SYNTHESIS AND APPLICATION OF MACROCYCLIC COMPOUNDS FOR METAL CATION SENSORS

by

SURESH VALIYAVEETTIL
B.Sc. Calicut University, Kerala India
M.Sc. Calicut University, Kerala, India
M.Tech. Indian Institute of Technology, New Delhi, India

A Dissertation Submitted in Partial Fulfilment of the Requirements
for the Degree of **DOCTOR OF PHILOSOPHY**

in the Department of Chemistry

We accept this thesis as conforming
to the required standard

Dr. T.M. Fyles, Supervisor
(Department of Chemistry)

Dr. A. Fischer, Departmental Member
(Department of Chemistry)

Dr. D.A. Harrington, Departmental Member
(Department of Chemistry)

Dr. T.W. Pearson, Outside Member
(Department of Biochemistry)

Dr.J.S. Bradshaw, External Examiner
(Brigham Young University, Utah)

Supervisor: Dr. Thomas M. Fyles

Abstract

This thesis comprises three chapters united by a single theme: development of alkali metal cation sensors based on ion complexing macrocycles.

In part 1, benzo-18-crown-6 and cryptand 2.2.2B were immobilised on polyacrylic acid backbone through an amide linkage. The benzo-18-crown-6 and 2.2.2B were functionalised using the Friedal-Crafts acylation reaction with ω-amino acids. The spacer between the polymer backbone and the crown ether was varied by using ω-amino acids with varying numbers of methylene groups ($(CH_2)_2$ and $(CH_2)_{11}$). Attempts to use ω-amino acids with an intermediate spacer length $(CH_2)_{4,5}$ failed due to formation of a cyclic imine. The amino crown ethers were immobilised on a poly(acryloyl chloride). Polymers **2a**, **5a-d** and **6a** failed to give self supporting membranes but a polymer blend with PVC/Plasticizer was employed for membrane fabrication. Ion Selective Electrodes (ISEs) and Coated Wire Electrodes (CWEs) were made from polymer blend membranes and their response to alkali metal cations was tested. The ISEs made with mobile carriers were active, while those prepared from immobilised carriers were inactive. The reverse was the case with CWEs. This dichotomy existed in all cases. The selectivity of the ionophores among the alkali metals was unaffected by linkage to the polymer backbone. However, the alkali metal/alkaline earth metal selectivity was enhanced. The effect of plasticizer and hydrophilic additives on electrode response was insignificant. The spacer length had considerable influence: the longer the spacer, the better the electrode response of the CWEs.

In part 2, the mass transport of ions across the polymer blend membrane under a temperature gradient was investigated. The immobilised polymers prepared in part 1 were used here to fabricate membranes from polymer blends with NOMEX. In thermodialysis experiments, a low level of ion transport was detected. These preliminary experiments led to a rediscovery of

membrane distillation. The scope of this latter process with hydrophobic membranes was explored in detail.

Part 3 was devoted to the design and synthesis of water soluble photoionophores. Three series of molecules were synthesised: captands, bis crown ether compounds and phenol derivatives of tartaro crown ether carboxylic acids. Captand molecules were synthesised by a capping reaction of crown ether tetraacid chloride **14** with 1,3-bis(aminomwthyl) benzene, 1,4-bis(aminomethyl) benzene and 2,2'-bis(aminomethyl) biphenyl. Crystals of meta- and para xylene capped molecules were grown and their structures solved to establish the conformation of the molecules. Fluorescence quenching studies of these molecules were done in 0.3% methanol:water (v/v). Quenching due to alkali metal ions was insignificant (< 20%) while copper and mercury cations quenched the emission significantly (> 90%). Stern-Volmer analysis showed an upward curvature indicating association between the ligand and the cations Cu^{2+} and Hg^{2+} cations, but dynamic and static components of the quenching could not be separated. Potentiometric titration with a potassium selective electrodes was carried out to obtain the stability constants for these ligands with potassium ion.

The bis crown ethers **28** and **29**, designed to increase water solubility, were prepared by the reaction of anhydride **27** with 9,10-bis(aminomethyl) anthracene and 1,2-bis(aminomethyl) benzene. The pK_a values of the ligands and their stability constants with alkali and alkaline earth metal ions were determined by potentiometric titration. Fluorescence quenching studies were done in aqueous buffer at pH 10. These compounds also failed to give an emission quenching in the presence of alkali or alkaline earth metal cations, but both copper and mercury cations showed a significant amount of quenching. Stability constants were derived from emission quenching studies for Cu^{2+} and Hg^{2+}.

Chromoionophores, phenol derivatives of tartaro crown ethers, were synthesised from the reaction of crown ether anhydrides and

2-aminophenol. The structure of the compound **31** was assigned as the *syn* isomer based on nmr data in comparison to literature reports. Absorption studies were carried out in water. The absorption spectra of compound **30** were perturbed by alkali metal as well as alkaline earth metal ions, while the absorption spectrum of compound **31** showed no response to varying cation concentration. The lack of response from compound **31** was attributed to the competitive binding of cations among *syn* carboxylic groups away from the *syn* phenolic groups.

Examiners:

Dr. T.M. Fyles, Supervisor
(Department of Chemistry)

Dr. A. Fischer, Departmental Member
(Department of Chemistry)

Dr. D.A. Harrington, Departmental Member
(Department of Chemistry)

Dr. T.W Pearson, Outside Member
(Department of Biochemistry)

Dr.J.S. Bradshaw, External Examiner
(Brigham Young University, Utah)

TABLE OF CONTENTS

LIST OF TABLES

LIST OF FIGURES

LIST OF SCHEMES

LIST OF ABBREVIATIONS

A -$CONMe_2$
AIBN -2,2'-Azo*bis*isobutyronitrile
amu -Atomic Mass Unit
c -concentration
CWE -Coated Wire Electrode
DMA -N,N-Dimethylacetamide
DMF -N,N-Dimethylformamide
DMSO-Dimethyl Sulphoxide
DOA -Dioctyladipate
DOP -Dioctylphthalate
F_0 -Emission Intensity with Zero Concentration of Quencher
F -Emission Intensity In presence of Quencher
HP -Hewlett-Packard
IR -Infrared
ISE -Ion Selective Electrode
LAH -Lithium Aluminium Hydroxide
mp -Melting Point
MS -Mass Spectroscopy
nmr -Nuclear Magenetic Resonance
NOMEX-trade name for the polymer
PVC -Poly Vinyl Chloride
r.t. -Room Temperature
SCOGS-Stability Constants of Generalized Species
THF -Tetrahydrofuran
TLC -Thin Layer Chromatography
TMAN-Tetramethylammonium Nitrate
TMAOH-Tetramethylammonium Hydroxide
Triton -Triton X-100
Ts -*para*-Toluenesulphonyl

IR DATA

s -Strong
m -Medium
w -Weak
br -Broad
sh -Shoulder
v -Very

nmr-DATA

s -Singlet
d -Doublet
t -Triplet
m -Multiplet
br -Broad

ACKNOWLEDGEMENTS

I would like to express my gratitude to Dr. T.M. Fyles for his support and guidance throughout this project.

I am also greatfull to Dr. P. Wan for all his help and allowing me to use the fluorimeter and accessories to do the photochemical investigations. Many thanks also go to my colleagues D. Budac, G. Cross, T. James, V. Iyer, K. Key, A. Pryhitka, D. Shukla and M. Zojaji for helpful discussions making the work atmosphere comfortable. Thanks are also due to my friends and other graduate students who helped in whatever way they could during my stay in Victoria (1987-1991). Special thanks also goes to K.C. Kaye for helping me to draw some of the pictures during the preparation of this thesis.

The crystallography was done by Dr. F.R. Fronczek and Dr. R.D. Gandour of Lousiana State University. Their efforts were greatly appreciated.

I would like to acknowledge Mrs. C. Greenwood for helping me run the nmr spectra reported in this thesis and Dr. D. McGillivray for the mass spectra reported here. Thanks are also due to the staff at the Chemistry Department for all their help.

To

my Parents, Brothers, Sisters and all my Professors

who inspired me to reach this stage.

CHAPTER 1

Overview

1.1 Supramolecular Chemistry

The discovery of cyclic ethers and their cation complexing properties opened a new branch of molecular chemistry which has become "Supramolecular Chemistry".[1] The importance of these molecules and the research in this area was recognised by the scientific community in the award of the 1987 Nobel prize for chemistry to three eminent pioneers: C. J. Pederson, D. J. Cram and J. M. Lehn. Today thousands of cyclic ethers, amines, sulphides and other molecules with designated topology are known. Interest in this field is growing, together with its implications and influence on other disciplines of molecular science to probe and create new dimensions of molecular interactions. The large number of reviews and monographs published to date express this fact.[2-7]

The terminology adopted to name these macrocycles is rather cumbersome, but is based on the topological aspects of the ligand.[2,8-10] A monocyclic ligand with any type of ligating atoms is called a coronand (coronate for the complex), polycyclic spherical coronands are cryptands (cryptate for the complex) and open chain multidentate ligands are called podands (podate for the complex). Most compounds belonging to the above

mentioned classes contain a hydrophilic interior and hydrophobic exterior (Fig. 1). The principle interest lies in the ability of such materials to form complexes. A complex is two or more molecules held together by distinct forces such as electrostatic interaction, hydrogen bonding, ion pairing, pi-acid to pi-base attractions, van der Waals attractive forces or partially made or broken covalent bonds.

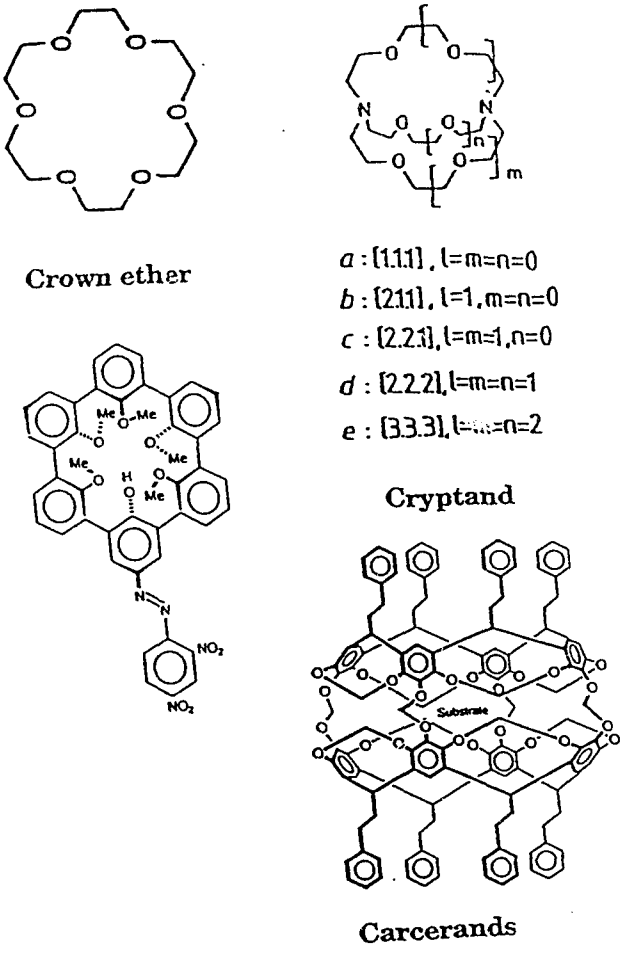

Figure *1* Examples of synthetic macrocycles

The stability of the complex depends on the geometrical, structural and functional complementarity of the two species. A complex is made of at least one host (whose binding sites converge in the complex) and one guest (binding sites diverge in the complex). A host may contain a cavity with more than two ligating sites, a reactive functionality or groups to control physical properties. The assembly of two or more molecules is also known as a supermolecule. Supramolecular chemistry involves the design and synthesis of macrocycles for a specific function and the exploration of the ability of the molecule to perform that function. The function can be molecular recognition, molecular catalysis or molecular or ionic transport through a medium.[11] Potential applications of these molecules include biochemical models in biochemistry, molecular devices and catalysts.

The central premise is that molecular architecture controls the shape and size of the host and the nature, number and the arrangement of the ligating sites and thereby determines the thermodynamics and kinetics of the complexation reaction. Complex formation and the stability of the complex can be approximately predicted by considering the force of attraction between the host and guest. Hard and soft acid base theory[12] is used to explain the electrostatic nature of these forces. According to this concept, hard acids such as alkali and alkaline earth metal ions prefer hard bases such as water etherial oxygens and carboxylates. Soft bases such as sulphur provide good ligating sites for soft acids such as late- and post-transition metal cations (eg.

Pb^{2+}, Cd^{2+} ions). Nitrogen prefers to stay in the middle with affinity towards transition metals like Ni^{2+}, Cu^{2+}, etc., at the same time without seriously diminishing the complexation of alkali metal ions.

The increased stability of the complex of a macrocyclic host with a cation relative to an open chain molecule is known as the macrocyclic effect.[13] Spherical recognition involves the size complementarity between the host having the spheroidal hydrophillic cavity and a ball-like guest where the cation fits nicely in to the cavity of the macrocycle. This is a simple analogy to the lock and key mechanism[14] of enzymology. The three dimensional encapsulation of a cation by a cryptand which results in 3 to 5 orders of magnitude higher stability than the macrocyclic effect is further known as a cryptate effect.[15] Size complementarity can further extend to other shapes and sizes (eg. tetrahedral, trigonal, central, lateral and linear recognition).

Another effect examined principally by D.J. Cram[16] involves the preorganization of the host to accommodate the guest species. The concept is revealed in the crystal structures of 18-Crown-6 and it's K^+CN^- complex.[17,18]

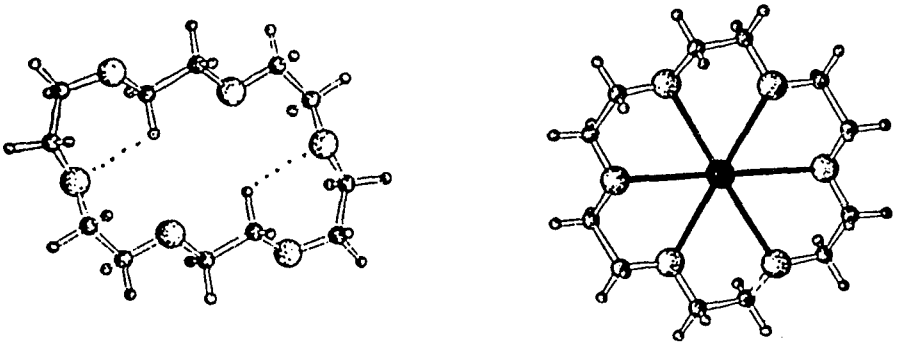

Fig. 2 Crystal structure of 18-crown-6 and its K^+CN^- complex.

The uncomplexed crown does not have a cavity whereas the potassium complex induces a convergence of the oxygen electron pairs to form a crown shaped object. The guest organises the host during complexation. Cram[16,19,20] has demonstrated that a highly preorganised rigid host shows better selectivity. For example, spherands undergo very limited conformational changes during complexation and are highly selective for their intended guest.

1.2 Analytical applications of Crown ethers:

Crown ethers and other macropolycyclic ligands are known to have high selectivity towards a specific guest species among similar substrates.[21] In principle, supramolecular chemistry can make use of the built-in properties (information) of a host molecule to associate with a specific guest species in order to tailor make molecular assemblies having well defined microscopic organization and macroscopic characteristics. These molecular assemblies could be molecular layers, membranes, vesicles, micelles or in general any type of molecular organization with well defined morphologies.[6] By designing and incorporating functional groups into these molecular assemblies or supramolecular systems, it is possible to develop supramolecular devices. These include molecular photonics, electronics and ionics, devices for information storage and signal transduction.[22]

In all the above mentioned devices or supramolecular assemblies the output signal generated would depend on the integrated signals of each of the molecules of the assembly. The architecture of the molecule to perform a specific function involves incorporating the proper functional group into the individual molecule and assembling them in the proper medium. The molecule recognising element is also attached to a monitoring device to record the cumulative response of individual molecules as distinct from the bulk medium. When the tailor-made molecule comes in contact with a species with a complementary functionality, the association of the two species generates a supermolecule. The supermolecule can respond to an external stimulus such as light, electricity or heat. A supermolecule which responds to electricity or an electrical gradient can be used construct electrochemical sensors. In general, any ionophore (molecule which associates with ions) incorporated into a membrane can be used to construct electrochemical sensors. These sensors, or electrodes, monitor the concentration of an ionic species which selectively interacts with the membrane material. It is then possible to detect and quantify (with the help of a calibration graph) the analyte in solution. Electrochemical sensing involves sensing of a charged species in an analyte solution by either potentiometric or amperometric techniques. Both techniques involve an electrode sensitive to the charged species, to produce a reading which corresponds to the amount of charged species or the relative changes in the absolute amount. The electrodes are generally constructed from a

membrane incorporated with an ionophore selective to the ion to be measured. The most common electrochemical sensors are Ion Selective Electrodes (ISE) and their relatives, Coated Wire Electrodes (CWE).

Photonics represents an area in which the molecular assembly responds to light. The necessary component of this device comprises a light sensitive functionality incorporated into the molecule. The formation of supramolecular entities from light sensitive components leads to changes in the ground and/or excited state properties of the individual species. These changes in the properties may lead to processes like photoinduced energy migration,[23] charge separation by electron or proton transfer,[24] perturbations in optical transitions and polarizabilities,[25] photoregulation of binding properties,[26] etc. The active ionophores in this area are divided into two main categories: fluoroionophores and chromoionophores depending upon the nature of photophysical process of the molecule. Effectively the chemical signal generated by the association or interaction of the analyte and the ionophore is transformed by the supermolecule into spectral changes of the host molecule.

Crown ethers, because of their high selectivity and easy synthesis, have established central status in supramolecular chemistry and its applications in analytical chemistry. My research in the past couple of years has concentrated on developing sensors for alkali metal ions in water based on crown ether ionophores. The study of membrane separation processes in our laboratory led us to study membrane based potentiometric electrodes. The lifetime of these

electrodes depends on the property of the membrane, which, in turn relates to the rate of leaching of water soluble components from the membrane to the analyte solution. In order to avoid leaching and thereby to increase the life time of the electrodes a novel approach of immobilising the ionophore to the back bone of the polymer was explored.

Membrane transport studies involving mass transfer across a membrane has been an active area during the past decade or so. In an ideal situation, a robust and thin membrane is impregnated with an ionophore selective to a particular ion. The membrane should be able to transport the given ion selectively from one aqueous phase to another. The second section of this thesis details an attempt to develop an ion selective transport membrane using a temperature gradient to drive the process. This process, if successful, would be an example of thermodialysis.

Transport of metal ions, especially the alkali metal ions, through biological membranes has also attracted considerable attention from research groups all over the world. These studies have focused on the development of ion transport systems such as ion channels,[27] pores[28] and carriers.[29] The transport is usually monitored by suitable sensors within the experimental system. Photometry plays an important role in monitoring the ion concentration because of its high sensitivity, high selectivity and simple analytical procedures. Fluoro- and chromoionophores developed to date are mainly soluble in organic solvents like acetonitrile and methanol. The *in situ*

monitoring of ion concentration for most biological transport requires a water soluble sensor molecule. The third section of this thesis deals with our efforts in this direction. We designed and synthesised three groups of compounds exploiting the known structural features of crown ethers containing tartaric acid units which can be used as fluoroionophores or chromoionophores. The main thrust of this project is to develop water soluble and efficient fluoro- or chromoionophores.

CHAPTER 2

Ion Selective Electrodes and Coated Wire Electrodes

2.1 Introduction

The progress in molecular recognition during the last two decades has resulted in a great deal of understanding about molecular interactions based upon structural and geometrical considerations. A number of molecules have been designed and studied to improve the selectivity and specificity of cation binding, especially of the alkali and alkaline earth metal ions. These studies span the spectrum of molecular chemistry from organic chemistry to analytical chemistry. The significant development in analytical chemistry was the development of sensors from molecules selective to specific metal ions. Two well known types of sensors are Ion Selective Electrodes (ISEs) and Coated Wire Electrodes (CWEs).

A brief history of the development of neutral-carrier-based ion-selective electrodes was given by W. Simon *et al*[30] in 1986 and a more recent one by R.L. Solsky (1990)[31] covers the significant developments in this area. A large number of reviews and monographs are available which deal with Ion-Selective Electrodes and membrane based electrodes in general.[31-35] The most important applications of these sensors are in the clinical and biochemical field where

sodium, potassium and calcium in urine and blood samples are analyzed routinely.[36-38]

Conventional ion-selective electrodes are comprised of a plasticized poly(vinyl chloride) (PVC) membrane containing an ionophore to provide ion discrimination. A plasticizer, which comprises up to 65% of the membrane, improves the mechanical properties of the membrane and provides a fluid phase to hold the active ionophore. The active membrane of appropriate diameter for the ISE is cut from a master membrane and mounted as a physical barrier between a reference solution and the analyte solution.

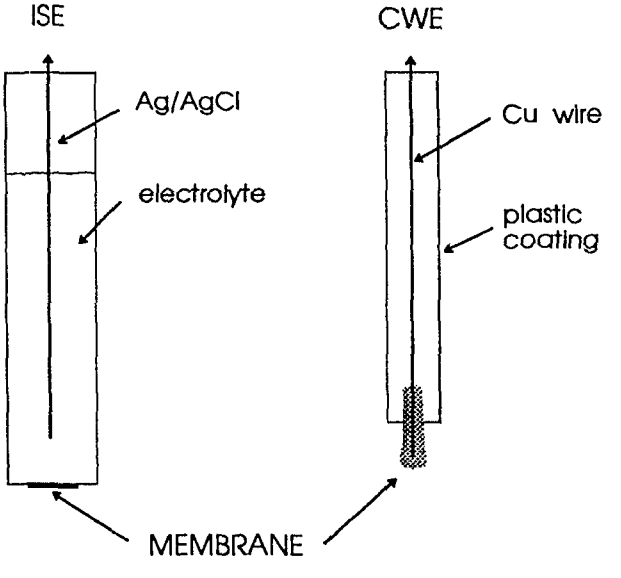

Figure *3* Schematic diagrams of an Ion Selective Electrode (left) and a Coated Wire Electrode (right).

Coated wire electrodes are relative new-comers in this area which offer some advantages over conventional ISEs. These are very easy to construct and

the cost of a single electrode is a few cents. At this point they are considered to be disposable electrodes. CWEs can be made in any shape (wire, disk, cylinder, thin film, etc.) by selecting an appropriately shaped conductor. The sensor is constructed by simply coating the conductor with the ionophore incorporated in a polymeric membrane. An excellent review on this topic was published by Cattrall and Hamilton in 1984.[39] The significance of this ever growing field in medicine and industry can be seen from the number of patents issued on this topic during the last few years.[40-43]

One unique feature of CWEs is the absence of an internal reference solution. The fundamental principles behind CWEs are not understood completely. This factor has never been a barrier in developing a large number of CWEs which respond to a given ion, or to their use in clinical, environmental and industrial analysis. A variety of polymeric materials such as polyvinyl chloride, poly(methyl methacrylate) and epoxy are usable in CWEs as the polymeric membrane.[44] In the first two polymer categories, a solution of polymer, plasticizer and ionophore is used to coat the tip of the conductor.[45] In the case of epoxy, the ionophore is mixed with the curing agent and combined with the epoxy resin.[46] In either case, the tip of the conductor is then dipped into the mixture to create a small bead, and allowed to cure. The conductors used are normally platinum or copper.

The efficiency of these sensors (CWE or ISE) depends on the selective absorption of the ion of interest into the polymer membrane. Absorption of

charged ion causes a concentration gradient across the membrane interface which in turn generates a membrane potential. This potential, being dependent on the selective absorption of the specific metal ion, can be used to measure the concentration of the metal ion in solution. One of the main impediments in developing a molecule based sensor, lies in the construction of the sensor without losing the inherent properties of the sensing molecule.

The main drawback of both ISEs and CWEs is their limited life time in real environments, limited chemical resistance, and in some environments, limited physical stability. The useful lifetime of electrodes is limited by the leaching of the ionophore from the polymer matrix into the analyte solution. The most widely studied ionophores include crown ethers,[47] ammonium salts,[48] valinomycin and other antibiotics,[49,50] calixarenes,[51] and open chain polyethers.[47] All of these materials are relatively polar and can be leached from the membrane over time. The lifetime decreases rapidly with increase in the solubility of the ionophore in water. Both detection limit and response of the electrode degrade as the ionophore is leached from the membrane.[44,48-50]

An obvious solution to the problem of decreased lifetime is the covalent immobilization of the ionophore on the polymer matrix of the membrane.[44] Alternatively, the use of a matrix with the same solubility as the ionophore would produce self-polishing electrodes. Covalent immobilisation of the active ionophore to the polymer matrix backbone has been exploited by various researchers.[51-53]. Compound specific methods have been adopted to graft the

ionophore to the polymeric back bone. In the most common method, a preformed polymer is modified to incorporate simple ion-exchange sites and the ion-selective membrane is cast from the polymer.[50] The number of reports available on this methodology points out the simplicity of the technique.[51-56] One simple example is the fabrication of an anion ISE by alkylation of the amino sites on a PVC backbone to create quaternary ammonium centres. Ion exchange with sodium dodecylsulphate yielded a polymer sensitive to anions.[56]

A recent paper by Bachas[57] explored the possibility of using immobilised benzo-15-crown-5 in constructing ISEs. The synthesis involved a carbodimide mediated coupling of an amino crown ether with the carboxyl groups of carboxylated PVC, and was claimed to produce 6.4% (w/w) ionophore loaded to the polymer. Kimura *et al*[58] synthesised polymers containing 12-crown-4, 15-crown-5 and 18-crown-6 by the condensation reaction of poly (ethylene-co-maleic anhydride) and the appropriate hydroxymethyl crown ether derivative. They blended these products with polyvinyl alcohol for membrane casting. The membranes were then treated with an aqueous solution of formaldehyde containing sulphuric acid to crosslink the poly(vinyl alcohol), and thereby decrease the solubility of the entrapped crown ether containing polymer in water.

The second alternative involves polymerisation of an ionophore/monomer to give a polymer sensitive to ions. There are two major developments in this

area: i) a simple monomer is polymerised in presence of ion exchangers or ionophores. One example involved radical polymerisation of vinyl chloride initiated with $SO_3^{\cdot-}$.[57]. The ionisable proton of the sulphonate end groups can be exchanged with a surfactant cation to produce cation exchange membrane electrodes. ii) The ionophore is covalently bound to an acrylic monomer and (photo) polymerised to give an ion responsive polymer.[59] Okahara *et al*[59] synthesised a polymer from N-acrylyl- and N-methacrylyl aminomethyl crown ethers through radical polymerisation. A related novel approach, developed by Harrison[60] uses a photopolymerisable plasticizer as the solvent for an ionophore/PVC solution. The designed solid state sensor in which the ionophore was entrapped in the polymer was produced by polymerisation of the plasticizer.

Extended lifetimes of polymer immobilised ionophores compared to conventional solvent polymeric membrane electrodes are commonly reported, together with improved detection limits and improved stability in some cases.[56] The immobilization also affects the nature of ion translocation and the rate of diffusion of the ionophore inside the membrane.

The molecular translocation across a membrane can be facilitated by different mechanisms[61](Figure 4). In general, there are three different mechanisms: i) a carrier mechanism in which the transporter diffuses across the membrane to facilitate ion transport, shipping substrate from the concentrated side to less concentrated side; ii) a channel mechanism where the

transporter spans the membrane like a tube, through which an ionic or neutral molecule can diffuse from one side to the other; or iii) a relay mechanism where the ion hops from one binding site in the transporter to another across the membrane.

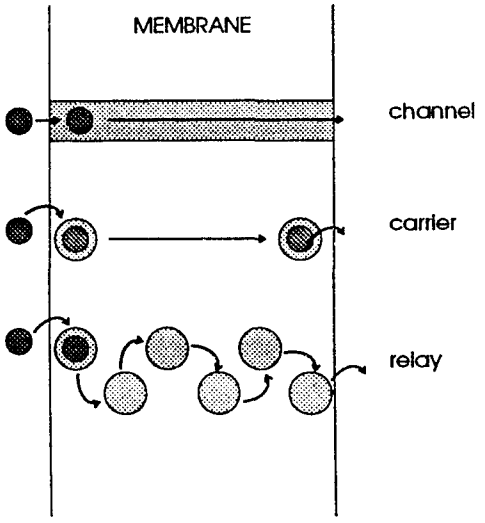

Figure *4* Mechanisms of membrane transport

Polymer immobilization of ionophores compels the metal ion transport to occur through a relay mechanism. This could lead to high ionic mobilities relative to ionophore diffusion via a carrier mechanism. In most cases of immobilization, the diffusion of the ionophore is effectively removed. Moreover, ionophore leaching from the membrane requires a chemical reaction to cleave the covalent bond between the ionophore and the polymer backbone.

Membranes fabricated from a hydrophobic polymer such as PVC, or immobilised PVC with proper plasticizer, provide a macroscopically and

microscopically homogenous medium through which an ion can diffuse from one side to the other. In cases of ionic polymers like Nafion, the possibility of microscopically heterogenous phase separation occurs inside a macroscopically homogenous membrane. This phenomenon is based on the tendency for the ionic sites on an ionic polymer to cluster along the polymeric backbone. The channel mechanism suggested by H. Freiser and C.R. Martin[62] for ISEs based on an ionic polymer involves the formation of ionic clusters (~ 40 Å in diameter) mutually connected by small channels (10 Å in diameter). These clusters, distributed randomly throughout the polymer matrix, contain the polymer attached ion, its counter ion, and water of hydration. The study also revealed that ions can diffuse through the channels.

The central influence of anionic site concentration present in the membrane, the presence of added inorganic salt, and the nature of anions on the response and selectivity and stability of the electrode has been examined thoroughly.[63-66] Buck *et al*[63] clearly demonstrated the effect of the anion site concentration in the membrane on the electrode response. They concluded from selectivity and impedance measurements that only a negligible portion of the total site concentration of carboxylated PVC is dissociated and available as counterions for transport of cations.[63] The negative site concentration in the membrane affects the membrane properties. It decreases the membrane resistance and increases the water uptake by the membrane. Any effect due to the dielectric constant of plasticizer was absent in the case of membranes

made from polymers containing ionic sites because of the high uptake of water by the polymer blend. Anionic interference can be eliminated by using a plasticizer with a low dielectric constant. However, the plasticizer o-nitrophenyl pentyl ether gave enhanced signal, slope, selectivity, and linearity of the calibration graph when compared to o-nitrophenyl octyl ether for PVC membranes containing crown ether ionophores.[68] Additives like potassium tetraphenylborate (KTPB) help to increase the cation sensitivity of the membrane, reduce interference of the interfering lipophilic anions, may increase the cation selectivity, and lower the electrical resistivity of the membrane considerably.[66] The lipophilicity of the TPB^- ion also reduces the water content inside the membrane.

The detailed study by S.C. Ma *et al*[65] on response properties of ISEs prepared with aminated and carboxylated PVC has shown that the presence of carboxyl or amine functional groups have little effect on the response and selectivity of neutral carrier based electrodes. This is true even if the amount of functional group exceeds the molar amount of the ion carriers, provided that these excess functional groups are associated and do not interact with the carrier directly.

The viscoelastic nature of the polymeric membrane is important to get a reasonable electrode response from a membrane.[69] This can be achieved by keeping the temperature of the membrane (during the analysis) above the glass transition temperature (T_g). Unplasticized PVC has a T_g of 80°C. Below

T_g, its electrical conductivity is 10^{-10} mho/cm and its dielectric constant is 3. Above 80°C, electrical conductivity can increase up to 10^{-9} mho/cm and the dielectric constant to 15. The plasticizer has a profound effect on the membrane response. It not only decreases the T_g of the polymer, but also provides a liquid phase for the diffusion of neutral carriers across the membrane. This is important in the case of neutral carrier based membrane electrodes where the amount of ionophore is only 0.1 wt % of the membrane composition.

The response of CWEs are much better than conventional ISEs in many cases.[71] However, understanding the mechanism of charge conduction inside the membrane and the polymer-substrate interface requires detailed investigation of interfacial ion transport. Contradicting evidence has been obtained in different studies.[72,73,74] For example, studies of temperature dependent ion conductance indicated an electronic mechanism similar to organic semiconductors,[72] whereas studies of the pressure dependence of conductance pointed to an ionic conduction mechanism.[73] Since E^0 values depend on the metallic nature of the conductor, it is reasonable to assume that a redox couple acting at the interface might be providing an internal reference for the CWE.

Our interest in polymer immobilised ionophores in sensor technology stems from polymer immobilized ionophores for membrane separations. Polymer blend membranes can be prepared from crown ether containing

acrylamide polymers dispersed in a robust support polymer which forms the membrane barrier. This approach combines the known physical properties of the support polymer with a simplified polymer synthesis problem. The "active component" polymer need not have a high molecular weight, nor be particularly suited on its own for the ultimate application (for example: mechanical properties for separation membranes). The immobilized ionophore polymers can then be designed to exploit favourable synthetic chemistry, simple structural characterization, or any other critical factors. This technology has advantages over conventional single polymer membranes: i) it provides an opportunity to covalently attach highly water soluble ionophores; ii) it can reduce electrical resistance due to the presence of ionisable groups; iii) it could improve the adhesion properties of the polymer blend to a solid surface especially on a silica surface to produce solid state sensors;[75] iv) it could increase the water intake and thereby increase the ion mobility inside the membrane; and, v) it could increase the cation sensitivity and decrease interference from anions present in the analyte solution.

The other variable which has been shown to influence the electrode response is the "spacer" length. By varying the spacer length, or the length of an alkyl chain between the polymer backbone and the ionophore site, the microscopic mobility of a bound ionophore inside the membrane can be manipulated. The shorter the length of the chain, the less will be the mobility. The movement and alignment of ionophore inside the membrane influences the

ion translocation through the membrane, especially when a relay mechanism is favoured among other mechanisms. Earlier work by Neilsen and Jansen[76] indicated the effects of chain length on the response of a nitrate selective electrode. The linear calibration range was extended with extension of the alkyl chain length on tetraalkylammonium nitrate from C_3 or longer.
Since ionophore immobilised polymers are known to provide robust and high flux membranes for ion separations,[77,78,79] it is potentially interesting to explore the properties of sensors from these same polymers. It is surprising to see that in the literature, the number of PVC-immobilised, or even polymer immobilised ionophores, used to improve the response and the lifetime of potentiometric sensors is very few.[57] The obvious questions that arise are: i) can these polymeric ionophores, or blends made from two different polymers, give thin membranes which can be used in ISEs and other related sensors? ii) can immobilisation increase the lifetime of the electrode? iii) is the selectivity of the ionophores affected by the immobilisation? and, iv) is there any effect of chain length (spacer between the polymer backbone and the crown ether) on the response and lifetime of the electrodes?

We expected that a polymer blend with PVC and a second polymer bearing the active ionophore could combine ionophore derived selectivity with extended lifetime and could continue to enjoy the advantages of plasticized PVC as a matrix for ISE's and CWE's. The polymer bearing the ionophore will also contain free acid groups to provide more anionic sites to assist in

hydration, cation sensitivity and cation diffusion. This project seeks to demonstrate the approach using simple 18-crown-6 derivatives grafted to carboxy-PVC or poly (acrylic acid). If the concept has merit, it could then be extended to synthetic ion binding sites with better discrimination, or to other polymeric crown ether systems.

2.2 Theoretical description of the EMF response.

Ion-Selective Electrodes (ISEs) and Coated Wire Electrodes (CWEs) are electrochemical sensors whose potential responses have a linear relationship with changes in concentration or activity of a given ion.[80] An ISE is composed of a polymeric membrane, an internal filling solution, and an internal reference electrode (Fig III). The membrane is composed of a continuous layer of polymer which is responsible for electrode response and selectivity, and either physically covers a structure or separates two electrolyte solutions. The internal reference electrode is an electrode inside the ion selective electrode, generally a silver/silver chloride electrode in contact with solution containing chloride and of a fixed concentration of the ion for which the membrane is selective. The electrochemical cell is made up of this electrode and a reference electrode, connected by a wire and placed in the analyte solution. A reference electrode has a constant potential under the experimental condition, and serves

to measure the potential of a test electrode. For a determinant X, the Nernst equation for the response of a cell containing an X selective electrode may be written as

$$E_{ISE} = E^0 + 2.303\ RT/Z_XF\ \log a_X \qquad \text{---------- 1}$$

where E_{ISE} is the potential difference between the sample solution and internal filling solution, E^0 is constant potential difference including the boundary potential difference between the internal filling solution and the membrane, a_X is the activity of ion X in the sample solution, R is the gas constant (8.31441 $JK^{-1}mol^{-1}$), T is the absolute temperature (in K), F is the Faraday equivalent ($9.648670x10^4$ $Cmol^{-1}$), and Z_X is the charge of ion X. Nernstian response refers to a linear slope of 2.303 RT/z_xF mV/decade ($59.16/Z_X$ mV per unit of log a_X at 25°C) for an ion selective electrode when the potential of the electrode in conjunction with a reference electrode is plotted against the logarithm of activity (concentration) of a given species (X) over a given range. The intercept E^0 of the linear response function is a temperature dependant constant; the slope is the Nernst factor.

In order to account for the large deviations at low activities, Nicolsky and Eisenman[81] introduced a semi-empirical extension for the emf of the measuring cell as

$$E = E_0 + 2.303\ RT/Z_XF\ \log [\ a_X + K_{X,Y}^{pot}(a_Y)^{Zx/Zy}] \qquad \text{---------- 2}$$

where $E_0 = E_i^0 + E_R + E_D$ and E is the experimentally observed potential of a cell (in mV), E_i^0 is the constant potential difference including the boundary

potential difference between the internal filling solution and membrane, E_R is a constant consisting of the potential difference between the metallic lead to the solution in both the ISE and the reference electrode, E_D is the liquid junction potential generated between the reference electrolyte and the sample solution, Z_X and a_X are the charge number of the primary ion X and its activity in the sample solution, Z_Y and a_Y are the charge number of any interferent ion Y and its activity in the sample solution, and $K_{X,Y}^{pot}$ is the potentiometric selectivity factor. E_D is variable and sample dependent, whereas, the sum of E_i^0 and E_R is independent of sample composition. The Nicolsky formalism reduces to the Nernst equation in either of two cases: i) a perfectly selective electrode where $K_{X,Y}^{pot}$ reduces to zero; or, ii) the sample solution contains no interfering ion (i.e., a_Y is zero). The potentiometric selectivity coefficient ($K_{x,y}^{pot}$) defines the ability of an ion-selective electrode to respond to a single ion in the presence of other interfering ions in the same solution. It is measured in terms of the EMF response of a mixed solution containing both primary ion (X) and interfering ion (Y). A smaller value of this constant is preferred for practical application. An interfering ion is an ion, other than the ion being measured, which affects the potential output of the sensor, either by interacting with the ionophore or with the polymer material of the membrane. For a membrane electrode with neutral carriers that predominantly form 1:1 isosteric complexes with cations of same charge, the selectivity coefficient is determined as:

$$K_{X,Y}^{pot} = K_{S,Y} / K_{S,X} \quad \text{---------- 3}$$

where K_S is the stability constant of the respective complex in water. Single ion activity can be calculated by using the equation $a_X = C_X\gamma_X$, where γ_X is not equal to 1. The mean activity coefficient γ may be calculated in terms of the concentration of all ionic moieties, according to Debye-Huckel formulae:[82]

$$\log \gamma_{\pm} = [(AI^{1/2} / Z_+Z_-) / (1 + BaI^{1/2})] + cI \quad \text{---------- 4}$$

$$I = 0.5 \Sigma C_nZ_n^2 \quad \text{---------- 5}$$

where A = -0.509 and B = 0.328 at 25°C in water, I is the ionic strength of the solution, C_n, Z_n are concentration and charge of any ion in solution and a and c are constants (ion dependent) for fitting the theoretical relationship to measured values of γ. According to the conventions proposed by Debye and Huckel, the activity coefficient of a single ion is given by:

$$\log \gamma_+ = |Z_+/Z_-| \log \gamma_{\pm} \quad \text{---------- 6}$$

$$\log \gamma_- = |Z_-/Z_+| \log \gamma_{\pm} \quad \text{---------- 7}$$

ISEs can be calibrated in three ways:[83] i) by choosing a calibration solution of known composition that resembles the unknown sample in every respect as closely as possible; ii) by bracketing the expected range of activity of the samples to be processed with two or more calibration solutions and then interpolating the results; or, iii) by a standard addition or known addition method. Both procedures i) and ii) are affected by changes in thermal equilibrium, rinsing of electrodes to alleviate memory effects, presence of electroactive species, etc. Procedure iii) is trivial and involves small additions

of the ion investigated or buffering of the ionic strength. By any technique, the calibration curve is a plot of potential of a given ion selective electrode assembly (ordinate) versus the logarithm of the ionic activity or concentration (abscissa) of a given species. The convention $pI = -\log a_i$ is frequently used through analogy to the pH definition.

2.3 Results and Discussion

All electrode responses were measured versus a double junction standard calomel electrode (Fischer Scientific) with 0.1M tetra-methylammonium nitrate as external filling solution. Detailed examination of the electrodes was done with an automatic titrimeter and automatic buret controlled by a microcomputer HP85. The titrant was added at a controlled rate and activity was calculated and recorded at each addition along with the cell potential and the time taken to reach the equilibrium. Slope and detection limits were calculated from the calibration curves. Potentiometric selectivity was measured using a fixed interference method, typically at 10^{-2}M in interfering ion concentration.

2.3.1 Synthesis and Membrane Fabrication

The immobilization of crown ethers involves a covalent bond-forming step between the ionophore and the backbone of the desired polymer. The coupling of acid chloride and amine was used to achieve this goal. Previous work with an amino derivatized crown ether from tartaric acid relied on a series of functional group interconversions to add the amino group and spacer to the crown ether moiety.[84] Although reliable, the process was lengthy and we sought a simpler and more general method for the preparation of reactive crown ethers.

The well-studied Friedel-Crafts reaction has been used to synthesize

amino-functionalised benzo-18-crown-6. This particular strategy was first reported by Quici.[85] The high yield and easy accessibility of the derivatives through the acylation reaction was exploited to generate crown ethers with different spacer lengths. The synthesis was carried out by treating the benzo-18-crown-6 with the ω-amino acid of the specific "spacer length" with polyphosphoric acid catalyst (Scheme I), purification of the product involved extraction of the acylated derivative of crown with chlorocarbons.

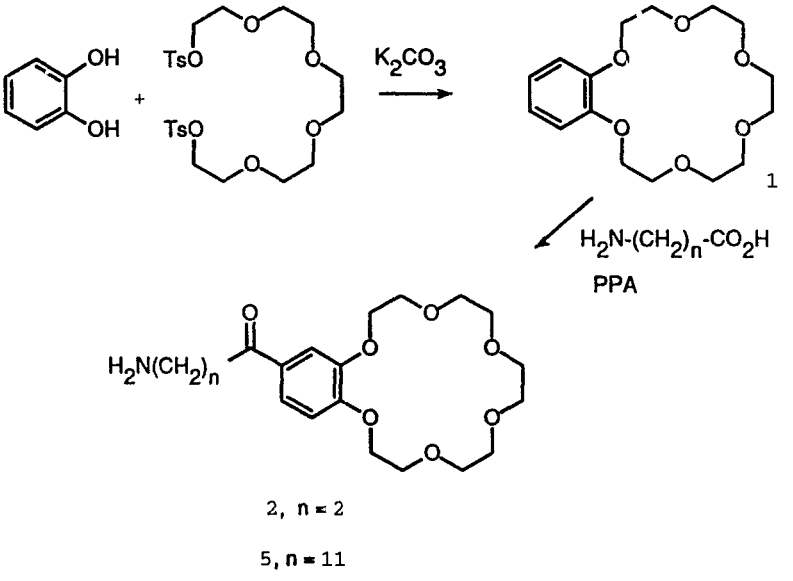

Scheme 1 Synthesis of benzo-18-crown-6 derivatives **2** and **5**.

The first compound synthesised in this series was 4'-(3-aminopropanoyl)benzo-18-crown-6 (**2**) by the reaction of 3-aminopropanoic acid with benzo-18-crown-6 in the presence of polyphosphoric acid. The reaction was found to be sluggish when compared to other derivatives prepared. The presence of a peak at 198.0 ppm (C=O) and two peaks at 44.8 and 38.1 ppm

(side chain carbons) in the ^{13}C nmr spectrum and the characteristic splitting pattern of a 1,2,4-tri-substituted aromatic ring in the ^{1}H nmr spectrum indicates the presence of an alkyl phenone chain attached to the benzo-18-crown-6 moiety. Other evidence came from the molecular ion peak (m/z 383) in the mass spectrum.

The second derivative prepared was 4'-(12-aminododecanoyl)benzo-18-crown-6 (**5**), by treating 12-aminododecanoic acid with benzo-18-crown-6 in the presence of polyphosphoric acid. The product was identified by its ^{13}C and ^{1}H nmr spectra. The ^{13}C nmr spectrum showed a peak at 199.2 ppm (C=O) and eight peaks below 33.0 ppm corresponding to the alkyl chain carbon atoms. The ^{1}H nmr spectrum showed two triplets corresponding to the methylenes adjacent to C=O and $-NH_2$ groups at 2.6 and 2.8 δ respectively. The presence of a singlet (7.4 ppm) and two doublets (7.5 and 6.8 ppm) corresponding to the three aromatic protons also identifies the presence of the desired product. The other structural confirmation came from the mass spectrum (m/z 509).

The acylation of benzo-2.2.2.-cryptand with 12-aminododecanoic acid yielded 4'-(12-aminododecanoyl)benzo-2.2.2-cryptand (**6**). The structural characterisation was achieved by the spectroscopic studies of the compound. The ^{13}C and ^{1}H spectra of the compound were found to have characteristic peaks similar to those described for compound **5**. The product also showed the expected molecular ion in the mass spectrum at m/z 622.

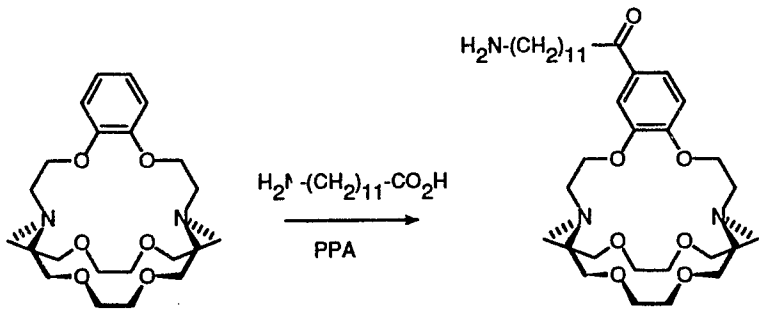

Scheme *2* Synthesis of benzo-2.2.2B derivative (**6**)

Attempted synthesis of crown ethers with intermediate spacer lengths (n=3,4) did not produce any free amine containing products. The end product of acylation of benzo-18-crown-6 with 5-aminopentanoic acid (valeric acid) was identified as the imine which arose from the intramolecular cyclization of the amino group with the keto group. In the ^{13}C nmr spectrum the single low field peak observed at 164.4 ppm could be assigned to the imine (C=N) carbon and the four peaks at 49.5, 26.5, 21.7 and 19.6 ppm could be assigned to the methylene carbons on the cyclic side chain. The absence of any peak above 165 ppm indicates the lack of a C=O functional group in the structure. The strong IR absorptions at 2870 (C-H stretching), 1625, 1590 and 1575 cm^{-1} (C=N stretch) indicate the presence of imine functionality in the molecule. The absence of absorption at 1650 to 1750 cm^{-1} ruled out the possibility of a keto group in the molecule. The strong molecular ion peak at m/z 393 in the mass spectrum corresponds the cyclic imine, instead of m/z 411 for the amine. An $(M+1)^+$ peak at m/z 394 and $(M+29)^+$ and $(M+41)^+$ peaks at m/z 422 and 433

confirm the cyclic imine structure instead of the free amine.

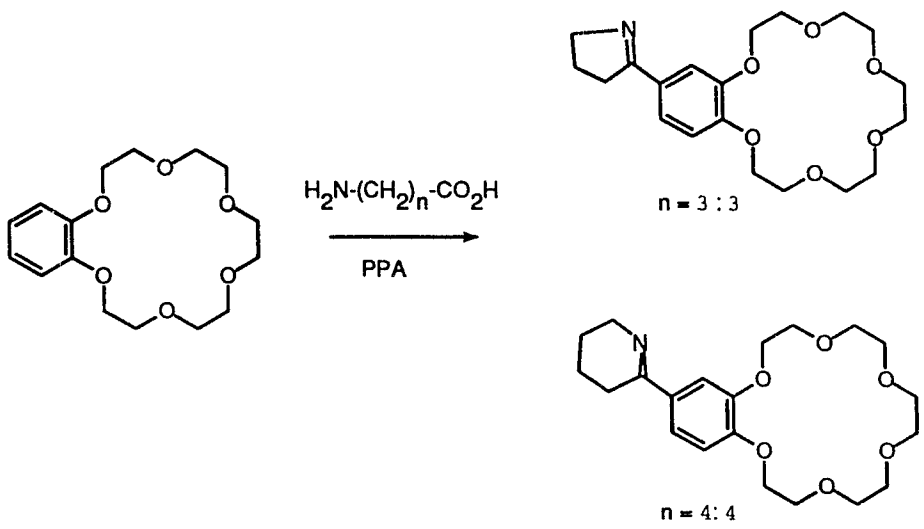

Scheme *3* Attempted synthesis of derivatives of benzo-18-crown-6 with intermediate spacer length (**3,4**).

A comparable result was observed in the acylation of benzo-18-crown-6 with 4-aminobutyric acid where the presence of a 5 membered cyclic amine attached to the benzene ring of benzo-18-crown-6 was established from ^{1}H and ^{13}C nmr spectra. The molecular ion peak at m/z 380 $(M+1)^{+}$ in the mass spectrum was a final confirmation of the cyclic imine structure in this case as well.

Attempts to generate free amines from these cyclic imines were not successful under Clemmenson conditions[86] (Zn/HCl) or a variety of conventional reductive conditions[87,88] ($LiAlH_4$, H_2/Pd/C/HCl). The end product of reduction was identified as the imine starting material from spectral

analysis.

The "aminocrowns" **2, 5** and **6** were then immobilised on the polymer backbone. The poly(acrylyl chloride) was produced from free radical polymerisation of the monomer acrylyl chloride.[84] The molecular weight and the acid content were determined separately. The acid chloride content was 10.4 mmol/g from titration with standard base solution and 11.2 mmol/g from the chloride determination from $AgNO_3$ titration. The molecular weight was determined by viscosity measurements of the methyl ester derivative prepared by reaction of poly(acrylyl chloride) with dry methanol. The value was found to be in the range of 15000-17000 g/mol. This is too low to form a self supporting film, but polyacrylamides of this molecular weight have previously been used in polymer blend applications.

Carboxylated PVC was converted to the acid chloride by treatment with thionyl chloride. For either polymer, the coupling reaction was carried out between the aminocrowns and polymers in dry THF with triethylamine as the base. The polymer was then purified by washing with methanol and in certain cases by dialysing the remaining traces of triethylammonium chloride with water. IR spectra of these polymer derivatives showed the absorption due to the amide group at 1650 and 1585 cm^{-1}. The percentage loading of ionophore to polymer was varied in terms of the acid content of the polymer and the amount of aminocrown used in the immobilisation step.

Immobilisation of aminocrown ethers on carboxylated PVC consistently

failed to give the persuasive absorption bands in the IR spectrum. This suggested that the reaction was sluggish relative to the rate of adventitious hydrolysis of the acid chloride. To summarize a large number of experiments: immobilizations on carboxy-PVC via the acid chloride (PVC-COCl) were generally poor, although some samples were prepared. Conversion to the acid chloride was incomplete and the subsequent amide formation reaction was also incomplete. The net result was a very low loading of crown ether in the PVC matrix.

Immobilization on poly(acrylic acid) backbones via the acid chloride (PA-COCl) were much more successful. The poly(acrylyl chloride) prepared was essentially a homopolymer containing very few unreacted acrylic acid groups.

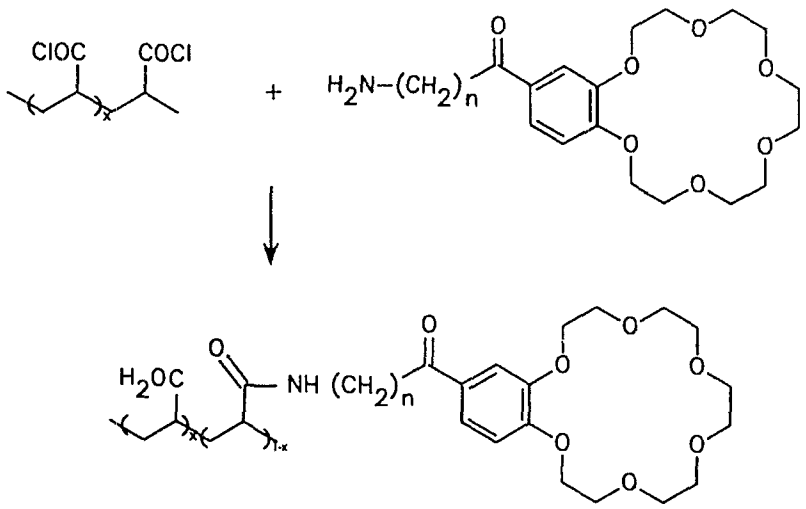

Scheme *4* Immobilisation of ionophores on polymer backbones

This polymer also provides an easy access to a large number of acid chloride functionalities which can be used for further immobilisation reactions with amino crowns. The polymers prepared from **2,5** and **6** had variable proportions of carboxylic acid and crown ether amide units randomly dispersed within the polymer. The % loading on the polymer was controlled by the known amount of acid chloride content on the polymer and using the appropriate amount of amino crown.

Three different types of crown ether immobilised polymers were prepared, two of which had benzo-18-crown-6 ether as ionophore and the other a cryptand 2.2.2B. The spacer length between the ionophore and the polymeric back bone was varied by selecting the appropriate aminoacid for the acylation reaction.

Table *1* Classification of immobilised polymers

Ionophore	Immobilised polymer	% Loading*
2	**2a**	20
5	**5a**	14
	5b	20
	5c	70
	5d	90
6	**6a**	20

* % loading = (moles of amino crown ether/ moles of acid chloride in the starting polymer) x 100

ISEs and CWEs were constructed from these immobilised polymers by making a polymer blend with high molecular weight PVC. Attempts to fabricate membranes directly from the immobilised crown ether polymers were in vain because of the sticky nature of the polymer. A membrane cast on a glass surface was difficult to peel from the surface; solutions of the blended polymers were more successful. Immobilised crown ether polymer and PVC were dissolved in THF along with plasticiser and the membrane was cast on a glass by slow evaporation of the solution. The same plasticizer can be used for both polymers. In the case of ISEs a 6mm diameter disk was cut from this membrane and mounted on a electrode body using 0.1M KCl as the internal solution.

CWEs were made by using the method described by H. Freiser.[89] This involved making a homogenous solution of the immobilised polymer, PVC and plasticiser in THF and dipping a copper wire into the solution followed by air drying of the polymer solution. Successive dip/drying cycles built a polymeric bead of 0.6 to 1 mm in diameter. The rest of the copper wire above the bead was covered with parafilm. The size of the bead was controlled by keeping the composition of the solution constant and using a constant number of dip/dry cycles. All electrodes were kept in 0.1M KCl solution for 24hrs before titrating.

Polymers **5 (a-d)** and **6a** were freely soluble in THF and appeared to form homogeneous blends with plasticized PVC. Polymer **2a** was sparingly

soluble in THF and formed two phases when blended with plasticized PVC under most conditions. Blends from **2a** and PVC/plasticizer in DMF were apparently homogeneous, but undoubtedly contained residual solvent.

2.3.2 Electrode characterization

The performance of ISEs and CWEs prepared from the immobilized ionophores as K^+ sensors is summarized in Table *2*.

Table *2* Response of electrodes made from immobilised ionophores[$]

Electrode	Immobi--lised Polymer	% Loading of ionophore on the polymer backbone	slope mv/de-cade	Detection Limit[‡]	Slope[*] mv/de cade	Detection Limit[‡*]
CWE	**5a**	14	-52 -52	4.8	-32 -34	4.1
ISE	**5a**	14	9.9 9.2	4.9	NR	NR
CWE	**5b**	20	-57 -56	4.6	-46 -45	4.3 4.4
ISE	**5b**	20	-11 -10	4.8	-8.9	2.9
CWE	**5c**	70	-45 -45	4.9	-64	3.4
ISE	**5c**	70	-12	3.8	-11	2.7
CWE	**5d**	90	-56 -56	4.3	-46	4.1
ISE	**5d**	90	-15	4.5	- 7.3	3.3

see footnotes on the next page

$ Membranes prepared from PVC:ionophore:plasticizer 25:10:65 wt% and tested against 10^{-5} - 5 x 10^{-2} M KCl solutions.
* In presence of 0.001M NaCl solution
‡ Detection limit was taken as the logarithm of activity or concentration of K^+ at the point of intersection of the extrapolated linear segments of the calibration curve (Fig. *5*).
NR No response

The striking feature of the data is the mediocre performance of ISEs relative to CWEs of the same composition. A typical example is illustrated in Figure *6*, which compares an ISE and a CWE prepared from **5b**.

An active CWE is formed (slope -49.1 mV/decade; lower bound of linear range about 5x10^{-4} M) but there is effectively no response to potassium ion activity by the ISE of the same polymer blend. In stark contrast, ISEs and CWEs prepared from **5** as a mobile carrier exhibit the opposite behaviour (Figure *5*).

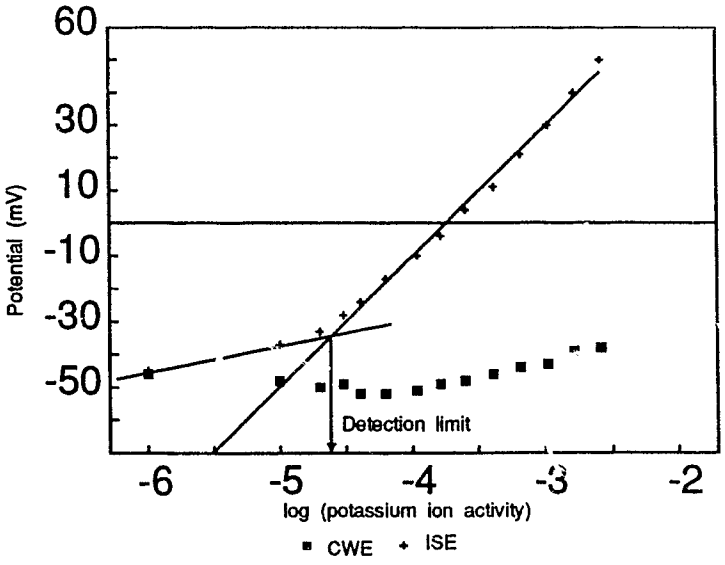

Figure *5* Comparison of CWE and ISE fabricated from the mobile carrier ionophore **5**

The ISE from **5** responds to potassium ion activity, but the CWE is essentially unresponsive. This dichotomy extends throughout the data of Table 1 and to all the polymer blend electrodes examined to date. In no case do we find high quality electrodes for polymer immobilized ionophores in ISEs. The converse is not the case: mobile carriers are active in CWEs.[3] This anomaly can not be explained completely with the present data.

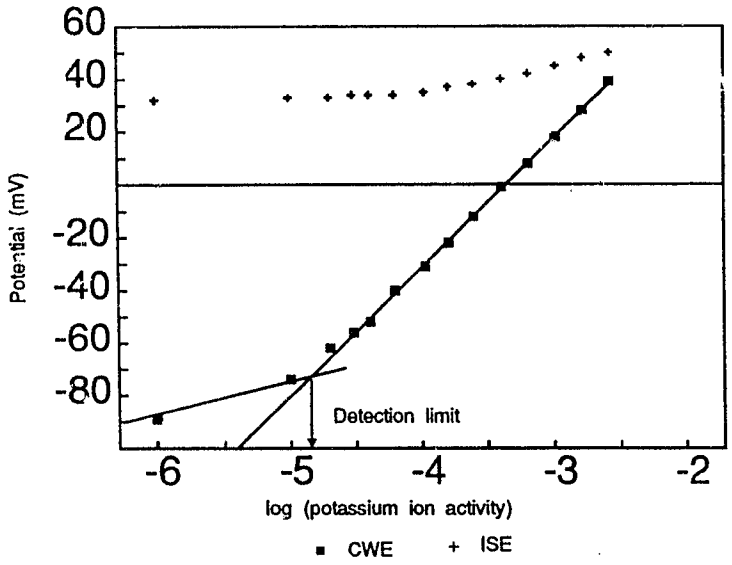

Figure *6* Comparison of CWE and ISE fabricated from the immobilized ionophore **5b**

Table *3* Comparison mobile vs immobilised carrier on electrode response.

IONOPHORE	ELECTRODE	SLOPE (mv/decade)	DETECTION LIMIT‡
5b	CWE ISE	-57 -12	4.6 4.8
5*	CWE ISE	-24 -45	4.2 4.3

$ Membranes prepared from PVC:ionophore:plasticizer 25:10:65 wt% and tested against 10^{-5} - 5 x 10^{-2} M KCl solutions.
* Membranes prepared from PVC:ionophore:plasticizer 34:1:65 wt% and tested against 10^{-5} - 5 x 10^{-2} M KCl solutions.
‡ Detection limit expressed as -log a_{K+}; lower limit of linear response.

The dichotomy of a mobile carrier which gives good ISE response but poor response in CWE response needs some comment. The mechanism of ISEs is well studied and generally well understood. In contrast, theoretical understanding of the mode of action of CWEs is virtually absent from the literature. Of the three known ion translocation mechanisms through a membrane (carrier, channel or relay), it is often suggested in the case of mobile carrier that the carrier mechanism is predominant over the other two (Fig. *4*). So an ISE made with mobile ionophore incorporated membrane shows a good response towards the metal ion of choice due to the diffusion of the ionophore-metal ion complex into the membrane phase.

The significant difference observed in this study between a mobile and an immobilised carrier in ISEs contradicts other reports where an immobilised carrier also functions in ISEs. A reasonable way to rationalize this observation

is to assume a microheterogenous phase separation in the ISE membrane. Even though the ISE membranes cast were macroscopically uniform and transparent, they may have microscopic polymer/ion clusters inside the membrane. This clustering phenomenon is known in the literature. For example, H. Freiser[62] observed this phenomenon with Nafion-based membranes. The ion transport through these membranes can only take place through "channels" which join the clusters. However, the concentration of immobilised poly acrylic acid in PVC might not be sufficient to produce channels connecting all ionic clusters inside the bulk membrane. Isolated clusters can not participate in transporting an ion from one side of the membrane to the other. Alternatively, the hydrophobic PVC polymer chains can disrupt the communication of ion channels inside the membrane.

The mode of casting the membrane and the mobility of ionophores inside the membrane dictate the difference in response of ISEs and CWEs studied. ISE membrane is cast over a long period of time by slow evaporation of solvent to deposit a "homogenous" membrane of desired thickness on a surface. The chance of having a uniform single layered membrane is very high and it might contain clusters on a molecular level. CWE membranes are made as multiple dip/drying cycles of the homogenous solution of the polymer and ionophore. The chance of having thin but distinct membrane layers one on top of the other with residual solvent at the interfaces is a good possibility. This itself could cause a change in the behaviour of the sensors.

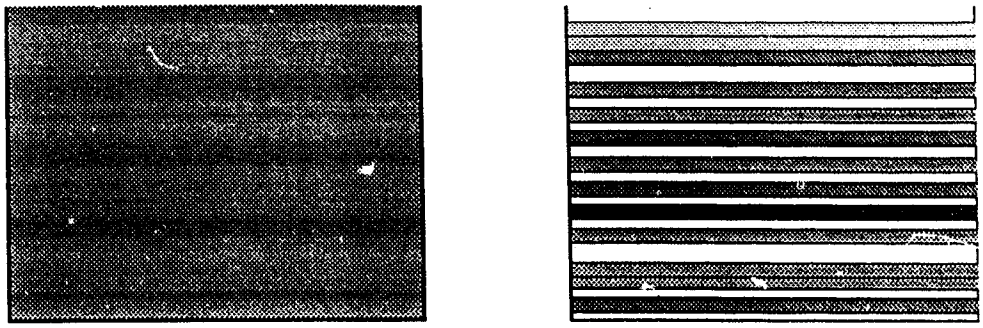

Figure 7 Cartoon of cross section of the membrane of an ISE and a CWE

If we accept this condition, then CWE membranes containing a mobile carrier could result in an accumulation of the ionophore to the interphases between membrane layers leaving polymeric non-conducting layers (or vice versa). This separation obviously would decrease the response of the CWE sensor by limiting the diffusion of the ionophore. In the case of an immobilised carrier, the question of free diffusion of the carrier does not arise at all. It is reasonable to assume that a relay mechanism of ion transport would accomplish the observed signal generation. In CWEs the preferential concentration of the carriers at the interphases can not happen. If microphase separation does occur the domains could be large enough to span the thin layers in CWEs. The cluster could then be in contact through the bulk of the

electrode.

The question of the events occurring at the interface of the metal and the membrane can not be solved by a single experiment and would require a thorough investigation beyond the scope of this project. Our naive approach to this particular problem was to substitute copper wire with platinum. The poor response from platinum in place of copper points a finger at the nature of interaction between the membrane and the metal surfaces. The result is contradictory to the literature evidence[90] where CWEs made by using platinum as conductor gave a reasonable response. Despite the rigorous cleaning of the copper surface to remove any oxide film, the possibility of having a thin layer of copper oxide can not be ruled out. Defects on the surface which are partly responsible for the good adhesion of the polymeric membrane, solvent molecules or even the traces of moisture trapped in between the membrane and the metal surface also increase the conductance at the metal-membrane interface. The significant and repeated failure of CWEs based on platinum wire with the same polymer blend indicates the lack of contact between the membrane and the platinum surface. An operating redox couple on the metal surface could act as an internal reference. It has also been observed in the past that only E^0 values change by changing the metallic conductor, while the response of the electrode maintains same. In our studies, the response of the electrode changes with the metallic conductor. This could be attributed to the polymer blend based membranes adsorbing more strongly on the copper

surface than on platinum.

Other differences between the compositions and structures of the ionophores are relatively minor in comparison. The degree of substitution along the acrylic acid backbone is apparently not critical. Poly(acrylic acid) itself also gives a reasonable electrode response, albeit with lower slope (-41 mv). This is consistent with the literature data[91]. Even though this does not clearly indicate the mechanism of ion movement through the membrane, it is reasonable to assume that the relay mechanism is predominant over the others. The effect of the spacer length between the ionophore site and the polymer backbone is more critical. A polymer with a two methylene-unit spacer between the ionophore and the backbone (**2a**), gives a mediocre CWE when compared to the eleven methylene spacer (**5b**).

This observation is in turn explained by the increased mobility of the ionophore in a hydrophobic medium with increase in the spacer length. As predicted, the benzo-2.2.2 cryptand derivative (**6a**) is also an active ionophore in CWEs but not in ISEs.

Table *4* Effects of the spacer length on electrode response[$]

Derivatised Ionophore	Spacer Length	Electrode	Slope mv/decade	Detection Limit[‡]
2a	n=2	CWE	-23.3	4.4
		ISE	-10.4	4.9
5b	n=11	CWE	-57.6	4.6
		ISE	-12.0	4.8
6a	n=11	CWE	-56.8	4.5
		ISE	---	---

$ Membranes prepared from PVC:ionophore:plasticizer 25:10:65 wt% and tested against 10^{-5} - 5 x 10^{-2} M KCl solutions.
‡ Detection limit expressed as -log a_{K+}; lower limit of linear response.
--- No response

The effect of plasticizer on electrode response is given in table (*5*). The ester plasticizers, dioctyl phthalate and dioctyl adipate are comparable with that of the *ortho*-nitrophenyl octyl ether. In both cases the effects were insignificant and random. This could be attributed to the nature of the polymer blend. Since water intake of an ionic polymer like polyacrylamide is much higher than that of PVC, the dielectric constant of the plasticizer has little effect on membrane response. This too, is a general result for polymer blend CWEs.

Table 5 The effect of plasticizer, % loading and KTPB additive concentration on electrode response[$]

Plasticizer	% loading of the Ionophore on the polymer*	Wt% of KTPB	Slope (mv/decade)
DOP	14	0.0	-49.4
NPOE	14	7.4	-52.6
DOP	20	0.0	-61.7
DOP	20	7.2	-32.6
DOA	20	0.0	-38.3
DOA	20	6.8	-50.2
NPOE	20	0.0	-48.1
DOP	70	0.0	-34.9
NPOE	70	7.4	-45.8

$ Membranes prepared from PVC:ionophore:plasticizer 25:10:65 wt% and tested against 10^{-5} - 5 x 10^{-2} M KCl solutions.
* Calculated based on the acid chloride content of the polymer and the amount of aminocrown used for immobilization
Abbreviations: DOP, dioctyl phthalate; DOA, dioctyl adipate; NPOE, ortho-nitrophenyl octyl ether; KTPB, potassium tetraphenylborate.

The addition of potassium tetraphenylborate also affects the electrode performance; poor slope with DOP as plasticizer but enhanced in the case of DOA and NPOE as plasticizer. This can also be attributed to the hydrophillic polymeric blend. Water mobility inside the membrane could be high. The addition of potassium tetraphenylborate does not increase the hydrophilicity significantly to match the changes in dielectric constants of the plasticizer and the nature of the blend itself.

The amount of polymer ionophore added makes relatively little difference on electrode response. The same is the case with the amount of crown ether on the polymer back bone with 20% and 90% giving better response to the other two. These results are too random to comment on in detail but likely follow the general trend of steric crowding or cluster formation for the alignment of ionophores to have an ion hopping mechanism. The 20% immobilisation is the optimum loading to give a reasonable response. The 90% immobilization takes to a saturation of the number of ionophores inside the polyamide, but is too large an investment of ionophore to get a responsive electrode.

Potentiometric selectivity constants for various interfering ions were determined by the fixed interference method. Table *6* reports the results for **5b** in CWEs containing different plasticizers. Literature results for benzo-18-crown-6 as a mobile carrier in an ISE and as a complexing agent in methanol solution are given for comparison. Polymer blend electrodes from **5b** show strong discrimination between mono- and divalent ions, with poorer discrimination between different monovalent ions. The plasticizer influences the detailed selectivity patterns; greater selectivity is achieved with ortho-nitrophenyl octyl ether than with dioctyl phthalate or dioctyl adipate. Similar results have been noted previously, and is probably related to the influence of solvent on ion extraction to the membrane phase.[68]

The monovalent/divalent selectivity of polymer blend electrodes is much

more pronounced than in ISE's[68] or in solution.[92] The two series of like charge, Ca^{2+}, Sr^{2+}, Ba^{2+}, Pb^{2+} and Li^{+}, Cs^{+}, Na^{+} both have similar trends to decreasing selectivity in solution and in CWEs from (**5b**). The ion binding site is apparently controlling the selectivity, but the polymer blend matrix and the plasticizer enforces a monovalent cation selectivity. This indicates that the crown ether sites act in isolation within the matrix. Were there cooperative interactions between crown ethers, low K^{+}/Cs^{+} selectivities typical of bis (benzo-18-crown-6) derivatives would be expected[93].

Table *6* Comparison of potentiometric selectivity of CWEs prepared from immobilised polymer 5b for various plasticizers ($\log K_{K+,i}^{pot}$)‡.

Metal Ion	Plasticizer				
	DOP	DOA	NPOE	ISE*,[68]	Sol'n.[92,] c
Na^{+}	-0.45	-0.68	-1.1	-0.58	-1.08
Cs^{+}	-0.22	-0.55	-0.98	0.91	-0.91
Li^{+}	-1.5	-2.0	-0.68	-0.35	
Mg^{+}	-3.4	-5.2	-5.3	-1.2	
Ca^{2+}	-3.8	-5.5	-4.3	0.21	-2.6
Sr^{2+}	-3.3	-4.9	-4.2	0.60	-0.18
Ba^{2+}	-2.9	-4.8	-3.9	1.7	0.18
Pb^{2+}	-1.7	-2.3	1.6	2.3	0.21
Zn^{2+}	-3.8	-5.1	-4.7	4.5	
Cd^{2+}	-3.6	-5.0	-4.3	4.1	
La^{3+}	-4.7	-7.9	-6.1	6.6	

see footnotes on the next page

$ Membranes prepared from PVC:ionophore:plasticizer 25:10:65 wt% and tested against 10^{-5} - 5 x 10^{-2} M KCl solutions.
* Data for an ISE containing PVC, benzo-18-crown-6 and NPOE, ref.
c Solution selectivity = log K_{ion} - log K_{K+}

The useful lifetimes of the electrodes were investigated. ISEs formed from 5 as a mobile carrier have short lifetimes. The ionophore is freely soluble in water and presumably can be leached to aqueous solutions relatively rapidly. CWEs formed from **5b** with DOP as plasticizer are much more stable. CWEs were stored in 0.1M KCl, in 3M HCl or in running tap water, and were periodically monitored for slope and detection limit. After 95 days, the electrodes stored in HCl and in running water behaved as they had on the first day. The electrode stored in KCl was completely inactive, presumably because the membrane was saturated with potassium ions. The immobilized cryptand **6a** contains 3° amine sites which are protonated by neutral and acidic solutions. This limits both the useful pH range of the electrode and its lifetime. The potential for highly selective potassium electrodes based on this ionophore was not realized.

2.4 Conclusion

Polymer immobilized ionophores can be fabricated into ion-selective CWEs that preserve and enhance the inherent selectivities of the ion-binding unit. The Friedel-Crafts acylation reaction is a general method to provide a

linkage between a polymer backbone and a synthetic ionophore containing an activated aromatic ring. A large number of interesting and selective ligands fulfil this requirement (calixarenes, cyclophanes, spherands) and are potential candidates for fabrication of sensors. Conventional ISEs from the same materials are possible, with lifetimes dependent upon the characteristics of the ionophore. What is apparently impossible is the fabrication of polymer blend ISEs using the methods developed here.

The work of Bachas[57] demonstrates that immobilization of the ionophore in carboxy-PVC and fabrication of an electrode without blending a second polymer is feasible. Apparently there is no inherent problem with the immobilization step. The major disadvantage is the lack of flexibility in % loading of the ionophore and the availability of the remote functional group (-COOH,1.8 Wt%) on the PVC back bone. In this study both of these drawbacks have been taken into consideration to produce new polymeric blend membrane electrodes. This technology, beside its drawbacks has merit in cases where the % loading of the ionophore is significant or in immobilisation of sterically bulky ionophores like enzymes. This could also extend to the design of new applications in immobilization of electrophilic ionophores.

Our differences with the Bachas results, and our inability to form ISEs from immobilized ionophores must stem from the nature of the blends produced. Both CWEs and ISEs are cast from the same solutions, but the CWE process is quicker and involves thin layers of membrane to build up in

successive steps of 1-2 minutes duration. The ISE casting process gives a single layer membrane over a period of 12-24 hours. A likely possibility is fractionation of the polymer blend during solvent removal. We do not detect two phases in the samples but these need not be very large in order to completely disrupt ion mobility within the polymer matrix. The casting of CWEs might produce a metastable blend in which ion mobility extends over larger distances than in the membranes produced under equilibrium conditions of slow evaporation. The results, even though somewhat unexpected, are interesting and may provide an insight into the mechanistic difference between the dynamics of ISEs and CWEs. This area has never been studied in detail and this comparative study of two sensors from the same ionophore is first of the kind and opens up a new area of research.

2.5 Experimental

General Details:

Instruments and procedures are described in section 4.5. All plasticizers used were the best commercial grades available and were not purified further except for drying. Carboxyl substituted PVC (PVC-CO_2H; 1.8% CO_2H) was used as received from Aldrich. Acrylyl chloride was obtained from Aldrich and freshly distilled before use. All solvents were freshly distilled and dried prior to their use. Benzo-18-crown-6 was synthesised by using the known procedure[94] and benzo-2.2.2-cryptand was bought from Aldrich.

4'-(3-aminopropanoyl)benzo-18-crown-6 (2)

A homogenous slurry was made by mixing benzo-18-crown-6[94] (5.02 g, 16 mmol), polyphosphoric acid (35 g, excess) and 3-aminopropanoic acid (7.73 g, 87 mmol, excess) was added while stirring with a mechanical stirrer at 80° C. The stirring was continued for six hours and quenched with water (50 ml). The mixture was allowed to cool and sodium hydroxide pellets were added to give pH 14. The solution was then diluted with water (50 ml) and extracted with dichloromethane (2 x 250 ml). The aqueous extract was then subjected to a continuous extraction with dichloromethane overnight. All chlorocarbon extracts were collected, dried over sodium sulphate and evaporated to dryness

to give a pale yellow solid. The solid was then taken in a dialysis membrane and subjected to dialysis with water at pH 7 to remove the traces of the 3-aminopropanoic acid. The compound was characterised as 4'-(3-aminopropanoyl)-benzo-18-crown-6 by ^{1}H, ^{13}C nmr spectra(see table 7) and its molecular ion peak at m/z 384 $(M+1)^{+}$, pale yellow oil, Yield 3.6 g (60%).

Preparation of 4'-(12-aminododecanoyl)benzo-18-crown-6 (5)

Benzo-18-crown-6 (5.0 g,16 mmol), polyphosphoric acid (35 g, excess) and 3-aminododecanoic acid (3.5 g, 16 mmol) were mixed and stirred to make a homogenous slurry with a mechanical stirrer at 80° C. The stirring was continued for six hours and quenched with water (50 ml). The mixture was allowed to cool and sodium hydroxide pellets were added to give pH 14. The solution was then diluted with water (50 ml) and extracted with dichloromethane (2 x 250 mls). The aqueous extract was then subjected to a continuous extraction with dichloromethane overnight. All chlorocarbon extracts were collected dried over sodium sulphate and evaporated to dryness to give a pale yellow solid and characterised as 4'-(12-aminododecanoyl)benzo-18-crown-6 by ^{1}H, ^{13}C nmr spectra (see table 7) and its molecular ion peak at m/z 510 $(M+1)^{+}$, m.p (65° C), Yield 7.2 g (88%).

4'-(12-aminododecanoyl)benzo-2.2.2-cryptand (6)

Benzo-2.2.2 cryptand (150 mg, 0.3 mmol), polyphosphoric acid (PPA, 15

g) and 11-aminododecanoic acid (200 mg, 0.928 mmol) were added together and stirred vigorously to give a homogenous slurry. The stirring was continued for six hours at 80° C and quenched with water (20 ml). The mixture was allowed to cool and sodium hydroxide solution (25 ml) was added to get pH 14. The solution was then extracted with dichloromethane (2 x 250 ml). The aqueous extract was then subjected to continuous extraction with dichloromethane overnight. All chlorocarbon extracts were collected, dried over sodium sulphate and evaporated to dryness to give a pale yellow solid which was characterised as 4'-(12-aminododecanoyl)benzo-2.2.2 cryptand by ^{1}H nmr, ^{13}C nmr spectra (see table 7) and its molecular ion peak at m/z 622 $(M+1)^{+}$, m.p. oil,
Yield 0.15 g (80%).

Attempted synthesis of 4'-(4-aminobutyroyl)-benzo-18-crown-6 (3)

A homogenous slurry was made by mixing benzo-18-crown-6 (1.52 g, 4 mmol) and polyphosphoric acid (30 g, excess) and 4-aminobutyric acid (602 mg, 6 mmols) was added while stirring with a mechanical stirrer at 80° C. The stirring was continued for six hours and quenched with water (40 ml). The mixture was allowed to cool and sodium hydroxide pellets were added to give a pH 14. The solution was then diluted with water (50 ml) and extracted with dichloromethane (2 x 250 ml). The aqueous extract was then subjected to a continuous extraction with dichloromethane overnight. All chlorocarbon extracts were collected dried over sodium sulphate and evaporated to dryness

to give a pale yellow solid and characterised as cyclic imine **3** by ^{1}H, ^{13}C nmr spectra (see table 7) and its molecular ion peak at m/z 380 $(M+1)^{+}$, Yield 1.7g (88%).

Attempted synthesis of 4'-(5-aminopentanoyl)-benzo-18-crown-6 (4)

The procedure described above for **3** was followed: Benzo-18-crown-6 (1.5 g, 5 mmol), 5-Aminopentanoic acid (5-aminovaleric acid) (1.2 g, 10 mmol), and polyphosphoric acid (30 g). The compound was characterised by it's ^{1}H and ^{13}C nmr spectra (see table 7). Yield 1.7g (90%) molecular ion m/z 394 $(M+1)^{+}$.

Synthesis of Poly(acrylyl chloride)

Freshly distilled acrylyl chloride (36.5 g) was dissolved in dry benzene and was purged with nitrogen for 30 minutes. A few crystals of AIBN (< 100 mg) was added to this solution, the solution was heated at reflux overnight and cooled to give a yellow oily bottom layer and a clear top layer which were separated. The yellow oil was dissolved in dry dichloromethane (freshly distilled over phosphorous pentoxide) which was then evaporated to give a white foamy solid. The solid was washed with dry ether (2 x 100 ml) and dried on a vacuum pump for 24 hours. IR (thin film, cm^{-1}): 3500 (w, acidic OH stretch) 2890-3000 (s, C-H stretch.), 1810-1790 (vs, C=O stretching), 1440 (vs, CH deformation). The amount of acid was 10 mmol per gram of the polymer

from base titration. The chloride content of the poly (acrylyl chloride) (11.43 mmol per gram) was determined by titrating an aqueous solution of the polymer with standard silver nitrate. The molecular weight was determined by viscosity measurements on the methyl ester of the polymer. The molecular weight was 15,000-17,000 g/mol. Yield 28 g.

Synthesis of the acid chloride of carboxylated polyvinyl chloride

Carboxylated polyvinyl chloride (10 g, 1.8% -COOH) dissolved in 100 ml of THF was stirred at reflux with 25 ml of thionyl chloride overnight. The excess thionyl chloride and THF were removed at reduced pressure and dry benzene was added. The solvent was then removed at reduced pressure and the benzene washing/evaporation cycle (2 x 50 ml) was repeated to remove traces of $SOCl_2$. The white solid was then dried at high vacuum. The acid content was determined as 0.8 meq/g corresponding to 0.4 meq/g COCl by titration of a THF solution of the polymer with a standard base. IR (thin film, cm^{-1}): 2980-2840 (s, C-H stretch), 1800-1750 (s, COCl) plus residual CO_2H at 1720 (w). Complete conversion of acid to acid chloride on PVC was never achieved in repeated trials.

Immobilisation of 4'-(3-aminopropanoyl)benzo-18-crown-6 on poly(acrylyl chloride) (2a)

Poly(acryloyl chloride) (1g, 10.4 meq COCl) was dissolved in 10 ml of

dry THF. Triethylamine (2 ml) was added followed by the amino ionophore 4'-(3-amino propanoyl)benzo-18-crown-6 (3 g, excess). The mixture was stirred at 50 °C for 16 hr., poured into ether:pentane 1:1, and the fibrous precipitate was collected by filtration, washed with methanol to remove the excess of amino-crown ether and dried. The product polymer was insoluble in THF. The polymer showed IR absorptions (thin film, cm^{-1}) at 3550-3300 (b, acid OH stretch), 2980-2880 (s, CH stretch), 1750-1700 (s, acid C=O stretch), 1660, 1585 (vs, amide C=O stretch, I and II), 1110 (s, C-O-C stretch). N_2 analysis expected 2.8% observed 2.64%.

Immobilisation of 4'-(12-aminododecanoyl)benzo-18-crown-6 (5a-d)

Poly(acrylyl chloride) (1.0 g, 10.4 meq COCl) was dissolved in 10 ml of dry THF. Triethylamine (2 ml) was added followed by the amino ionophore 4'-(12-aminododecanoyl)benzo-18-crown-6 (amount varied according to the required % loading on the polymer back bone). The mixture was stirred at 50 °C for 16 hr., poured into ether:pentane 1:1, and the fibrous precipitate was collected by filtration, washed with methanol to remove the excess of amino crown ether and dried. IR: (thin film, cm^{-1}) 3600-3200 (b, acid OH stretch), 2960-2840 (s, CH stretch), 1700 (s, acid C=O stretch), 1655, 1580 (vs, amid C=O stretch, I and II), 1100 (s, C-O-C stretch). The N_2 analysis : **5a** expected 2.2%, observed 2.2%; **5b** expected 2.3%, observed 2.34%; **5c** expected 3.0%,

observed 3.12%; **5d** expected 3.6% observed 3.92%.

Immobilisation of 4'-(12-aminododecanoyl)benzo-2.2.2-cryptand (6a)

Poly(acrylyl chloride) (1.0 g, 10.4 meq COCl) was dissolved in 10 ml of dry THF. Triethylamine (2 ml) was added followed by the amino ionophore 4'-(12-aminododecanoyl)benzo-2.2.2-cryptand (61 mg, 20% loading)). The mixture was stirred at 50 °C for 16 hr., poured into ether:pentane 1:1, and the fibrous precipitate was collected by filtration, washed with methanol to remove the excess of amino cryptand and dried. The immobilised polymer was soluble in THF. IR: (thin film, cm^{-1}) 3650-3200 (b, acid OH stretch), 2980-2820 (s, CH stretch), 1725 (b, acid C=O stretch), 1665, 1580 (vs, amid C=O stretch, I and II), 1450, 1250, 1100 (s, C-O-C stretch).

Electrode preparation

Ion-selective electrodes:

Due to the low percentage loading of ionophore on polyvinyl chloride, electrodes were not made of any of the PVC immobilised polymers. A polymer blend containing 10 wt% ionophore immobilised polymer (**2a**, **5a-d**, **6a**) and 25 wt% high molecular weight PVC (B.F. Goodrich, Canada) and 65 wt% plasticizer (DOA, DOP, NPOE) was prepared by dissolving the components in THF. Membranes were cast on a glass plate by slow evaporation of the THF solution held in a glass ring of 24 mm diameter. Disks (6.5 mm dia.) were cut

out of this master membrane and mounted in a Phillips type IS561 electrode body with 0.1 M KCl as internal fill solution. All electrodes were soaked in 0.01 ml of KCl for 24 hr. before first use.

Coated-wire electrodes:

Copper wire was used as a conductor in all CWE construction. The tip of the wire was cleaned with emery paper to remove the oxide film over the surface and washed with acetone and dried in an air stream. Polymer blend membranes were dip cast on copper wire tip to make a uniform bead (to the naked eye) from a THF solution of the composition described above. After each dip, solvent was evaporated in a stream of air for 1 min. between dipping cycles and the dipping process was continued until the electrode tip was completely encased in a translucent bead 0.6-1.0 mm in dia. The consistency of thickness of the bead was controlled by holding the composition of the solution and the number of dip drying constant. The remaining exposed copper surface above the bead was encased in Parafilm. Electrodes were soaked in 0.01 M KCl for 24 hr. before first use.

Potential measurements

All electrode potentials were measured vs. a double junction standard calomel reference electrode containing 0.1 M tetramethylammonium chloride as the external junction electrolyte. The cell for the ion-selective electrode was:

calomel | 4 M KCl | 0.1 M Me_4NCl | sample solution | membrane | 0.1 M KCl | Ag-AgCl. The cell for the coated-wire electrode was: calomel | 4 M KCl | 0.1 M Me_4NCl | sample solution | membrane | Cu. Survey work was done using separate solutions. Detailed examination of electrodes used the automatic titration system and the procedures previously described.[95]

Detailed analysis of electrodes was done with an automatic titrimeter (Metrohm E536) and automatic burette (Metrohm Dosimat 655) controlled by a microcomputer (Hewlett-Packard HP85). The titrant was added to an initial volume of distilled water (10 ml) in a thermostated cell (25.0 ± 0.2 °C) with efficient stirring. The activity of the measured ion in the solution was calculated and stored along with the cell potential and the time required to achieve an equilibrium potential. Slope and detection limit were calculated on operator specified portions of the calibration curves. Potentiometric selectivity constants were calculated by the method of fixed interference, typically at 10^{-3} M in interfering ion. The reproducibility of the measurement were tested by repeated titrations and the values were computed by using a microcomputer HP85. A graph of log a_{K^+} vs the pH meter readings in mV was generated and slope and detection limits were calculated from the graph. The detection limit was calculated by taking the intercept of the extrapolated lines.

Table 7 ^{1}H and ^{13}C nmr data for compounds prepared[a]

Compound	nmr	Ar-ring	Ether ring	C=O	C=N	CH_2-CO	CH_2-NH_2	-CH_2-CH_2-
2	^{1}H	7.4(d,1H),7.3(s,1H), 6.7(d,1H)	4.6-3(m,22H)	---	---	---	---	2.6(t,4H)
	^{13}C	148.6,130.3,122.9, 112.6,111.9	77.2, 70.6-68.8(8peaks)	198.0	---	38.1	44.8	
3	^{1}H	7.5(s,1H),7.2(d,1H) 6.8(d,1H)	4.2-3.6(m,20H)	---	---	---	2.9(t,2H)	1.9(m,4H)
	^{13}C	150.8,146.6,127.2 121.6,112.3,111.8	77.1, 70.5-70.8(6peaks), 69.4,69.3,68.8,68.7	---	172.4	34.7	61.2	22.7
4	^{1}H	7.4(s,1H),7.2(d,1H) 6.8(d,1H)	4.2-3.6(m,20H)	---	---	1.7(m,2H)	2.5(t,2H)	1.6(m,2H)
	^{13}C	150.3,148.4,133.0, 119.3,111.0	70.4-70.7(6peaks), 69.4,69.3,68.7,68.6	---	165.0	26.7	49.4	21.7,19.6
5	^{1}H	7.5(d,1H),7.4(s,1H) 6.8(d,1H)	4.2-3.6(m,20H)	---	---	2.6(t,2H)	2.8(t,2H)	1.7-1.2 (m,18H)
	^{13}C	152.8,148.4,130.4, 122.8,112.4,111.6	70.8-70.3(6peaks), 69.3,69.2,68.8,68.7	199.2	---	38.0	41.9	33.0,29.4-29.4(5peaks), 26.7,24.6
6	^{1}H	7.6(d,1H),7.5(s,1H) 6.9(d,1H)	4.2-4.1(m,4H), 3.5-2.6(m,30H)	---	---	2.1(t,2H)		1.5-1.2 (m,18H)
	^{13}C	153.4,148.7,130.5, 123.0,114.1,112.9	77.2,70.7,70.6,69.8, 68.3,68.2,67.8,56,0, 55.9,55.2,55.0,54.9	199.3	---	38.2	41.9	33.2,29.5-29.4(3peaks), 26.9,24.7

a In $CDCl_3$ versus TMS or D_2O versus ext. TMS
--- Inappropriate

CHAPTER 3

Non Isothermal Membrane Transport

3.1 Introduction

A membrane is defined by its function irrespective of its composition. As is generally understood, it can be defined as a distinct phase separating two liquid phases and allowing particles and ions to pass through depending upon the trans-membrane gradients (concentration, pressure, temperature etc.) applied to the system. Membranes may vary by source (nature, synthetic laboratory) and by function (life processes, separations and sensor applications). There are a large number of reviews available on the role of membranes in industrial and biological applications from a number of different perspectives.[96-102]

This section focuses on the properties of polymer based membranes and their potential applications toward academic and industrial separation problems. The study of synthetic polymer membranes was started in 1846, followed by the work of pioneers in the field of membrane processes.[103-109] However, the golden age of membranology started only in 1960, initiated by Loeb and Sourirajan[110] and their ingenious discovery of a hyperfiltration membrane based on cellulose acetate. This golden age continues today in

terms of developing new membrane materials, new fabrication methods and above all the exploration of the membrane application studies. A brief history of this period and the significant developments were given by R.E. Kesting in 1985.[111]

Polymer membranes can be classified according to their nature or their mode of preparation. Another common way to classify membranes is based on the use of the membrane.[112] There are three major sections: i) membranes with good physical, chemical and electrical properties for fundamental ion transport studies; ii) membranes which can mimic natural membranes, and; iii) simple or composite membranes for specific applications. Membranes belonging to the first category are further divided into homogenous and heterogenous membranes. The heterogenous membranes can be further divided as non-reinforced membranes, reinforced membranes, chemically treated membranes, mechanically treated and formed polymers, and membranes from photochemical methods. The membranes which mimic natural membranes are generally made from fatty acids, phospholipids, and modified fatty acids, whereas, the speciality membranes are prepared from cationic and anionic exchange materials to give diverse electrical properties. These polymers can be further subdivided into three categories: a) concentration of cationic and anionic sites optimised to give an amphoteric membranes; b) membranes with distinct cationic and anionic sites, and; c) membranes with cationic and anionic polymer layers (step-junction bipolar

membranes).[113]

The suitability of the membrane for a particular process is decided by the mechanism of separation, mechanical, and chemical stability of the membrane, and the compatibility of the membrane with the contacting solutions. Membrane separation processes are based on three different mechanisms: i) a sieve effect where the separation is based on the size of the permeants (all filtration processes); ii) an electrochemical effect where charge of the permeant plays an important role in separation (electrodialysis); and iii) a solubility effect where the solubility of the permeant in the membrane phase dictates the flux (eg. reverse osmosis, pervaporation and other concentration gradient driven processes).[114] Thermosmosis, membrane distillation and pervaporation are temperature dependent processes, or in other words non-isothermal membrane processes, which are the central issue in this section.

The transport across a membrane can be considered active or passive depending upon the direction of flux. If the flux is against a gradient then it is defined as active, and if it is along the gradient it is passive.[115,116] In nature, active transport is always coupled to another process inside the cell. The transport is often activated by a transporter inside the membrane.[117] This is called facilitated transport. The facilitated transport can be further classified as symport or antiport[61].

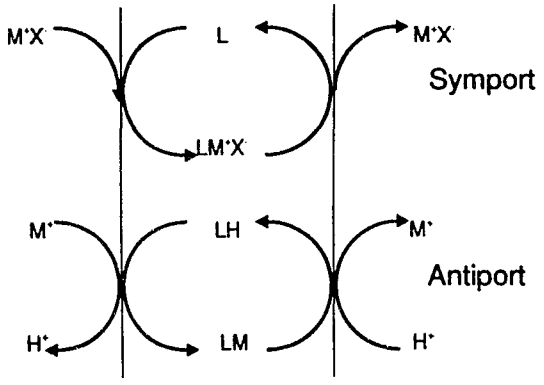

Figure *8* Cartoon of symport and antiport mechanisms

Symport implies transport of an ion with its counter ion from the same side of the membrane, whereas the antiport involves the transport of one species driven by counter transport of another species from the opposite side of the membrane. N. Ogata and co-workers[77] have examined a fixed site polymer membrane to achieve an anion proton pump driven by a pH gradient. By incorporation of ionophores having ionisable groups into a polymeric membrane, a cation-proton counter transport membrane system is designed to establish selective transport of cations under a pH gradient.[84,119-121]

T. Uragami *et al*[122] explained an active transport of metal ions driven by a pH gradient through a special polymeric membrane fabricated from

poly(isobutylene-alternat-co-maleic anhydride) and poly(vinyl alcohol), using the terms chemical and physical active transport.[122] In chemical active transport, the dissociation of the carboxylate on the basic side extracts metal ions from solution. When protons neutralise the carboxylate so formed, metal ions are released and transferred to the acidic side under an electric potential gradient. Physical active transport involves the swelling of the polymer on the basic side of the membrane due to the intake of M^+ and OH^-, and the subsequent contraction due to neutralisation of the carboxylate by the diffusing proton from acidic side to the basic side. Here the released metal ions and hydroxyl ions inside the polymeric membrane, being in a "wilful" state can migrate to either side of the membrane.[122]

In the absence of any other external stimuli like magnetic and gravitational factors, the driving forces which are responsible for a flux through a membrane separating two solutions involve: i) a difference in chemical potential; ii) a difference in electrical potential; iii) a difference of pressure; and iv) a difference in temperature. The table below summarises the relationship of flux to driving force.

Table *8* Definition of membrane processes

	ΔP	$\Delta\mu$	ΔE	ΔT
Solvent flux	Permeation	Osmosis	Electro-osmosis	Thermo-osmosis
Solute flux	Filtration	Dialysis	Electro-dialysis	Thermo-dialysis

Permeation is the process of movement of *solvent* due to a pressure gradient through a polymeric membrane by sorption and diffusion. If selectivity is shown by the membrane as different rates of solvent transport the membrane can be used as a semipermeable membrane. Permeation through a membrane involves three consecutive steps: dissolution of molecules on one side of the membrane, diffusion of the molecules through the membrane, and the desorption on the other side of the membrane. Focusing on solute movement, filtration is defined as separation or rejection of *solutes* by a membrane under a pressure gradient.

Dialysis is the diffusion of solute molecule from the concentrated side to a dilute solution side driven by the chemical potential difference (concentration difference). If a solvent molecule diffuses across the membrane then that process is known as osmosis. Dialysis and osmosis occur simultaneously but in opposite directions.

Electroosmosis and electrodialysis involve the transfer of solvent and solute respectively under an electric potential gradient through a membrane. The same relationship applies for thermoosmosis and thermodialysis for transfer of solvent and solute under a temperature gradient.

Electrophoresis is defined as a molecular diffusion of solute under an electric voltage gradient. This process does not necessarily involve a membrane but can occur in a single medium. Thermophoresis refers to the related solute diffusion under a temperature gradient in a single phase.

Thermoosmosis involves a transmembrane solute flux, generally from a hot side to a cold side under a temperature gradient.[123] The related process of membrane distillation involves the same translocation of solvent (solvent flux) through a porous hydrophobic membrane. In order to effectively carry out membrane distillation a gaseous phase must be immobilised inside the porous membrane.[124] This requires the pressure on either side of the membrane to be less than the capillary force in the pores. The temperature gradient establishes a vapour pressure gradient within the gaseous phase entrapped inside the pores. Solvent vapour diffuses through the gaseous phase from the high vapour pressure side to the low vapour pressure side when condensation occurs. The crucial property of the membrane to be active in membrane distillation is non-wettability (ability to hold the gaseous membrane), and pore size of the membrane.[124] Selectivity arises from the difference in partial pressures of the components on the hot side of the cell.

Pervaporation is another non-isothermal process which also involves a concentration gradient. A dense hydrophobic membrane separates a solution phase from a vacuum or condensing phase. The partial pressure of the solvent vapour is low on the condensing phase to drive the process. In order to increase the rate of transport or condensation, a vacuum or sweeping gas is employed to strip the vapours away from the membrane and condense the transported solvent in a receiver placed outside of the cell. The flux mainly depends on the vapour pressure gradient and on the nature of the membrane.

Solvent is absorbed by the membrane and diffuses within the bulk membrane phase. Selectivity arises from differential partition to the membrane and differential mobility within the membrane.[125]

Membrane transport of metal ions has been a subject of investigation during the last several years.[126-128] The exponential growth of supramolecular chemistry has produced a series of macrocycles which can selectively extract and transport a single species from an aqueous medium to another through a lipophilic medium. The stability and the selectivity of macrocycles (or host molecules) can be exploited to design specific membrane processes for different disciplines such as analytical chemistry (membrane based sensors),[37,39] bio-mimetic chemistry (ion transport)[29], and industrial application (desalination, gas separations and purifications, metal recovery).[124,125]

The membranes containing ionophores have been shown to transport and separate ions.[116,119,120] The overall efficiency and practical utility of such processes depends on the stability of the membrane. Most of the common ionophores are water soluble. Because of this property, the ionophores tend to leach out of the membrane which drastically reduces efficiency and lifetime.[44,48-50] In order to solve this problem, an ionophore immobilised polymer could be used.[44,51,52] Ionophore immobilised polymers have been used to transport ions selectively and large number of reports are available in the literature.[53-56] All studies to date have been conducted in an isothermal environment. Non-isothermal mass transfer has received a lot of attention in the case of liquid

and gas separation processes.[123]

Temperature control of complexation has been reported, but this has not yet been extended to metal ion transport driven by a temperature gradient. Warshawsky *et al*[129] successfully synthesised and characterised a copolymer of styrene-divinylbenzene containing pseudo-crowns as a part of the polymer chain, a series of polymers containing benzo-18-crown-6 and polymeric diaza-pseudocrowns. The complexation of these polymers under different temperatures (0 to 60 °C) was studied and a complete decomplexation at 60 °C was observed. The temperature regulated release of metal ions by the polymer depends on properties of the polymer, interaction of the ligand with metal ions (low binding constant) and insolubility of the polymer in the reaction medium. It is also significant to note that only crown ether complexation-decomplexation was affected by the temperature dependent mechanism. The decomplexation of metal complexes formed from ion-exchange with catechol groups on the polymer backbone was not observed.

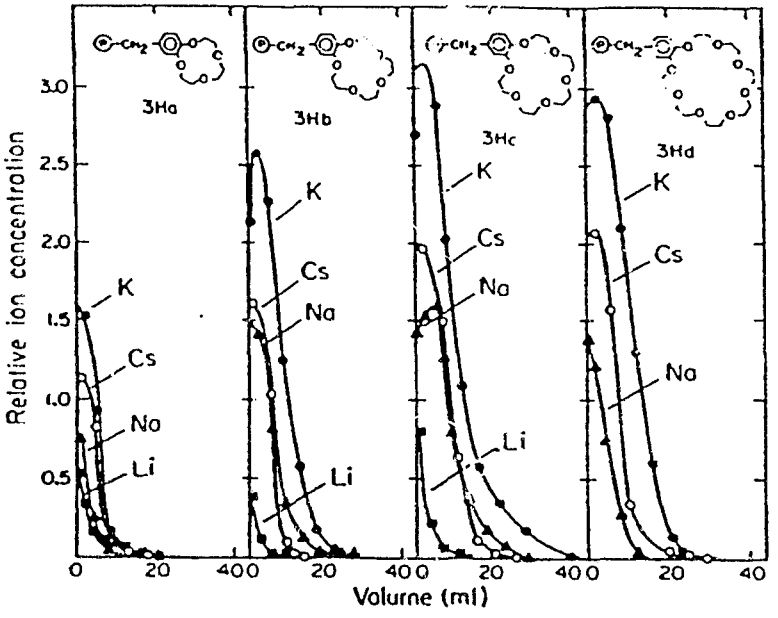

Figure *9* Temperature controlled decomplexation of crown ethers[129]

Our studies in this area originated from our interest in employing the immobilised ionophore polymers of *chapter 2* for the selective transport of alkali metal ions. Results from previous transport studies based on liquid membranes and polymeric membranes incorporating immobilised ionophores have encouraged us to look into the temperature controlled transport of alkali metals across a membrane. Based on the Warshawsky data, the crown ether immobilised on poly(acrylic acid) would be an ideal candidate to conduct the transport experiment. Crown ether immobilised poly(acrylic acid) has free carboxyl groups to increase the mobility of ion transport inside the polymeric medium, while at the same time the decomplexation of the carboxylate-metal

complex would be independent of temperature gradient. The knowledge of the stability constants of crown ethers and their temperature dependent complexation-decomplexation properties suggests that the Warshawsky's result[129] is general - complexation will be favoured on the low temperature side and disfavoured on the high temperature side of the membrane. The performance of the crown ether incorporated polymer would be based on the crown ether-metal interaction only. By changing the ionophore from a crown ether to macrocycles with higher binding constants (cryptands and cavitands), it might be possible to elute and separate alkali metal ions selectively from solution.

3.2 Results and discussion

The polymers of *chapter 2* involving benzo-18-crown-6 immobilized on poly(acrylyl chloride) provided the materials for this study (Scheme *4*, Table *1*). Since these polymers do not form self-supporting membranes, a polymer blend has to be adopted for the process. Previously Nomex membranes containing an immobilised polymer were made and used to study the transport of ions or solvent using concentration gradients.[84]

Previous studies on Nomex membrane characteristics indicated the structure of the membrane.[84,130,132] The membrane has a porous structure and by mixing with immobilised polymer the porous nature as well as the mechanical support of the membrane can be used to explore the transport properties of ionophore immobilised polymer. The membranes were made by dissolving Nomex polymer and the crown ether immobilised polyacrylamide in N,N-dimethylacetamide.[84] The solution was then spread uniformly on a glass plate with a casting thickness of 300 μm using a TLC spreader. The glass plate with the film was then left in an oven for 5 minutes at 100 °C to cure, and then immersed in cold water. The separated membrane was then left immersed in water overnight to remove traces of N,N-dimethylacetamide. When dried in air the final thickness was 30-50 μm and had a total area of 10 x 20 cm^2. A membrane with an area of 10 cm^2 was cut and mounted between the two compartments of a cell with a volume of 32 ml. The temperature gradient was created by circulating hot water through one side of the cell, and

cold water through the other. The temperature measurements were made by thermocouples inserted on each side of the cell. The cation concentration on either side was monitored by atomic absorption or emission spectroscopy. A typical sample preparation consisted of an aliquot of 5-50 µl of solution withdrawn from one compartment of the cell and diluted to 1 ml with 5% HNO_3.

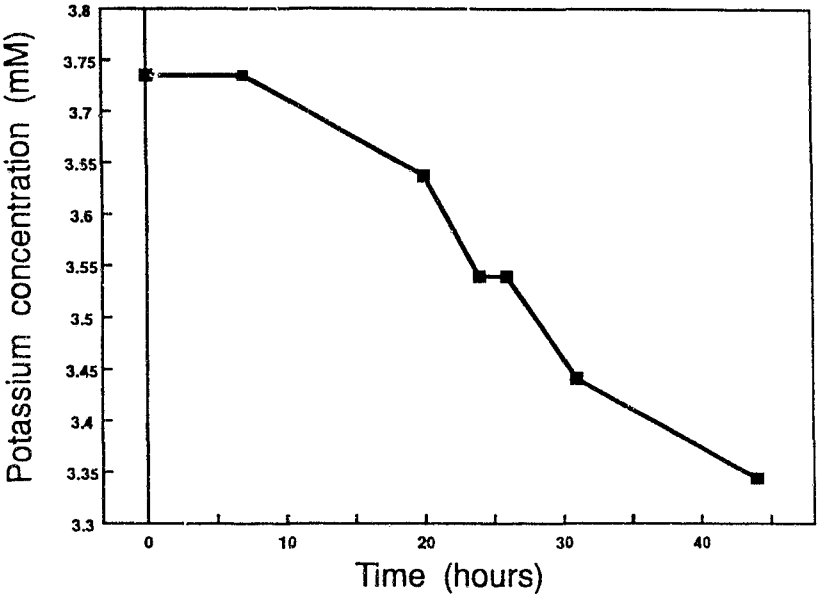

Figure *10* Potassium concentration as a function of time for the hot side of the cell with a membrane fabricated from a blend of immobilised polymer (**5b**) and NOMEX under a temperature gradient of 40 °C

The transport studies were done with $KClO_4$ (approx. $4x10^{-3}$ M) solution on both sides of the cell. The transport of salts from the hot side to the cold side was expected on the basis of the greater solvation energy at the lower temperature. A quick glance at the results shows that the transport of K^+ was from hot to cold but the process was slow. The polarity of the Nomex

membrane increases considerably by blending with crown ether immobilised polyacrylic acid. This in turn increases the water uptake of the membrane. The mobility of ionic species inside the membrane increases with increase in water content. The temperature gradient induces a chemical potential gradient across the membrane. It is then reasonable to assume that, in the absence of any significant solvent movement, the induced chemical potential gradient drives the metal ion transport from hot side to the cold side. The sluggish rate of transport across the membrane supports this hypothesis. Unfortunately the rate of transport of salt across the membrane was slow.

At about the same time, it became apparent that ISEs made out of the immobilised polymer did not give good responses. The lack of bulk transport through the polymer blend membrane prompted us to look into other options such as porous support membranes. This would be equivalent to using the porous membrane to support numerous micro-membranes of the active polymer within the pores of the support. When hydrophobic membranes like PTFE and GORTEX were used as support membranes and coated with the immobilised polymer (**5b**), the salt concentration gradients were established with experimental conditions as described above. In these early experiments the cell volumes were enclosed, so the net transfer of solvent was difficult to detect. Control experiments with the untreated commercial membrane itself showed the same amount of salt gradient production even without the immobilized polymeric coating. This phenomenon was observed only when the

support membrane had hydrophillic properties. For example, the porous cellulose membranes did not give any salt gradient even after a prolonged period.

The same experiment was repeated with a PTFE membrane, using a Triton solution in KCl on the hot side. Since Triton is a detergent it destroys the non-wettability of the hydrophobic membrane. In this experiment no significant water movement was observed. Thus, from these experiments it is likely that the process observed was membrane distillation, where the solvent vapour diffuses through the gaseous phase of the membrane from the hot side to cold side.

An extensive study on membrane distillation for desalination has been carried out and reported by other groups working in this area.[124-126] The theoretical background is also well understood.[123] In our exploration of this process, we extended the method to separation of both inorganic and organic water soluble substrates as solutes. In all cases when separation was observed the solute remained on the hot side and the water was efficiently removed from the hot side to the cold side. Azeotrope forming compounds transferred from the hot to cold side along with the water. This is consistent with the proposed gas membrane mechanism.

The experiments were done in a cell with two compartments and each compartment had a thermocouple and a graduated glass tube attached vertically to measure the volume changes inside the cell (Refer Fig. *13*). All

experiments were performed with equal volumes of solvents on each compartment on either side of the membrane. The liquid level in the sight glasses were made equal at room temperature. In all cases pure water was in the cell with a cold water jacket and the water solution of the solute of interest was in the other compartment with hot water jacket. The temperature gradient was established by circulating externally heated water and cold tap water through the corresponding sides. The contents of the compartments were stirred with magnetic stirrers and the temperature equilibrium was established in a few minutes. An initial fluctuation in the sight tube level on the hot side due to the expansion of the liquid was observed. After 5 to 10 minutes a steady state was established followed by a constant increase in the water level in the sight tube over the cold side in parallel with a steady decrease in the sight tube volume level on the hot side. The volume change on both sides of the cell was monitored in each case. Even after the removal of the temperature gradient this difference in the volume stayed as long as the membrane was hydrophobic and stable. A control experiment with pure water on each side of the cell was carried out to determine the flow rate of water from the hot to cold side. The volume change in the cold side appeared to be following a linear relationship with time. Typical examples are illustrated in Figures *11* and *12*. The former used water on both sides of the cell; the latter used 0.5 M urea on the hot side of the cell.

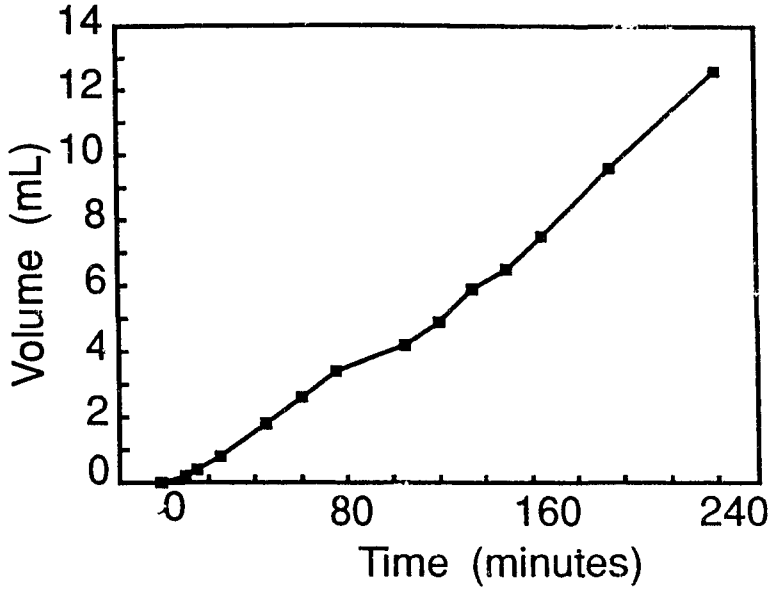

Figure *11* Volume on the cold side of the cell as function of time indicating water flux during the experiment from hot to cold using a Teflon membrane. Pure water on either side of the cell.

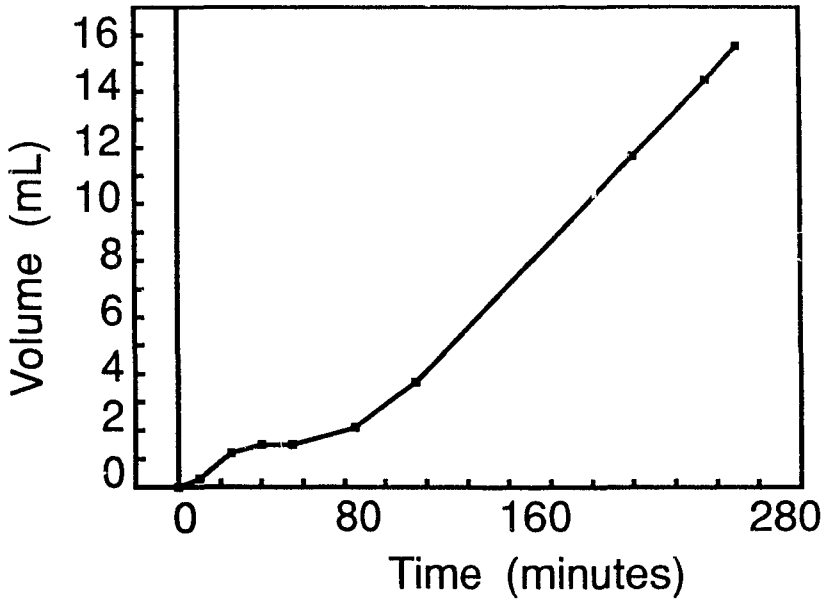

Figure *12* Volume on the cold side of the cell as a function of time indicating a water flux from hot side to cold using a Teflon membrane. Urea solution on the hot side; pure water on the cold side.

Among the inorganic compounds tested in these experiments were $CaCl_2$, NaCl, K_2SO_4 and NH_4Cl. The organic water soluble compounds separated from water included urea, sucrose, tartaric acid, and pentaethylene glycol. In none of these cases was any trace of the dissolved solute detected on the cold side of the cell.

The cases where the dissolved solutes did pass through the membrane involved water solutions of methanol, ethylene glycol, ethanol, propanol, butanol, and phenol. All of these compounds are known to form azeotropes with water. The comparison of phenol (b.p. 150 °C) and H_2O_2 (b.p. 156 °C) is instructive. It is not the boiling point that is critical, but the absence of azeotrope formation which controls the separation.

The results of these experiments can be explained by considering the gas membrane as bubbles of vapour inside the hydrophobic support membrane. When the membrane is immersed in a liquid with high vapour pressure, the vapour diffuses into this gas membrane trapped inside the pores. As the temperature of the hot side of the cell increases, the vapour pressure of the liquid on the hot side increases and more vapour diffuses into the gaseous membrane which imbalances the equilibrium distribution of vapour pressure on either side of the membrane. In order to maintain the equilibrium, vapour from hot side of the cell diffuses to the cold side and condenses. This creates a continuous driving force for convection and continues as long as the temperature gradient stays. Once the temperature gradient is removed, the

equilibrium of the vapour pressure is re-established and the flow of water (or more precisely, the convection of the water vapour) through the membrane stops. The membrane can then hold the difference in the water level. By re-introducing the temperature gradient the process can be restarted until the water, or any solvent with high vapour pressure, on the hot side is effectively pumped to the cold side of the cell.

Membrane distillation (MD) has great potential in dealing with environmental pollution, industrial waste concentration and treatment, and desalination of water. The energy required for membrane distillation is low when compar ` to the normal distillation, as the MD occurs at modest temperature. For most waste treatment problems, the industrial waste often comes with excess low level heat from the plant. Maintaining a temperature gradient suitable for MD would not involve any extra expense of energy. In the original area of thermophoresis the design and development of the membrane with enough specificity and selectivity for a particular metal ion or a single species in general requires more work. Supramolecular chemistry offers a great deal of potential in this area. The availability of a large number of macrocycles with high selectivity for a single substrate warrants a detailed investigation in this promising area. The only disadvantage of this process is the energy consumption to provide a temperature gradient across the membrane.

3.3 Experimental

Fabrication of Membranes

Membranes for thermophoresis/thermodialysis were prepared as a blend of Nomex (polyaramid) and the ionophore immobilised polyacrylic acid (**5b**). Nomex polymer (E.I. du Pont de Nemours & Co., Willington, DE) was used as purchased. The synthesis and characterisation of the immobilised polymer **5b** was described in the second chapter of this thesis. Solvent N,N-dimethylacetamide (DMA) was distilled before use, LiCl was used as received from Aldrich (analytical reagent grade).

Nomex (1.5 g) was dissolved in hot (80 °C) N,N-dimethylacetamide (8 ml) containing LiCl (200 mg) to increase the solubility. The crown ether immobilised polymer **5b** (75 mg) was added to it. The mixture was allowed to stir for 20 minutes at a temperature of 120 °C. The clear solution so obtained was allowed to stand for 10 minutes on the bench to allow the bubbles to migrate to the surface. A film of 300 μm thickness was cast on a glass plate using a TLC plate spreader. The membrane was cured in an oven at 100 °C for 2 hours and then placed in water to induce gelation and separation of the membrane from the glass plate. The membrane peeled free from the glass plate and was allowed to soak overnight in water to remove traces of DMA. The resultant membrane had an approximate thickness of 30-50 μm and was 10 x 20 cm^2 in area. The appropriate size of the membrane for the cell was cut

out from this master membrane.

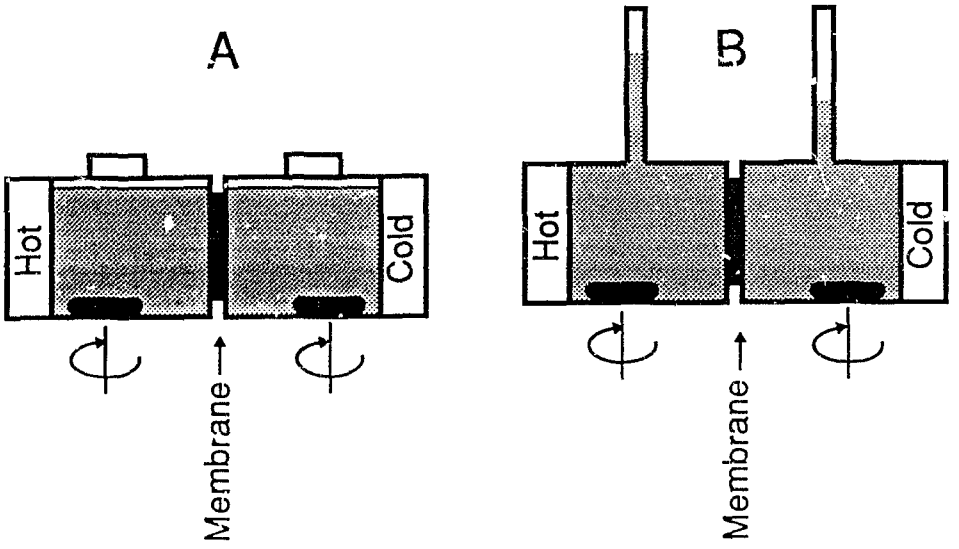

Figure *13* Sketch diagram of the cell used for thermodialysis (A) and membrane distillation (B).

Thermodialysis experiment

The thermodialysis studies were carried out in the cell illustrated in Figure *13A*. The temperature gradient was applied by circulating hot water through a heat exchange element on one side of the cell and cold water through a similar element on the other side of the cell (labelled Hot and Cold in Figure *13*). The solutions contained on either side of the cell were stirred

at a constant rate. The transport of metal ions was monitored by withdrawing samples at specific time intervals from each side and analyzing the concentration by atomic absorption spectroscopy. Aliquots of 5-50 µl of solution were diluted with 1 ml of 5% HNO_3 for analysis.

Membrane distillation experiment

For all membrane distillation experiments, a commercial polytetrafluoro-ethylene membrane of 0.5 µm thickness was used. The membrane was mounted in a cell with a sight tube to measure the volumes of the two phases contacting the membrane (Figure *13B*). The initial volume in each side of the cell was made constant. The temperature gradient was created by circulating hot and cold water through heat exchange elements on opposite sides of the cell. Typically the solute solution was on the hot side of the cell, and deionised water on the cold side. The temperature on each side was monitored by a thermocouple and samples were withdrawn at specific intervals of time. The sample analysis was done by atomic absorption spectroscopy or refractive index measurement. The samples for atomic absorption spectroscopy were prepared by diluting 5-50 µl aliquots with 5% HNO_3. For the organic solutes, the refractive index of the sample was measured using the sample withdrawn from the cell compartments without any pretreatment. The concentrations were determined from a standard curve.

CHAPTER 4

Photoionophores

4.1 Introduction.

The application of colorimetry for metal ion analysis is not a new technique and is widely used in clinical, industrial and academic laboratories.[133-135] Even so, the number of colorimetric reagents suitable for alkali and alkaline earth metal ions are few.[136] The discovery of the crown ethers by Pedersen[1] and investigation of the complexation chemistry of these metal ions stimulated research in this area. Much of the applied work is based on a demand for sodium and potassium sensitive sensors for analysis of samples of blood, urine or any body fluids of clinical interest.[137] The concentration of the metal ions in body fluids *in vivo* and *in vitro*, need to be determined accurately and rapidly.[138-141] The remote sensing of samples in an ongoing chemical reactor or inside a specific organ of a living organism or in a hazardous environment warrants highly sensitive and selective sensors.[142,143] In principle, macrocycles such as crown ethers and cryptands with a high selectivity and sensitivity for the alkali metals can be modified to develop a sensor which satisfy the requirements of any application.

Photometry deals with the measurement and recording of change in the

optical density of a medium. The principle cause of changes in optical density is due to the presence of photoactive molecules in the medium. Molecules which are photoactive as well as selective complexing agents towards specific ionic species are known as photoionophores. The complexation induces a perturbation in the ground and excited electronic states, which could, in principle, be studied by absorption or emission spectroscopy respectively. There are two main types of photoionophores: fluoroionophores in which the complexation induces change in the emission spectrum and chromoionophores in which complexation induces changes in the absorption spectrum of the photoionophore. The interest in this area was started by the synthesis of an ionophore containing chromogenic groups in 1977.[144,145] By incorporating a chromophoric group to a crown ether ring through a covalent bond, the electronic perturbations occurring in the crown ether structure due to complexation of a positively charged species could be monitored.[145] Absorption of light by the complexed species can induce several changes within the system such as charge separation by proton or electron transfer, perturbation of optical and physical properties, photoregulation of the binding properties and selective photochemical transformations.[22] The electronic perturbations affect the ground state as well as the excited state of the molecule, and can be visualised through the changes in the absorption and/or emission spectrum.[146]

Most of the photoionophores synthesised to date are based on aza-crown ethers or benzocrown ethers as the ion binding sites.[144,145,147,150] The common

chromophores used are phenols and substituted phenols.[144,145,147,151] Deprotonation of a phenolic group and complexation of the metal ion by a crown ether could occur simultaneously for these ligands. The main advantage of these mono and diprotonic chromoionophores is the large shift in the absorption maxima when they are deprotonated. Visible colour changes in the system indicate the extent of complexation and can be quantified to analyze for the added cation in a given sample. In a way, the chromophoric unit acts as a metal ion detector and the ionophore unit acts as complexation or extraction unit. However, the deprotonated phenolic groups also participate in ion binding provided the conformational requirements are met in the design of the chromoionophore.

The metal extraction properties of phenol incorporated azacrown ethers are well explored and it is recognized that the proper alignment of the phenolic group is necessary for the phenol to take part in complexation.[138,153] The flexibility of the side chain and the distance from the crown ether are the two major factors which determine the efficiency of the metal extraction.[149,153] For example: compare the C-substituted crown ether and N-substituted crown ether shown at the top of Figure *14*.

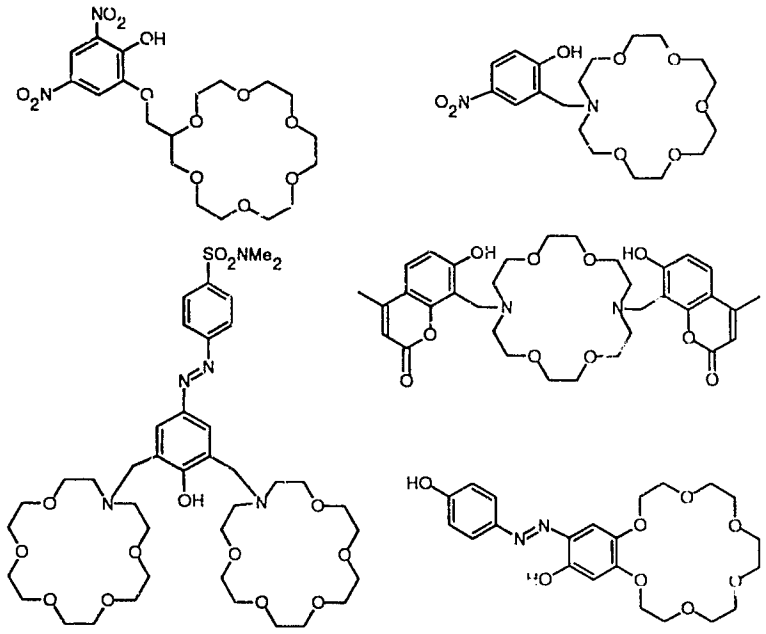

Figure *14* Examples of phenol incorporated chromoionophores

These two similar ligands showed different selectivities due to the fact that in the case of N-substituted crown ether, a stable 5 or 6 membered chelate ring of metal-phenolate co-ordination is possible, while in the C-substituted crown ether, a simple chelate is impossible. This factor is significant in case of a smaller cation.[149,153,154]

The crown ether incorporated with an azophenol group (Figure *14*, lower right) has shown a Li^+ dependent colour change in chloroform with pyridine as a base. Even though the colour change was selective to lithium ion, the other

alkali metal cations and alkaline earth metal cations caused interference in analytical measurements. Moreover, in extraction experiments, the azophenol based crown ethers have shown cation selectivity as $Ba^{2+} > Sr^{2+} > Li^{+} > Na^{+} > K^{+}$; the stoichiometry of complexation and the equilibria involved are not well resolved. The bis crown synthesised by Kitazawa *et al*[153] have shown a sodium selectivity probably due to the formation of a sandwich complex.

Aza crown ether derivatives with phenol as chromophoric units were more effective in extracting alkali metals to an organic medium when compared to the benzocrown derivatives. The reason for this was attributed to an increase in separation of chromophore from the complexed metal ion in the case of benzocrown ethers. The extraction efficiency increases with increase in the pH of the medium indicating the participation of the phenolic oxygen in complexation. The absorption spectra of these chromoionophores can show either bathochromic or hypsochromic shifts due to complexation with a metal ion.

The electronic perturbations induced by different cations through donor-acceptor type interactions often result in colour changes. The extent of colour changes follow the cation size order as illustrated by the azulene crown ethers of Figure *15*. The cation which has an optimum fit to the cavity induces the maximum shift and has the maximum complex stability. The azulene incorporated crown ether **a**, (λ_{max} = 618nm), synthesised by Vögtle and co-workers[155] (type I) showed a hypsochromic shift in the presence of Ca^{2+} (λ_{max}

=610) and Ba^{2+} (λ_{max} = 612nm), due to the direct interaction of the cations with the π-system whereas the type II molecule showed a bathochromic shift. The visible absorption band of **c** (λ_{max} = 477nm) is shifted bathochromically with salts (Ca λ_{max} = 492nm, Ba λ_{max} = 560nm).

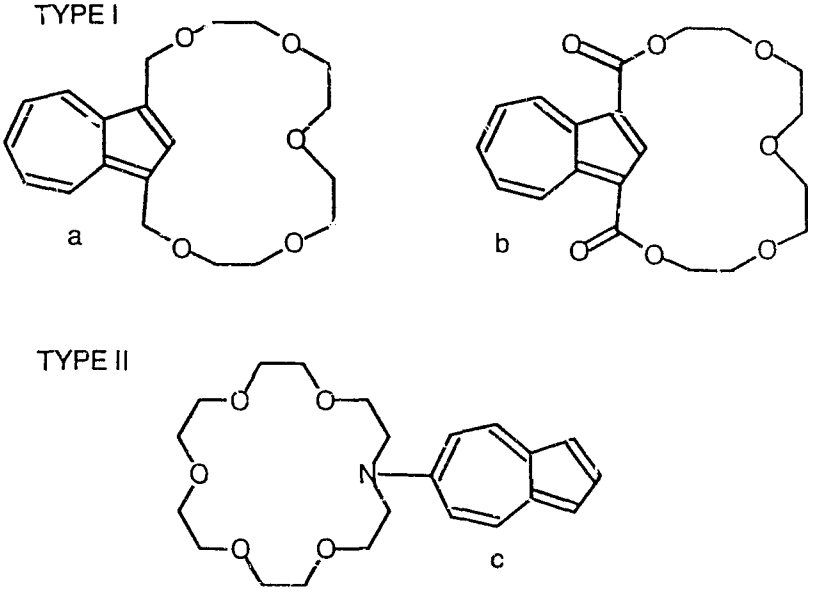

Figure *15* Azulene incorporated ionophores

The second category of photosensitive ionophores are called fluoroionophores in which the ionophore is attached to a fluorescent probe. The high sensitivity and high selectivity of fluorimetry could provide an excellent tool for analysis of alkali and alkaline earth metal ions in solution. A number of modified EDTA based fluoroionophores are available.[133,134] The interest in a derivatised macrocycle as a fluoroionophore has produced aza crown based molecules. Nishida *et al*[149] have designed and synthesised

fluoroionophores based on 4-methylumbelliferone which showed alkali metal affinity in extraction experiments. The naphthalene attached crown ethers synthesised by Sousa and Larson[156-158] demonstrated the effects of the orientations of the fluorescent group towards the complexed perturber metal ion (Figure *16*).

Exploratory fluorescence studies of the naphthalene incorporated crown ethers (Figure *16*) on the cation dependent quenching were done in alcohol glass at 77 °K. The molecules are designed in such a way that the complexed cation is held in a fixed orientation to the fluorescent groups. The results indicated that a cation held at the face of the π-system does not increase or decrease the overall perturbing effect when compared to the side or end of the naphthalene chromophore. The heavy atom effect due to spin-orbit coupling in the presence of cesium ion was higher when the cation was held near the face of the π-system rather than at the side or end.

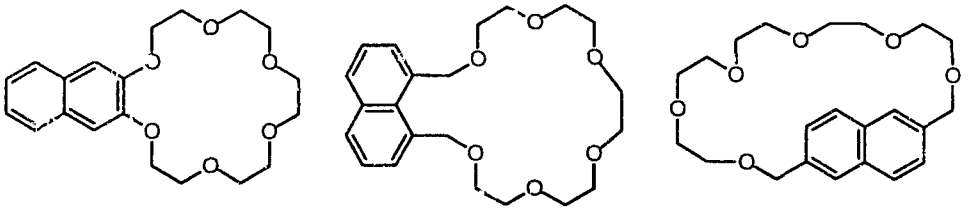

Figure *16* Naphthalene based fluoroionophores.

The recent observation by Forrest and Pacey[159] on phenol incorporated crown ethers indicated a bathochromic shift in the absorption spectrum of phenol when deprotonated, but no fluorescence quenching was observed in the presence of alkali metal ions. Anthracene substituted azacrown ethers have been synthesised and explored for developing a fluoroionophore by different groups. Vögtle *et al*[160,161] have synthesised the following anthracene derivatives (Figure *17*). The fluorescent quenching of these ligands with Cu^{2+} was used to study the phase transition of phosphatidylcholines.

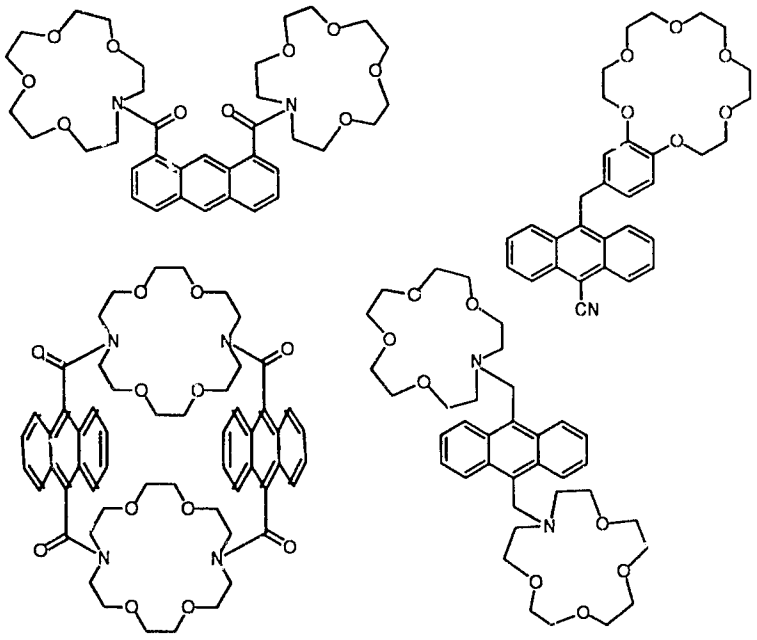

Figure *17* Examples of anthracene incorporated fluoroionophores

A more recent report by Silva and Sandanayake[150] on the development

of anthracene substituted azacrowns and benzocrown ethers as fluorescent photoinduced electron transfer sensors for alkali metal ions showed a high selectivity for sodium in the presence of other alkali metal ions. A bis crown ether containing an aza-crown ether and an anthracene fluorophore, designed by the same authors, has shown an alkyl chain length dependent quenching by α,ω-alkanediammonium ions in $CHCl_3 : CH_3OH$ (1:1 v/v).[162] The anthracene moiety was used as a spacer between the two azacrowns as well as the detecting unit in this case. These molecules are only soluble in organic solvents and the studies were exclusively done in non- aqueous solvents.

Immobilisation of fluoroionophores has also been achieved in the development of sensors known as optodes. A number of reviews are available in this area.[142,164-168] The high sensitivity, the absence of a sensitive liquid interfaces, the small size and the high suitability for remote sensing applications of these sensors make them potentially superior to other types of sensors. The developments in fiber optic technology, communication technology and the syntheses of cation sensitive and selective fluoroionophores enhances the chances of developing a cation selective optode. There are number of anion selective chromo- and fluoroionophores available in the literature,[150,160-162] but an efficient cation selective fluoroionophores which is insensitive to pH has not been developed yet. The biggest problem with the known cation fluoroionophore molecules is their overall insensitivity towards alkali metal ions. The change in optical properties induced by complex formation in these

molecules is rarely above 20% which is just not enough for use in a reliable application.

Membrane based sensors such as optodes work on the basic principle of selective extraction of the ion by the ionophore into the membrane phase. The extent of extraction can be monitored in different ways. Potentiometric sensors make use of the change in potential of the membrane due to the extraction of cationic or anionic species from solution.[44] Optical sensors monitor the changes in optical properties of the membrane components (e.g. dyes) such as the amount of light absorbed, transmitted or reflected, quenching of the fluorescence emission, phosphorescence or chemiluminescence.[166] In a simple optical sensor a polymeric membrane mounted between two transparent glass plates can be used to monitor the analyte concentration in a solution which is in contact with the membrane.

In a more advanced approach, an optical fibre coated or immobilised with an indicator species for the analyte in question could be developed.[169-171] This type of sensor could be applied in remote sensing. The indicator species, on interaction with the analyte would produce a change in the spectral properties as a linear function of the analyte concentration. By incorporating an ionophore unit to an indicator immobilised on a solid support or fibre, selective determination of a specific ion could be achieved.[171] There are three major categories depending upon the nature of the analyte a) ionic sensors (cations and pH optodes),[172,173] b) gas sensors (for vapours of NH_3, EtOH, Br_2,

I_2, N_2H_4 and CH_4)[174-175] and c) biosensors (Immunosensors).[176] In all these cases the performance of the sensor depends on the extraction efficiency of the ionophore rather than its transport efficiency which was crucial in the potentiometric sensors. Another type of optical sensor is based on changes in mechanical properties of the fibre due to the adsorption of the analyte (e.g. sensor for H_2 based on Pd coated optical fibre).[177] The optodes can incorporate a combination of carriers at least one of which has to be a photoionophore.[178] For the case of neutral carriers, the extraction efficiency depends on both cation extraction as well as on counter ion extraction. So a combination of cation selective and anion selective carriers can be used in the membrane.[179] By designing selective carriers in the "proper way" both anion as well as the cation concentration can be monitored at the same time with a single sensor. The "proper way" implies the optical properties perturbed by the two carriers should not be same and should be monitored individually. In principle, designing a fluoroionophore opens up an important area of analysis.

4.2 The design strategy

The key questions which need to be considered and explored to develop an ideal photoionophore are a) What are the metal ions to be determined by optical sensors? b) What type of ion binding units are necessary to achieve high selectivity? c) What chromophore gives maximum cation sensitivity of the analysis? d) What types of linkage and orientation of the chromophore are

necessary to achieve maximum interaction between the complexed cation and the chromophore? e) What type of structural modification of the photoionophore is necessary to develop an optode for the analysis of a given sample? f) How does a cation (analyte) change the optical properties of the photoionophore? and g) Can a water soluble photoionophore be prepared?

The last point is very significant in other areas of ongoing research in our group. The transport of metal ions especially the alkali metal ions through membranes has attracted considerable attention from research groups all over the world. These studies have focused on the development of ion transport systems like ion carriers, channels and pores.[29,180] This effort depends on monitoring the transport by developing suitable sensitive techniques. In our group, the main analytical problem is the determination of cation concentration in the inner phase of bilayer vesicles.[27] Fluorometry could play an important role in monitoring the ion concentration because of its high sensitivity, high selectivity and simple analytical procedures. The *in situ* monitoring of ion concentration requires efficient water soluble fluoroionophore molecules. Ideally, a large change in optical properties due to cation binding is required. The optical properties of the fluoroionophore should also be pH independent over a wide range.

By comparison of the requirements of the ideal fluoroionophore, the properties of the photoionophores reported in the literature fall significantly short of the goal.[138,146] All of the molecules hitherto known are insoluble in

water. When cation dependent changes are observed, the molecules are based on the functionalization of aza-crown ether moieties with chromophores and they, therefore, show an interference from the pH of the medium.[181,182] The known fluoroionophores are insensitive to the alkali metal ions, ie the quenching induced by the alkali metals was insignificant. From the design perspective, these factors challenge the possibility of developing an efficient water soluble photoionophore. However, phenol based ionophores do show some water solubility. Moreover, it is the distance of separation of the chromophore from the ionophore unit, that is crucial, and not the orientation of the chromophore with respect to the complexed cation.[138]

This background prompted us to look into the design of new photoionophores based on different ion binding units than previously investigated. The selection of tartaric acid derived crown ethers for this application is based on their simple synthesis and known cation complexation behaviour in aqueous solution.[183,184] The carboxylate units on the crown ether ring provide an electrostatic component to the cation complexation thereby increasing the complex stability constant. The stability constant for alkali metal complexation by tartaric acid crown ethers in water is as high as for cryptands in non-aqueous solvents.[185] The diaxial orientation of the carboxyl group gives a proper alignment for further functionalisation, such as addition of chromophores.

Three series of compounds were designed: two series of fluoroionophores

and one series of chromoionophores. Our goal was to explore the synthesis and survey the metal ion dependent spectral properties of the molecules so that their potential as water soluble photoionophores could be assessed. The manipulation of the chromophore unit was not done to maximize sensitivity. Rather the prime importance was given to development of a synthetic strategy which could be used to incorporate any chromophore units through simple functionalisation.

We call the first series of compounds captands,[186] derived by capping the crown ether above and below the macrocycle with a spanning chromophoric group. A similar strategy was used by Lehn to synthesise monocapped crown ethers.[187-189] In the Lehn synthesis, the diamines used were flexible hence the product contained both *syn*- capped as well as *anti*-capped isomers. The purification of these isomers was achieved but the yields were low. Since there was no chromophore in the diamine skeleton, the molecules were not usable as photoionophores.

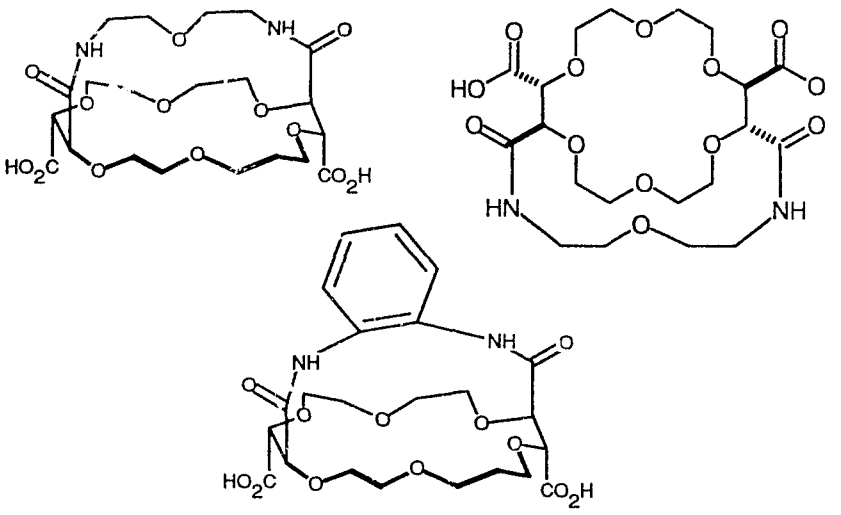

Figure *18* Examples of known monocapped crown ethers

Our synthetic strategy involves capping of a crown ether tetra acid chloride with rigid diamines of appropriate distance between the amino groups to give a tricyclic tetraamide (Figure *19*).

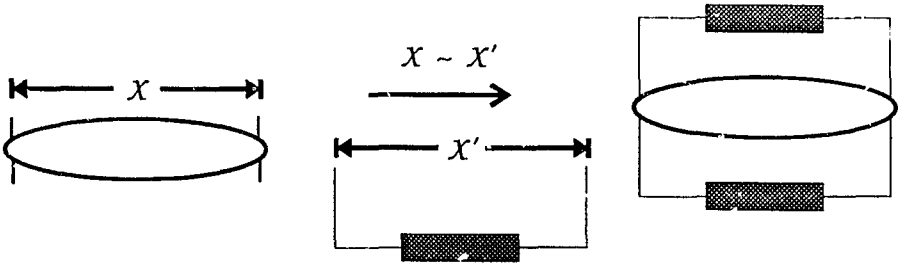

Figure *19* Cartoon of the design strategy for captands.

The appropriate span of the diamine was selected by comparison of the distance between the amino groups of candidate diamines determined by MMX calculation and the C=O group of the acid crowns derived from crystal structures. Rigid diamines are chosen to impose coupling of the acid chloride and amino group across the face of the crown ether. This limits the possibility for cross coupling or coupling to the opposite faces. Within the design limitation, the chromophore part of the diamine could be varied extensively. Capping of the crown ether macrocycle on both sides results in a highly pre-organised host which could enhance the stability of the complex with a metal ion.

Since the chromophore is connected to the crown ether on both sides of the molecule, electronic perturbations imposed by the metal ion might be twice as high as mono substituted photoionophores. Even though previous studies on naphthalene based fluoroionophores indicated that the orientation of the molecule did not effect the quenching properties[157], this hypothesis can be further tested in the case of captands where the chromophore orientation is highly controlled.

In a second series designed to have increased water solubility, bis crown ethers based on diacid crown ethers were designed. The main synthetic step involves treatment of an anhydride, prepared from the diacid, with various chromophore diamines. The product bis crown ether will have a free carboxyl group on each crown ether unit to enhance the electrostatic interaction of the

crown ether with the cations. I this series, the diamine could be either rigid or flexible. By manipulating the structure of the diamine, the spatial alignment of the crown ether with the chromophore can be varied. High water solubility of the compound due to the presence of hydrophilic functional groups in the structure is anticipated. As with other bis crown ethers, manipulation of spacer length should alter the selectivity and efficiency of the complexation.[152,162]

The third series explored were chromoionophores based on tartaric acid crown ethers. All hitherto known chromoionophores are based on azacrown ethers as the binding unit and their water solubility is marginal to insignificant.[138] They can be used to extract metal ions from water to an organic medium. Our interest piqued from the necessity of monitoring ion transport through a bilayer membrane in aqueous medium. The water insoluble molecules get partitioned to the bilayer membrane. This interferes with the monitoring of metal ion concentrations outside the bilayer.

The design strategy adopted here is very simple. The conformation of the carboxyl groups of the tartaric acid units incorporated to the crown ether ring was known from the crystal structure as well as nmr studies.[191,192,193] The diaxial orientation gives an ideal opportunity to orient a ligating atom just on top of the metal ion. By varying the distance between the phenolate group and the carboxyl C=O group we can increase or decrease the distance between the complexed metal ion and the phenolate group. The parent crown ether diacid

and tetracid are both soluble in water. The conversion of all carboxylic groups to amide functionality with lipophilic groups decreases the solubility considerably. For example captands[186] described earlier were insoluble in water, while the bis crown ethers were soluble in water. So at least one free carboxylgroup should be available to achieve water solubility.

Chromoionophores designed for monitoring the presence of metal ions in water by uv-spectroscopy involved the conversion of tartaric acid crown ethers to the corresponding anhydrides followed by treatment with o-aminophenol to give highly coloured mono and bis(phenol-carboxylic acid) compounds. The advantages discussed for the bis crown ether series are exploited in this case as well. In addition, the incorporation of a well studied chromophore (phenol) offers a standard to explore the other features. The easy synthetic accessibility of the phenol functionalization process provides a golden opportunity to generate alkali metal ion sensitive materials.

4.3 Results and Discussion

4.3.1 Synthesis of Captands

The synthesis of the required crown ethers from tartaric acid is straight forward and standardised in our laboratory.[194] The reaction involves a substitution of a sulphonate with the bis- alkoxide derived from tetramethyl tartaramide. In this case the dianion of tartaramide was made using sodium hydride as a base and followed by treatment with the tosylate of the appropriate glycol unit (Scheme *5*).

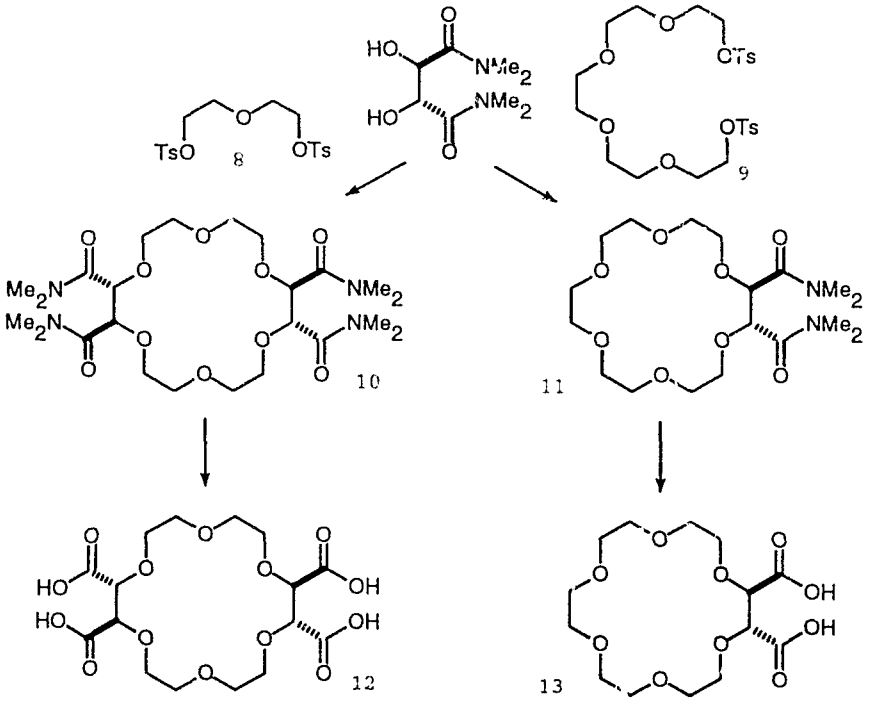

Scheme *5* Synthesis of tartaro-crown ethers.

Both diamides (**11**) and tetraamides (**10**) can be prepared in one pot in a reasonable yield.[194] Over the course of the project, the effect of solvent on the

yield of the reaction was explored. Both DMSO and DMA were found to be better solvents than DMF. The central problem is traces of formate in DMF which altered the stoichiometric ratio of anion to tosylate in the mixture. This decreased the yield of macrocyclisation product by quenching precursor intermediates. Hydrolysis of the amides with mineral acid gave the corresponding di- (**13**) and tetra-acids (**12**), identical in all respects with previously prepared samples.[195]

The synthesis of captands involved the conversion of the tetracid (**12**) to the tetraacid chloride **14** followed by capping the tetracid with an appropriate diamine (Scheme *6*). The selection of the appropriate diamine was based on information from crystal structure and molecular mechanics calculations. The crystal structures of the complexes of tetraacid with alkali metal ions has shown an average distance of 7.6 Å between the C=O groups of the carboxylic acids on the same side of the crown ether macrocycle.[191] We assume the diaxial orientation of the carboxyl groups of tartaric acid units is also important to align the carboxyl group during capping.

The selection of m- and p-xylylenediamines was based on molecular mechanics calculations. The structures of the diacetamide of several candidate diamines were minimised and the distance between the carbonyl carbons in the minimised structures was measured. For the meta-xylylene isomer the distance was 7.1 Å and for the para-xylylene isomer it was 8.2 Å. Only rigid diamines were considered initially.[196]

The capping of the tetracid chloride (**14**) with m-xylylenediamine yielded a captand (**15**, Scheme 6). The synthetic procedure involved a high dilution coupling of the m-xylyler diamine with 18-crown-6 tetracid chloride in dry toluene. The crude product was dissolved in water and extracted with dichloromethane. Quantitative coupling was observed - the crude reaction mixture contained only (**15**) and stoichiometric m-xylylenediammonium salt.

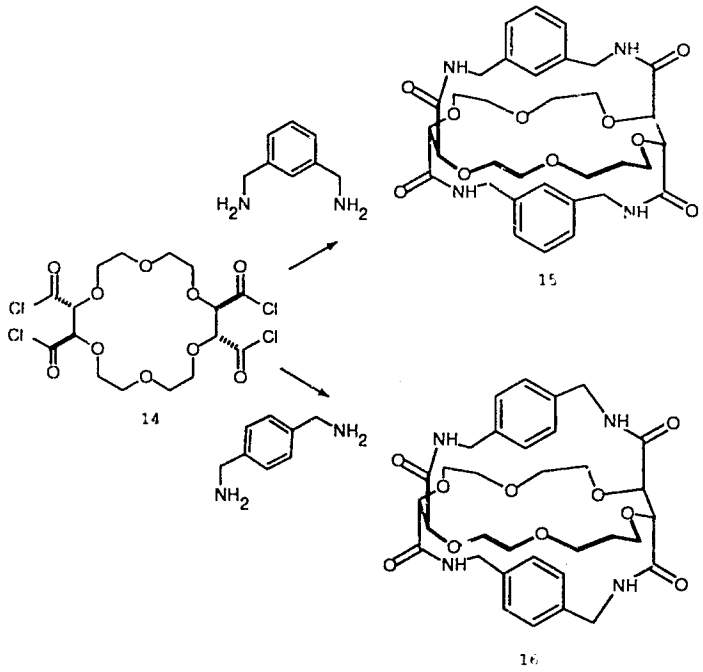

Scheme *6* Synthesis of Captands from m-xylylene - and p-xylylenediamines (**15,16**)

The ^1H nmr showed a doublet 7.6 ppm which could be assigned to the NH protons and a singlet at 7.2 ppm with intensity proportional to 3H which

could be attributed to the aromatic protons. A doublet of doublets at 5.0 ppm could be assigned to one of the diasteriotopic methylene protons and the doublet at 3.9 ppm could be assigned to the other methylene proton. The chemical shift difference between the two diasteriotopic methylene protons was 1.1 ppm which could be explained as due to the differential shielding of the methylene protons by the adjacent aromatic rings. Only one well resolved coupling was observed in case of the signal due to the NH indicating that one methylene proton forms a dihedral angle of about 90° with the NH. The sharp spectrum with defined couplings indicates a single dominant conformation about the -NH-CH_2-Ar unit. The ^{13}C nmr spectrum showed a peak at 169.3 ppm due to the amide $\underline{C}$=O, a single peak at 80.9 ppm from four identical $\underline{C}$H of the tartaramide units of the ring and a single peak at 42.4 ppm due to four identical Ar-$\underline{C}H_2$- of the molecule. The confirmation of the structure also came from its molecular ion at m/z 641 (M+1) in the mass spectrum, a crystal structure discussed below and elemental analysis.

The coupling reaction of p-xylylenediamine and tetracid chloride (**14**) was done in dry toluene (Scheme *6*). The product was purified by repeated extraction of the dichloromethane solution with water. The net yield of the captand **16** was only 40%. This could be attributed to the fact that the solubility of the p-xylylenediamine in dry toluene was lower than the m-xylylenediamine. Also the distances between the amino groups and their spatial alignment are different in the two compounds. The p-xylylenediamine

could have a *syn-* or *anti-* orientation whereas the m-xylylenediamine apparently lacks this freedom as assessed from MMX calculations.[196]

The ^{1}H nmr spectrum of compound **16** in $CDCl_3$ showed a singlet at 7.1 ppm corresponding to the aromatic protons and a doublet at 6.8 ppm due to the NH protons. The diasteriotopic methylene protons gave a doublet of doublets at 4.9 ppm and a doublet at 3.8 ppm. The methine proton resonance was seen as a singlet at 4.4 ppm and ethylenedioxy protons of the crown ether ring appeared as two multiplets at 3.5 and 3.4-3.2 ppm with a 1:3 intensity ratio. The large diasteriotopic shifts of the Ar-C$\underline{H}_2$- and crown ether -C$\underline{H}_2$- groups indicate well defined conformation in this structure. The ^{13}C nmr spectrum showed characteristic resonances of amide $\underline{C}$=O at 169.2 ppm. The single peak at 78.1 ppm ($\underline{C}$H of tartaramide unit) and 43.3 ppm (Ar-$\underline{C}H_2$-) confirms the symmetry of the molecule. The other structural confirmation came from the molecular ion peak at m/z 641 $(M+1)^+$ in the mass spectrum and the crystal structure discussed in the later part of this section.

Since m-xylylenediamine gave a quantitative yield in the capping reaction, we anticipated that the other diamines with the same distance between two amino groups on different fluorescent active groups would also give good yields. With this idea in mind, diamines of biphenyl and anthracene were chosen for the capping.

The selection of 2,2'-bis(aminomethyl)biphenyl was based on two features. The first factor was to explore the effect of rotational freedom of

diamines on the capping reaction. Rotation around the central bond between the two benzene rings is partly hindered and the two amino groups have a constrained but variable span. The other factor came from the expectation that the excited state of the biphenyl molecule would attempt to take a planar geometry instead of the twisted ground state conformation. The other feature of this diamine is that it could cap across the faces of the crown ether ring (*syn*-capping, between the acid groups of two different tartaric acid units) or along the edges (*ortho*-capping, between the acid groups of the same tartaric acid unit). This would be interesting to study in terms of the complexation behaviour and the spectroscopic characteristics. *Anti*-capping (between the two different tartaric acid unit spanning the two faces of the crown ether) is unlikely from an analysis of the models.

The choice of the 9,10-bis(aminomethyl)anthracene to cap the tetracid chloride was based on the intense fluorescence emission of anthracene at 425 nm. The concentration of fluorophore required to study the spectral characteristics would be in the range of 10^{-6} to 10^{-9} M. Because of the high emission intensity, the sensitivity of the anthracene fluorophore to the environment can be increased. Unfortunately the solubility of anthracene derivatives is very low in common solvents. However, the functionalisation of the anthracene moiety with the tetracid crown ether was expected to improve the solubility.

The 2,2'-bis(aminomethyl)biphenyl and 9,10-bis(aminomethyl)anthracene

were not commercially available. An easy route to "aminomethyl" functionalisation was to bromomethylate the corresponding aromatic group followed by conversion to the amine. An initial attempt with mesitylene was successful for the synthesis of the bromomethylated species in good yield using trioxane and hydrobromic acid as reported by Iyer and Mitchell.[197]

However, in the case of anthracene, the expected 9,10-bisbromomethylated product was found to be very impure and its nmr spectra were practically impossible to analyze. The related chloromethylation was attempted and pure 9,10-bis(chloromethyl)anthracene was isolated in 70% yield (Scheme 7).

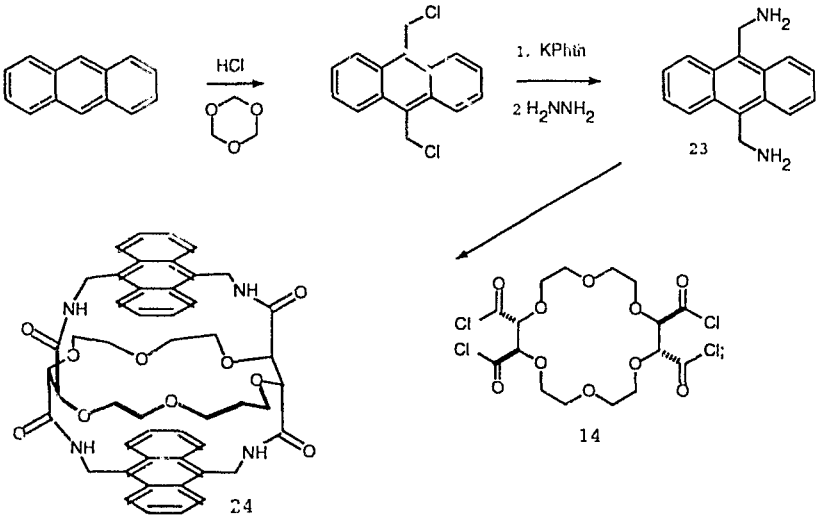

Scheme 7 Synthesis of captand **24** from 9,10-bis(aminomethyl)anthracene.

The required diamine (*23*) was prepared from this product using a

Gabriel phthalimide synthesis. The diamine (*23*) was essentially insoluble in all solvents. Because of this problem, spectral characterisation was very limited. The only structural evidence comes from the mass spectrum where a molecular ion m/z 237 $(M+1)^+$ corresponding to the diamine was observed.

Other structural evidence obtained in the latter stages of this project was the successful synthesis of bis crown ethers from this diamine. In the absence of firm structural confirmation, we proceeded with capping reactions with the notion that the crown ether moiety could increase the solubility of the anthracene unit. The capping reaction was done using a slurry of solid diamine (*23*) in dimethyl sulphoxide and the crown ether tetraacid chloride (*14*). The yellow product isolated showed an absorption at 3300-3500 cm^{-1} (-NH) and amide band at 1650 and 1530 cm^{-1} in the IR spectrum consistent with the required functional group. The product was insoluble in all common solvents and the full spectral characterisation of the product was impossible because of this insolubility. Since the aim of the project was to develop a water soluble fluoroionophore, the exploration of this compound was not pursued further.

2,2'-bis(aminomethyl)biphenyl was prepared from diphenic anhydride (scheme *8*) through a series of reactions ($LiAlH_4$ reduction, bromination with PBr_3 followed by aminolysis or Gabriel phthalimide synthesis). The diamine was characterised by ^1H, ^{13}C nmr and mass spectra. Its ^1H nmr spectrum showed, besides the peaks corresponding to the aromatic protons, a doublet of

doublets at 3.55 ppm attributed to the Ar-C<u>H</u>$_2$- protons and a broad singlet at 3.0 ppm which could be assigned to the Ar-CH$_2$-N<u>H</u>$_2$ protons. The ^{13}C nmr spectrum showed single peak at 48.8 ppm and 6 peaks in the range of 127.7 to 141.2 ppm. The diamine showed a molecular ion peak at m/z 213 $(M+1)^+$ in the mass spectrum.

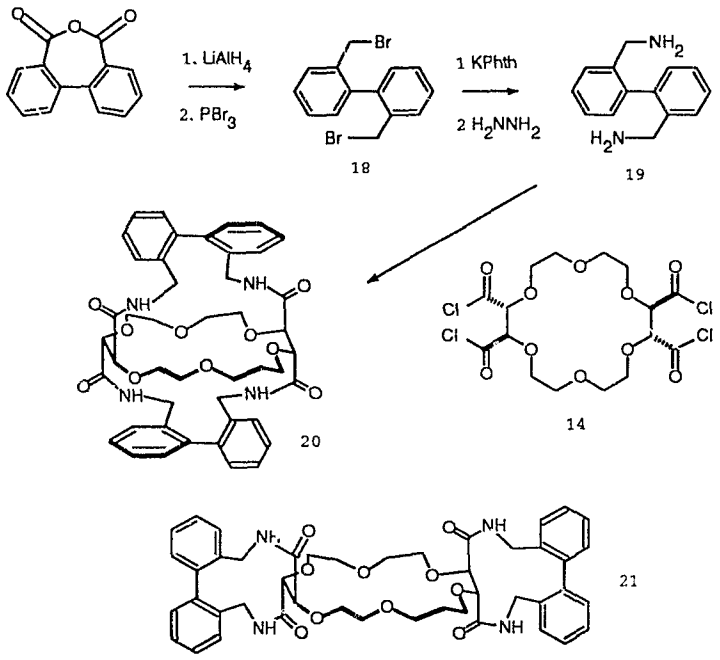

Scheme *8* Synthesis of captand **20** from 2,2'-bis(aminomethyl)biphenyl

The capping of the crown ether tetraacid with 2,2-bis(aminomethyl)biphenyl was done at high dilution in toluene using the tetraacid chloride *14* (Scheme *8*). The capped crown ether was obtained in an

80 % yield. Analysis of the ^{1}H and ^{13}C nmr spectra of the compound indicated some salient features of the molecule. The ^{1}H nmr spectrum showed relatively few but complex multiplets. The first group was at 7.7 ppm due to NH and a second group at 6.9-7.5 ppm could be attributed to the aromatic protons. The other multiplets at 4.71-4.85 and 4.60-4.69 ppm could be attributed to the methylene protons of the Ar-C$\underline{H}_2$- and the methine protons of the crown ether. The multiplet at 3.14-4.09 ppm could be assigned to the protons of the ethylendioxy group of the ring. The spectrum was much too complicated to analyze the fine structure. The ^{13}C nmr spectrum of the compound showed 4 peaks at 169.4, 169.5, 170.0 and 170.3 ppm which could be attributed to the amide $\underline{C}$=O and 4 peaks at 81.3, 81.9, 82.3 and 82.9 ppm assigned to the $\underline{C}$H of the tartaramide units of the ring. The other peculiar feature was the 4 signals corresponding to the Ar-$\underline{C}H_2$ at 41.4, 41.5, 42.0 and 42.4 ppm and two separate groups of ring carbons one at 70.7-71.6 ppm (4 signals) and the other at 76.7-77.4 ppm (4 signals). The analysis of the ^{13}C nmr spectrum is difficult because of the complexity of the features. However the presence of distinct 4 signals in the spectrum for $\underline{C}$=O, -$\underline{C}$H (ring tartaramide units) and Ar-$\underline{C}H_2$ indicates either an approximately 1:1 mixture of *syn-* capped (**20**) and *ortho-* capped (**21**) isomers each of which is undergoing rapid motion about the Ar-Ar bond or two slowly interconverting *syn-* capped isomers differing in the biphenyl chirality (only **20**, not **21**). The position of the peaks confirms that the molecule is in fact a crown ether tetraamide. As indicated earlier the

possibility of *ortho* capped (capping the two acid groups of the same tartaric acid unit in a side wise manner) isomers does exist. However, the thin layer chromatog2raphy of the compound showed only a single spot which discouraged any further separation of possible isomers. Attempts to grow crystals were not successful. The crystal structure of the molecule would prove the preferred conformation. The molecular ion observed at m/z 793 $(M+1)^+$ confirms the molecular structure and the elemental analysis suggests that if a mixture is present, it is a mixture of isomers.

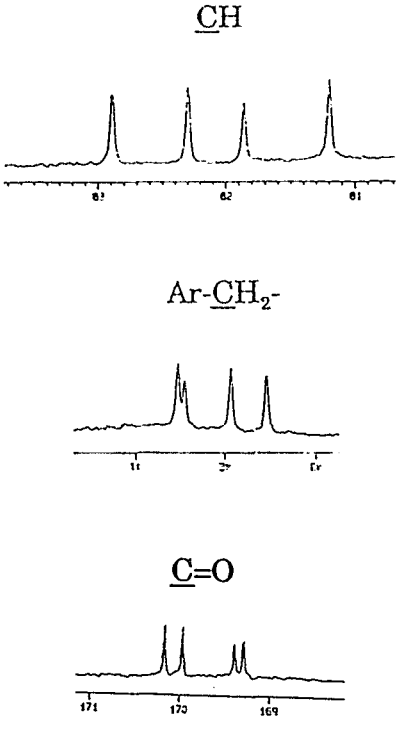

Figure *20* ^{13}C nmr of compound **20** (regions of C=O, CH and Ar-CH_2-)

The monocapped crown ether structure was another potential water

soluble fluoroionophore (scheme *9*). The free *syn* carboxyl groups could provide a site for further functionalisation as well as an increase in water solubility of the compound. The low solubility of the captand series in water prompted us to explore the synthesis of this type of compound. The synthesis was done by treating the 18-crown-6 dianhydride (**25**) with a diamine using high dilution conditions. The nmr spectra of the crude product showed the expected peaks. However all attempts to purify this compound were in vain. A metal free ligand was impossible to isolate from water but partly purified materials showed the expected nmr characteristics. The ^{1}H nmr spectrum showed a broad singlet at 7.1-7.3 ppm attributed to the aromatic protons and a multiplet at 3.9-4.3 ppm probably due to the Ar-$\underline{C}H_2$ protons. The ^{13}C nmr spectrum showed two peaks at 176.1 and 172.1 ppm which could be assigned to the $\underline{C}$=O group of the acid and amide respectively. The two peaks at 81.9 and 81.0 ppm could be assigned to the methine carbons of the tartaramide units and the peak at 45.0 ppm could be due to the Ar-$\underline{C}H_2$- carbon. Attempts to crystallise this compound were unsuccessful. All attempts to purify the compound by cation exchange, extraction or column chromatography failed. Other monocapped ligands were not prepared and we turned our efforts to a new strategy for water soluble fluoroionophores.

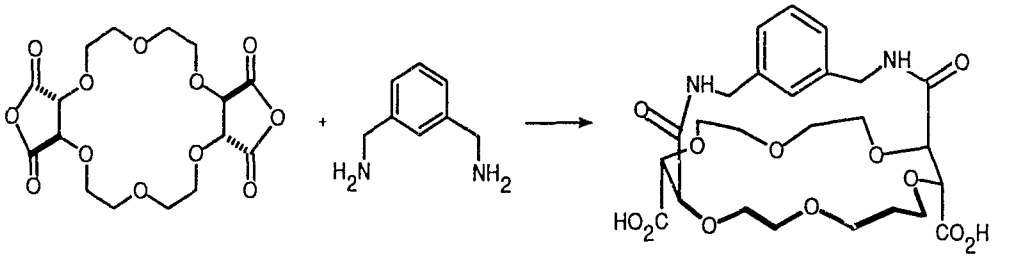

Scheme *9* Synthesis of monocapped crown ether **26**

4.3.2 Synthesis of Bis crown ether series

In a second series designed to have increased water solubility, we have successfully synthesised and characterised two fluorescent compounds based on the 18-crown-6 diacid as ionophore. By incorporating two crown ether units to a fluorophore, a host capable of multiple recognition could be envisaged.[6] The synthetic strategy is quite general and could be applied to any diamine.

The synthesis starts from the diacid derived from tartaramide and the ditosylate of pentaethylene glycol (scheme *5*). The method follows closely that for the tetraamide. The diamide (**11**) was hydrolysed and the anhydride was prepared from the diacid (**13**) by treating with acetyl chloride. The anhydride (**27**) was then treated with the diamines[198] (scheme *10*).

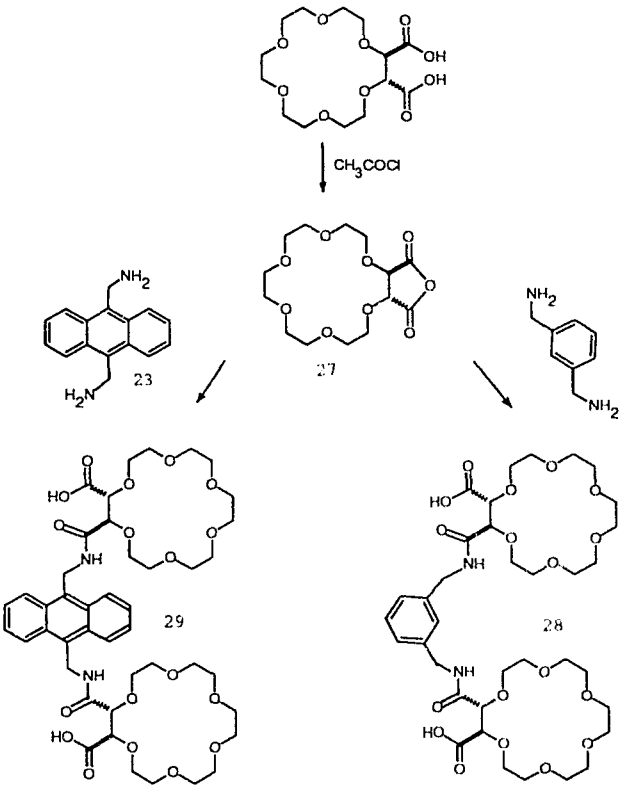

Scheme *10* Synthesis of bis crown derivatives **28**, **29**

The crude products were dissolved in water and extracted with dichloromethane. The m-xylylenediamine reacted with the anhydride to give quantitative yield of the bis-crown product. Purification was done by extraction from water into dichloromethane. Because of the high solubility of the product in water, the extraction was incomplete. The product obtained was passed through a cation exchange column to remove traces of ammonium salts

present. The two triplets observed in ^1H nmr spectrum at 7.31 and 7.24 ppm and the singlet at 7.29 ppm could be assigned to the aromatic protons and a broad singlet at 4.9 ppm which disappeared in D_2O was assigned to the N<u>H</u>. The doublet of doublets observed at 4.51 ppm was assigned to the methine protons of the tartaramide units of the ring and the doublet at 4.6 ppm was assigned to the Ar-C<u>H</u>$_2$ protons. The ring protons appeared in the range of 3.4-3.6 ppm. The ^{13}C nmr spectrum showed two distinct peaks at 171.7 and 169.4 ppm for the <u>C</u>=O of the acid and amide respectively. The two signals at 81.3 and 80.5 ppm could be attributed to the <u>C</u>H of the tartaric acid unit. The single peak at 42.8 ppm could be assigned to the Ar-<u>C</u>H$_2$ carbon. The mass spectrum showed a molecular ion peak at m/z 776 $(M+1)^+$.

Similarly the treatment of the crown ether anhydride with 9,10-bis(aminomethyl)anthracene was done in the same way and the product (**28**) was extracted from water with dichloromethane and further purified by passing through a cation exchange resin. The product was characterised by ^1H and ^{13}C nmr spectra. Its ^1H nmr spectrum showed two multiplets at 8.4 and 7.5 ppm with a total intensity corresponding to eight protons, assigned to the aromatic protons. The diasteriotopic methylene protons appeared as doublets at 4.7 and 4.3 ppm and the methine protons of the crown ether ring showed as two doublets at 4.3 and 4.4 ppm. The two peaks at 171.6 and 168.8 ppm in ^{13}C nmr spectrum could be assigned to the acid and amide <u>C</u>=O. Two peaks at

80.7 (CH of amide end) and 81.4 ppm (CH of acid end) could be due to the methine carbons of the tartaric acid unit and the single peak at 35.6 ppm could be attributed to the Ar-CH_2. Over a period of two months, the product decomposed in sunlight so subsequent samples were kept in brown vials covered with Aluminium foil.

4.3.3 Synthesis of Chromoionophores

The crown ether diacid anhydride (**27**) was treated with 2-aminophenol to give a highly coloured compound **30** (Scheme *11*). The purification involved extraction of the compound from water at pH 3 with dichloromethane and the dry compound obtained after the evaporation of the solvent, was again dissolved in water and passed through a cation exchange column to remove traces of triethylammonium chloride and other ammonium ions from the solution. The purified product was further characterised by its nmr and mass spectrum. ^{1}H nmr spectrum showed two doublets at 7.1 and 7.0 ppm, and two triplets at 7.3 and 6.9 ppm, all of which could be assigned to aromatic protons. The doublet of doublets observed at 4.4 ppm could be assigned to the methine protons of the tartaric acid unit of the crown ether. The broad singlet observed at 9.4 ppm could be assigned to the NH- protons. The ^{13}C nmr spectrum showed two distinct peaks at 171.2 and 169.1 ppm which could be assigned to the acid and amide C=O. Two peaks at 80.9 and 80.7 ppm could be assigned

to the methine carbons of the tartaric acid unit of the crown ether ring. The mass spectrum showed a molecular ion peak at m/z 444 $(M+1)^+$.

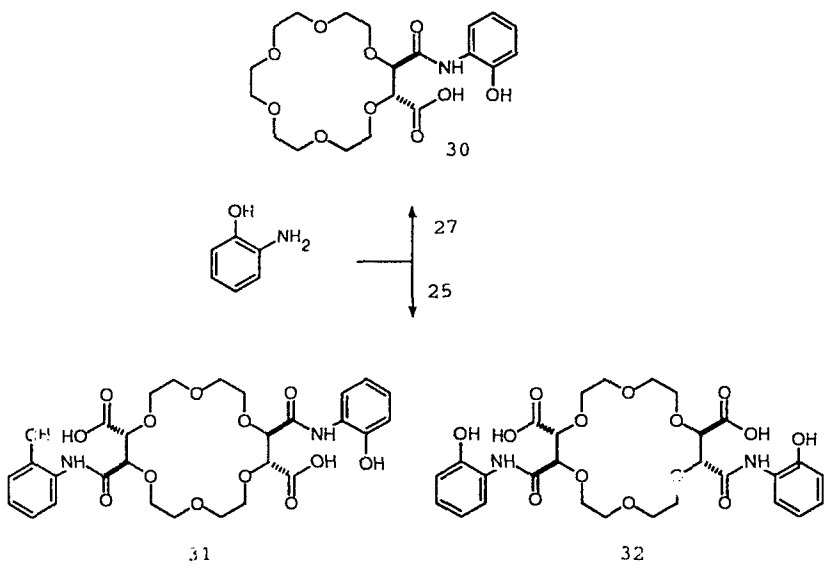

Scheme *11* Synthesis of chromoionophores **30, 31**

A related crown ether tetraacid derivative was also prepared by using the procedure described above. In this case, since the bisanhydride (**25**) is symmetrical, the possibility of the formation of *syn-* and *anti-* isomers exist. The reaction was done with triethylamine as base. These conditions are known to favour the formation of *syn-* crown ether amides. The purified product was characterised by its nmr and mass spectra. The ^1H nmr spectrum showed two doublets and two triplets due to the aromatic protons and a

doublet at 4.3 ppm which could be attributed to the methine protons of the tartaric acid units of the ring. A broad singlet at 8 ppm could be attributed to the -NH protons of the two amide groups. The ^{13}C nmr spectrum showed two peaks at 171.7 and 169.2 ppm due to the amide and acid C=O and two peaks at 81.2 and 79.9 ppm attributed to the methine carbons of the crown ether ring. The mass spectrum showed a molecular ion at m/z 623 $(M+1)^+$.

4.3.4 Survey of fluorescence and absorption spectra of photoionophores

Fluorescence is the emissive decay of a singlet excited state to a singlet ground state.[199,200] The excitation of an electron from a spin paired singlet ground state to a singlet excited state results in an electronic arrangement where the spin of the two electrons are still paired. Returning of this excited electron to the ground state leads to the fluorescent emission. The singlet excited state electron can also undergo a spin inversion to produce an excited triplet state where both electrons (ground and excited states) have the same spin. A change in spin orientation is necessary for a triplet excited state to return to a singlet ground state. The return of electron from a triplet state to a singlet ground state is quantum mechanically forbidden unless spin inversion is preceded. Since fluorescence is a quantum mechanically allowed transition it is a fast phenomenon (~10 nsec) whereas forbidden phosphorescence (triplet

excited state to singlet ground state) is the slow process. One characteristic feature of the active fluorophores is that these systems generally contain delocalised electrons. Anthracene, fluorescein and perylene are a few examples of highly fluorescent groups. Some of the lanthanide elements are also fluorescent due to the electronic transitions in their f orbitals (eg. europium and terbium ions).[201] The fine structure observed in some fluorescence spectra indicates the presence of different vibrational levels in the ground state. The photophysical processes involved are illustrated in the Jablonski diagram[202] below.

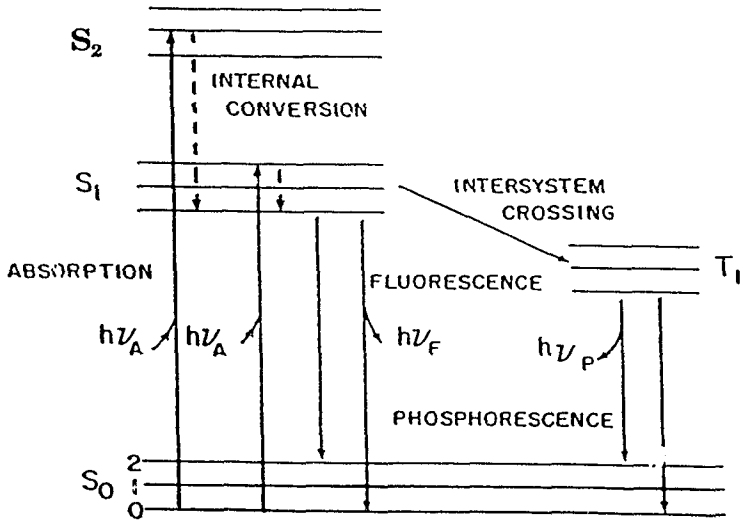

Figure *21* Jablonski diagram

The symbols S_0, S_1, and S_2 indicate the different singlet electronic states and the vibrational energy levels in each of these electronic states are represented

by 0,1,2 etc. The energy absorption of the molecules in the ground state is a fast process (10^{-15} sec). The light absorption by a fluorophore follows a series of processes. The excitation from the ground state to the vibrational levels of S_1 or S_2 is followed by very rapid internal conversion from the higher vibrational levels to the lowest vibrational level of the excited state (S_1). This process (10^{-12} sec.) generally goes to completion before the fluorescence emission (10^{-8} sec.) from this thermally equilibrated excited state (S_1). The return from this state to different vibrational states of the lower ground state appear as fine structures in the fluorescence emission. The thermal equilibration of these vibrational states to the lowest electronic level in the excited state (S_1) and ground state (S_0) goes to completion in 10^{-12} sec. All transitions from these thermally equilibrated states can appear in absorption and emission spectra of the molecule. For example the fine structure of the absorption spectrum represents the vibrational levels in the electronically excited state whereas the fine structure of the emission spectrum indicates the vibrational levels in the ground electronic state. In general the emission spectrum is the mirror image of the absorption spectrum (S_0 -> S_1 transition) for most molecules. This rule fails in the case of geometrical changes, or when reactions such as deprotonation or excimer formation occur in the excited state. The rule also fails if nuclear displacement occurs due to the long life time of S_1 state as would be the case for a biphenyl molecule. The intersystem crossing of molecules from the singlet excited state to the triplet excited state and

emission from the triplet state to the ground state occurs to a higher wavelength (lower energy) region.

The fluorescence lifetime of a molecule is defined as the average time a molecule spends in the excited state before its decay to the ground state and can be expressed as

$$\tau = 1/(T + k) \qquad \text{---------- 8}$$

where T is the rate constant of the radiative decay and k is the rate constant of non radiative decay. In the absence of non radiative decay the expression reduces to $\tau_0 = 1/T$

The fluorescence quantum yield indicates the ratio of the number of photons emitted to the number of photons absorbed.

$$Q = T / (T + k) \qquad \text{---------- 9}$$

where Q is the fluorescence quantum yield.

$$\text{or } Q = \tau / \tau_0 \qquad \text{---------- 10}$$

where τ is the lifetime in the presence of non-radiative decay and τ_0 is the lifetime in the absence of non-radiative decay.

Fluorescence spectroscopy is very sensitive to the molecular dynamics of the environment which occur during the fluorescence lifetime. The non-radiative decay of the excited state is the sole contributor of the depletion of the S_1 excited state and thereby quenching the fluorescence emission. Emission quenching can be either due to self quenching or quenching by another molecule. Using a dilute solution of the fluorophore can decrease the

amount of self quenching. Fluorescence quenching can be due to excited state reaction, energy transfer, electron transfer, complex formation as well as the collision of the excited state with other molecules.[200] Since we are interested in quenching the fluorophore emission by metal ions, only quenching by alkali metal and alkaline earth cations is considered here.

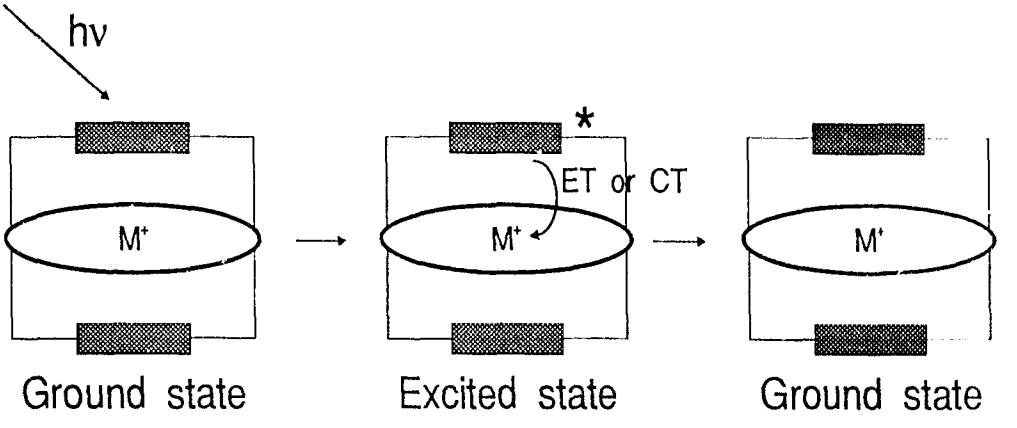

Figure 22 Cartoon of anticipated fluorescence quenching by energy, electron or charge transfer from fluorophore to metal ion

Fluorescence quenching can be classified as static quenching or dynamic quenching. For either type of quenching to occur, close proximity of the interacting molecules within the fluorescent life time of the fluorophore is necessary. In the case of static quenching, a complex is formed between the fluorophore and the quencher and the complex decays through a non radiative electron energy transfer process. This includes Columbic interaction (long

range ie, up to 100 Å) and electron exchange (short range). In dynamic quenching, the quencher molecule should contact the excited state of the fluorophore during the lifetime of the excited state.[203] Thus it depends on the diffusion rate of the quencher in the medium.

The mechanism of quenching can be the formation of charge transfer complexes (eg. anthracene-diethylamine),[204] exciplex formation (eg. α-cyanonaphthalene-olefins)[205] or spin-orbit coupling of the excited state (singlet) fluorophore and the quencher, followed by intersystem crossing to a triplet state which is quenched by another process having longer lifetimes, (eg. quenching by Cs^+, Br^-, I^- etc.).[206,207] Electron transfer quenching occurs due to transfer of electrons from the fluorophore to the quencher (eg. quenching by H^+, NO_3^-, Cu^{2+}, Pb^{2+}, Cd^{2+}, Mn^{2+}, fumarate).[207]

The Stern-Volmer equation for a dynamic quenching can be expressed as

$$F_0/F = 1 + k_q\tau_0[Q] = 1 + K_D[Q] \quad \text{---------- 11}$$

where F_0 and F are the fluorescence intensities in the absence and presence of quencher, k_q is the bimolecular quenching constant, τ_0 is the life time of the fluorophore in the absence of the quencher, [Q] is the concentration of the quencher and K_D is the dynamic quenching constant. In the case of dynamic quenching, the quenching ratio $F_0/F = \tau_0/\tau$ where the τ_0 and the τ are the fluorescent lifetimes in the absence and presence of the quencher.

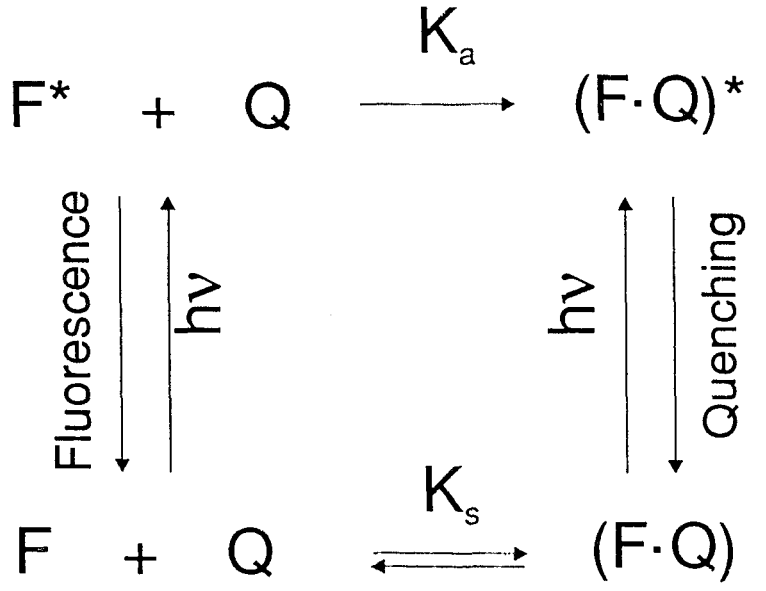

Scheme *12* Representation of static and dynamic quenching pathways

For static quenching, the Stern-Volmer equation can be derived based on the association constant of the fluorophore and the quencher according to the processes of Scheme *12*.

The ground state association is given by

$$K_S = \frac{[F.Q]}{[F][Q]} \qquad \text{---------- 12}$$

The total concentration of the fluorophore $[F_0] = [F] + [F.Q]$ at any concentration of Q is then given by:

$$K_S = \frac{[F_0]-[F]}{[F][Q]} = \frac{[F_0]}{[F][Q]} - \frac{1}{[Q]} \qquad \text{-------- 13}$$

or $F_0/F = 1 + K_S[Q]$ ---------- 14

Since only the lifetime of the non-fluorescing complex fluorophore is perturbed, the life time of the uncomplexed species is same as τ_0. So the ratio $\tau_0/\tau = 1$, or in other words for a static quenching the ratio $F_0/F = \tau_0/\tau = 1$. The easy way to differentiate static and dynamic quenching is to measure the life time in the presence and in the absence of quenchers.

If there is only one type of quenching (either static or dynamic) which occurs in the medium, a plot of F_0/F vs [Q] would give a straight line with an intercept at 1 and slope K_D (dynamic) or K_S (static). In cases where both of these quenching processes occur simultaneously, then the plot of F_0/F vs [Q] would have an upward curvature.

In a case where both static and dynamic quenching occur, the Stern-Volmer equation becomes

$F_0/F = (1 + K_D[Q])(1 + K_S[Q])$ ---------- 15

In principle, K_D can be calculated from life time measurements ($\tau_0/\tau = 1 + K_D[Q]$) and the dynamic component of the quenching can be separated. In cases where the life times are not available, the dynamic and static components can be separated from a plot of K_{app} vs [Q]

$F_0/F = 1+ (K_D + K_S)[Q] + K_DK_S[Q]^2$ ---------- 16

$= 1 + K_{app}[Q]$ ---------- 17

where $K_{app} = (K_D + K_S) + K_DK_S[Q] = (F_0/F - 1)/[Q]$ --------- 18

From a graph of $(F_0/F -1)/[Q]$ vs [Q], the slope of a straight line would

give K_DK_s and the $(K_D + K_S)$ would be the intercept. The individual components can be separated by solving the quadratic equation

$$K_S^2 - K_SI + S = 0 \qquad \text{---------- 19}$$

where S and I represent the slope and intercept.

4.3.4.a Fluorescence studies of Captands

The procedure of the fluorescence experiments involves the titration of a standard solution of the crown ether in 50% methanol:water with an aqueous solution of metal ions. Individual solutions with variable metal ion concentration and a fixed ligand concentration were made and the fluorescence emission spectra at a fixed excitation wavelength was recorded over a specific region. The stock solutions of the metal ions were made in deionised water. A typical sample for fluorescence emission studies consisted of a fixed volume of crown ether solution (20 µL) and metal ion solution (depending upon the required concentration) diluted to 3.0 mL (cell volume) with deionised water. The final solvent composition was 0.3% methanol in water. The excitation wavelength was determined by recording the absorption spectrum. For all three cases (**15, 16** and **20**) a strong absorption was observed in the range of 250 to 280 nm. Aqueous solutions are known to give a Raman scattering in the emission spectrum. The position of the Raman band depends on the excitation wavelength. The Raman band was identified by changing the excitation wavelength and a suitable excitation wavelength was chosen where

the Raman band was well separated from the emission maximum. For all the captands (**15**, **16** and **20**), 250 nm was found to be acceptable as an excitation wavelength. The emission spectra of solvents and metal ion solutions were recorded as a check of the purity; none of them showed any emission in the regions of interest.

The quenching by alkali metals can be monitored in two ways: 1) by monitoring the change in emission intensity of the fluorophores 2) by monitoring the change in fluorescent life time of the fluorophore in presence of metal ions. Only the first method was employed to survey the molecules in quenching studies. Since the final analytical method depends on the speed and simplicity of the measurement without compromising the sensitivity of the technique, this survey of analytical potential focused only on method 1. Even though lifetime measurements are more accurate than the intensity measurement, for the case of a weakly fluorescent fluorophore the lifetime measurement is rather difficult.

A survey of fluorescence quenching was completed with all three ligands and with alkali metals (Li^+, Na^+, K^+, Rb^+ and Cs^+) and alkaline earth metal cations (Ca^{2+}, Ba^{2+} and Sr^{2+}). The emission spectra were recorded and the change in emission intensity maximum was considered as a quenching efficiency in this preliminary survey. In all cases the concentration dependence of the fluorescence quenching was recorded by changing the concentration of the metal ion. A typical emission spectrum is given below.

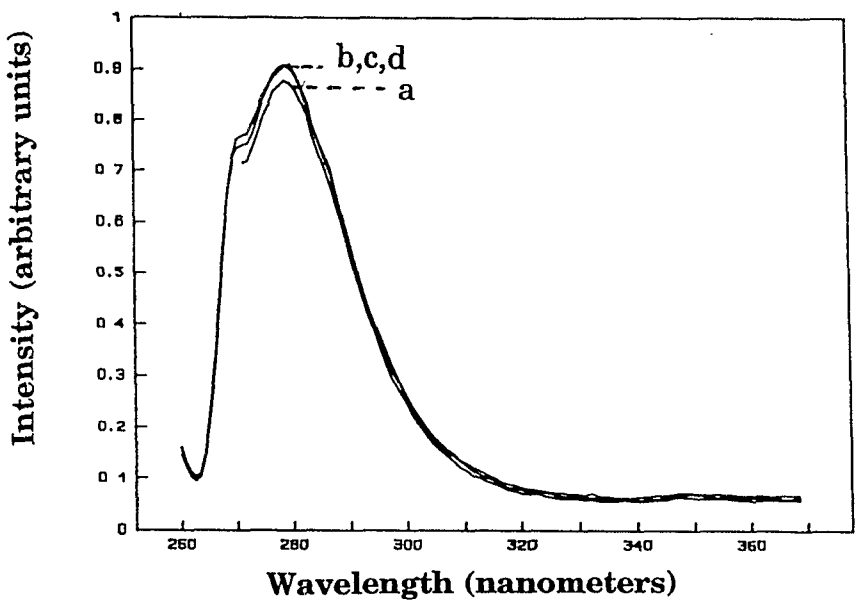

Figure *23* Emission spectrum of compound **15** (10^{-6} M in 3 ml cell) with varying concentrations of Rb^+; ExWl 250 nm, EmWl 260 nm, slits 5 mm/5 mm
a) Concentration of Rb^+ was 0.0 M in 3 ml cell
b) Concentration of Rb^+ was 3 x 10^{-4} M
c) Concentration of Rb^+ was 3 x 10^{-3} M
d) Concentration of Rb^+ was 2 x 10^{-2}M

For analytical purposes a change of less than 20% is of limited use. This typical example therefore is of little practical utility. In general, less than 20% quenching by metal ions was considered as an insignificant result. A quick glance at the results (Table *9*) indicates no significant quenching of the fluorescence by alkali metal ions in any case. These discouraging results fit well with previous studies by other groups.

Table *9* The quenching of the emission intensity of the captands **15**, **16** and **20** and bis crown ethers **28** and **29** with metal ions (expressed as a % of the metal free intensity)[*1,2,3].

Metal ion	Compounds				
	15[5]	**16**[5]	**20**[5]	**29**[4,6]	**28**[4]
Li^+	-4	-13	17	0	---
Na^+	-6	-9	11	-3	4
K^+	-2	-5	10	-1	1
Rb^+	-6	-13	13	2	---
Cs^+	-6	-8	7	-8	-8
Mg^{2+}	-3	-15	9	-5	---
Ca^{2+}	-2	0	15	6	---
Sr^{2+}	-6	-5	11	3	20
Ba^{2+}	-5	-12	12	4	25
Cu^{2+}	97[a]	99[b]	99[d]	57	86[g]
Hg^{2+}	92	90[c]	94[e]	88	93[h]
Cd^{2+}	-3	-6	12	---	---

*) + Indicates decrease in intensity and - indicates an increase in intensity
1) Concentration of fluoroionophore in 3.0 ml cell was 10^{-6} M
2) All measurements were done in 0.3 % methanol:water (v/v) unless otherwise mentioned
3) Concentration of metal ion was 0.01 M unless otherwise mentioned
4) Measurements were done in water
5) ExWL 250 nm, EmWL 260 nm; slits 5 mm / 5 mm
6) ExWL 360 nm, EmWL 370 nm; slits 5 mm / 5 mm
a) Concentration of metal ion in 3.0 ml cell was 1 mmol
b) Concentration of metal ion in 3.0 ml cell was 1.6 mmol
c) Concentration of metal ion in 3.0 ml cell was 16 mmol
d) Concentration of metal ion in 3.0 ml cell was 2 mmol
e) Concentration of metal ion in 3.0 ml cell was 24 mmol
f) Concentration of metal ion in 3.0 ml cell was 6 mmol
g) Concentration of metal ion in 3.0 ml cell was14 mmol
h) Concentration of metal ion in 3.0 ml cell was 8 mmol. --- Data not available

Only in the case of copper and mercury ions is a significant amount of quenching observed. A typical example of the emission quenching spectra of captand **20** and the Stern-Volmer plots in the presence of different amounts of Hg^{2+} is given below (Figure *24*).

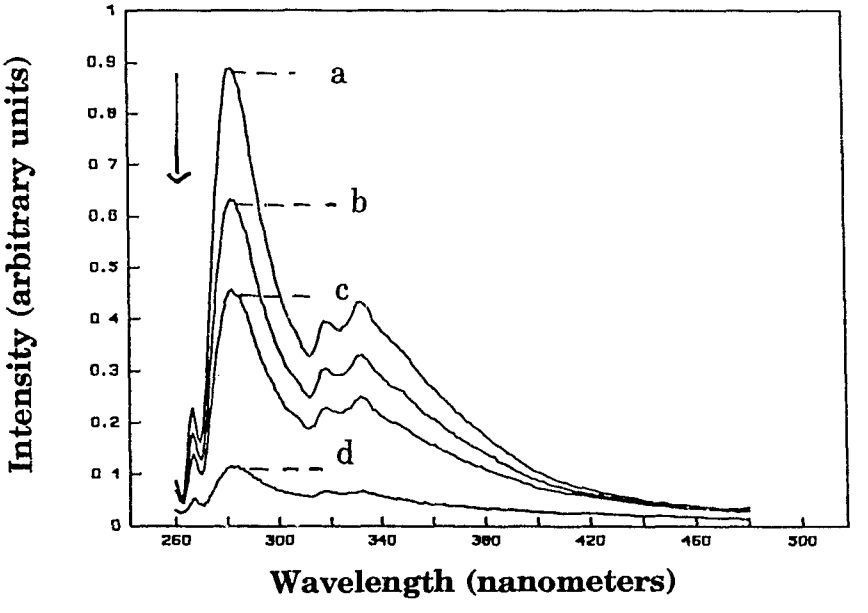

Figure *24* Quenching of emission spectra of the compound **20** with different amount of Hg^{2+}, concentration of the ligand was 8 x 10^{-6} M.
a) Concentration of Hg^{2+} was 0.0 M in 3ml cell
b) Concentration of Hg^{2+} was 4 x 10^{-4} M
c) Concentration of Hg^{2+} was 2 x 10^{-3} M
d) Concentration of Hg^{2+} was 2 x 10^{-2} M.

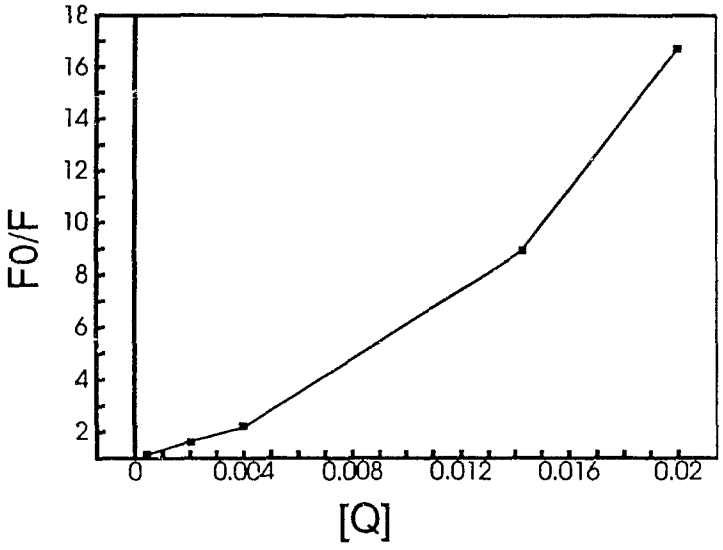

Figure *25* Stern-Volmer plot for the quenching studies of **20** with varying amount of Hg^{2+} (Emission spectrum is given as Fig. *24*)

It is clear from the above graph that the Stern-Volmer plot is not a straight line. The upward curvature indicates an association between the fluorophore and the quencher. This is common to all emission quenching studies with other fluoroionophores. The degree of upward curvature varies from one compound to the other. This can be seen in table *10* where the number of points in a straight line is different for each fluoroionophore and the r^2 values are much lower in all cases. The straight line portion of the graph was used to calculate the slope. The slope of the Stern-Volmer plot can be used to calculate the rate of quenching using the equation, provided the lifetime of the fluorophore is known in the specific solvent (water in this case).

$$F_0/F = 1 + k_q\tau_0[Q]$$

$$= 1 + K_D[Q] \qquad \text{---------- 11}$$

where K_D is the slope from the graph of F_0/F vs [Q].

Table *10* Parameters derived from Stern-Volmer plot of quenching studies Fluoroionophores[a,b]

Compounds/ Metal ion		Number of points lie on the straight line	r^2 value	Slope (x 10 M^{-1})	Intercept
15	Cu^{2+}	5	0.9874	645	0.9
	Hg^{2+}	7	0.9819	55	0.4
16	Cu^{2+}	---	---	---	---
	Hg^{2+}	4	0.9655	33	0.3
20	Cu^{2+}	3	0.9754	621	0.9
	Hg^{2+}	5	0.9839	57	0.6
28[c]	Cu^{2+}	9	0.9874	47	0.6
	Hg^{2+}	6	0.9969	16	1
29[c]	Cu^{2+}	6	0.9874	38	1
	Hg^{2+}	5	1	37	2

--- Indicates the graph was curved

a Concentration of the ligand was in the order of 10^{-4} M and metal ions Cu^{2+}, 10^{-5} M to 10^{-3} M, Hg^{2+}, 10^{-4} to 10^{-2} M.

b measurements were done in 0.3 % methanol:water (v/v)

c measurement was done in buffered aqueous medium (phosphate buffer, pH = 10)

No fluorescence life times (τ_0) of the fluorophores were available in water, because of low solubility and low intensity of the fluorescence emission. However, the life times of the *actual* fluorophores in cyclohexane is known[206]

and in a rough approximation can be used to calculate the rate of quenching of the molecules keeping in mind that the actual values of the life time in water (polar solvent) will be much less than that in a non-polar solvent (cyclohexane). The values calculated from the slope and the life time are given below

Table *11* Life time of similar fluorophores in cyclohexane[208]

Fluorophore	Lifetime in Cyclohexane
1,3-dimethyl benzene	30.8 nsec.
1,4-dimethyl benzene	30.0 nsec.
2,2'-dimethyl biphenyl	15.4 nsec.
9-methyl anthracene	4.6 nsec

Table *12* Rate of quenching (k_q $M^{-1}sec^{-1}$) of fluoroionophore with Cu^{2+} and Hg^{2+} ions calculated by using the equation *11* and parameters given in table *10*[a]

Fluoroionophores	Cu^{2+}	Hg^{2+}
15	2×10^{11}	2×10^{10}
16	-----	1×10^{10}
20	4×10^{11}	4×10^{10}
28*	8×10^{10}	8×10^{11}
29*	2×10^{10}	5×10^{10}

--- plot was highly curved,
* all mesurements were done in water
a measurements were done in .3 % methanol:water mixture

The diffusion rate constants of strong electrolytes in aqueous solution

(concentration of 0.01 M) are of the order of 10^5 cm^2 sec^{-1} and the rate of quenching observed in all cases were about five orders higher than the diffusion rate. This increase in rate can only be explained in terms of some association of the fluoroionophore and quencher. The use of lifetime of model compounds in the rate calculation may cause some error. However, the error caused by the assumption is unlikely to result in a factor of 10^5.

The application of equation 13 to separate the dynamic and static part of the quenching was carried out by plotting K_{app} vs [Q] as illustrated in figure *26*.

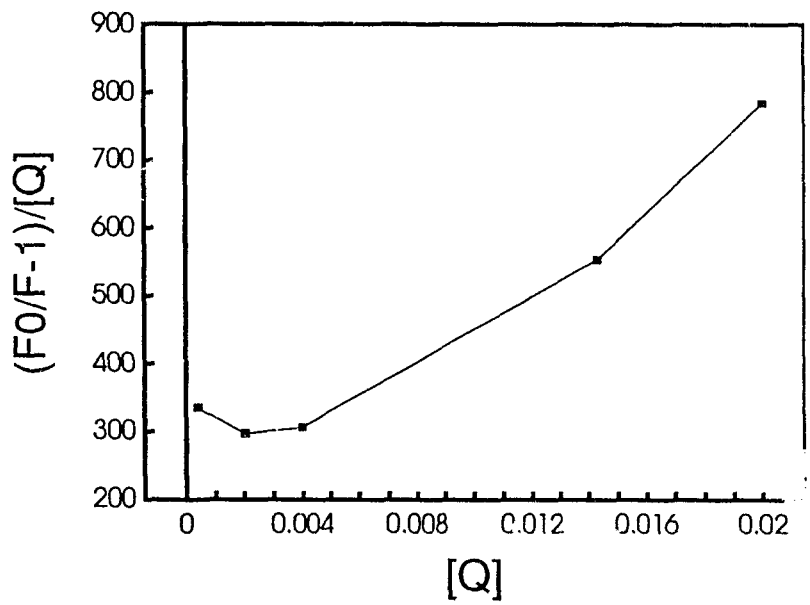

Figure *26* Plot of K_{app} versus [Q] for the quenching studies of compound **20** with Hg^{2+}

The graphs show a considerable upward curvature. The attempt to separate the quenching constant of the dynamic and static modes by equation

13 was unsuccessful as the survey data were not extensive enough and scattered considerably from the required straight line. This might be due to involvement of additional quenching processes such as the formation of 2:1 complexes. In any event, the plot of $(F_0-F/F)/[Q]$ vs [Q] showed a random distribution of points in the graph. In order to pinpoint the mechanism of quenching, a life time study is essential. Since the flourophores studied are weakly fluorescent, the life time measurement would be tedious. Moreover a cation analysis by this would be of limited utility, so an exploration along this direction was not initiated. To summarize, the upward curvature of the Stern-Volmer plot can not be explained by simple diffusion quenching, but an association of the cation and the fluoroionophore could explain increased rate of quenching as well as the upward curvature.

One other feature noted in the emission spectrum of biphenyl capped crown ether (**20**) was the presence of some structure in the long wavelength region (Figure *27*). All maxima in fig. *27* originated from a single species. This was established by recording the excitation spectra at different emission maxima. The excitation spectra were directly comparable and accounted for by a single species.

The other feature of the quenching studies of the biphenyl capped crown ether (**20**) was the appearance of a new emission band at long wavelength region (455 nm).

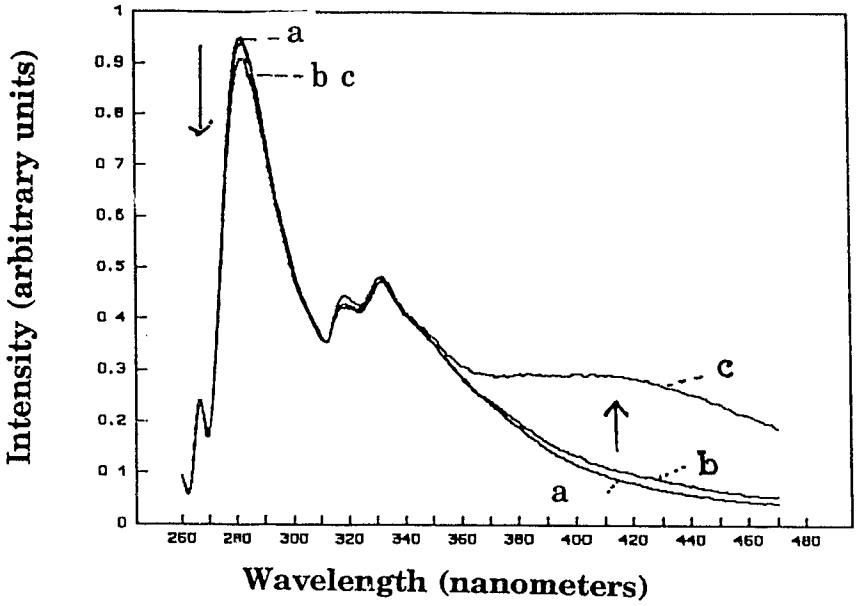

Figure 27 Effect of Na^+ ion concentration on the emission spectra of compound **20**[*,$]

* Concentration of the ligand was 8 x 10^{-6} M in 3 ml cell

$ ExWl 250 nM, EmWl 260 nM; slits 5 mm / 5 mm

a) Concentration of Na^+ in the cell was 0.0 M

b) Concentration of Na^+ in the cell was 0.001 M

c) Concentration of Na^+ in the cell was 0.02 M

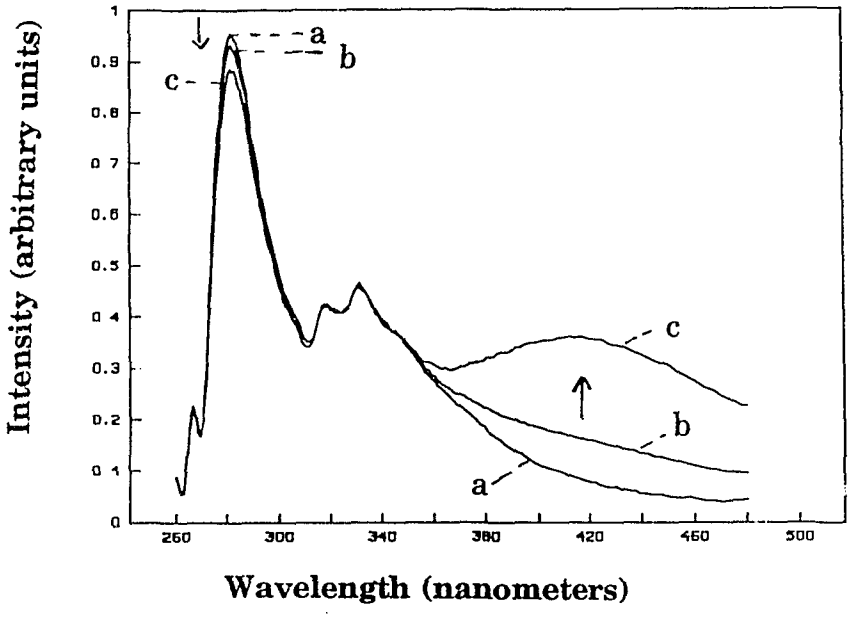

Figure 28 Effect of Cs^{2+} ion concentration on the emission spectra of compound **20**[*,$]

* Concentration of the ligand was 8 x 10^{-6} M in 3 ml cell

$ ExWl 250 nM, EmWl 260 nM; slits 5 mm / 5 mm

a) Concentration of Cs^{+} in the cell was 0.0 M

b) Concentration of Cs^{+} in the cell was 0.004 M

c) Concentration of Cs^{+} in the cell was 0.02 M

The new emission was observed only in the presence of sodium and cesium metal ions. The intensity of the emission at 455 nm increased with concentration of metal ion. The intensity of the normal emission did not decrease to a significant amount; the decrease in intensity of the normal emission band at 295nm is only 11% in the case of sodium and 7% in the case

of cesium. However, the increase in the emission band at 455nm is significant. In principle, this change can be used to exploit the possibility of a Na^+ or Cs^+ selective fluoroionophore.

The identification of the species responsible for this emission is very difficult to establish on the current experimental evidence. This baffling result is only seen in the presence of sodium and cesium ions. A reasonable explanation might be based on excimer formation of the biphenyl capped crown ether with the metal ion provided that the excimer emits much more intensely than the parent captand molecule. The slight decrease in intensity of the emission at 295nm could be due to the depletion of a population of either ground state or excited state of the free ligand to form an excimer. Since the intensity of emission was proportional to the concentration of metal ion, the excimer is presumably an inclusion complex of metal ion and the captand molecule. The scope of this project was to survey the ligands. This interesting observation was not pursued thoroughly due to the lack of understanding of the process, but offers some potential for a fluorescent assay, at least for Na^+ and Cs^+ cation.

4.3.4.b Fluorescence quenching studies in the Bis crown ether series.

The bis crown ether compounds synthesised from m-xylylenediamine (**28**) were highly soluble in water whereas the 9,10-bis(aminomethyl)anthracene derivative (**29**) was only soluble in water: methanol (92:8 v/v). All fluorescent studies were done in a buffered (pH 10) medium. The emission intensity was recorded as a function of wavelength at different metal ion concentrations. The required metal ion concentration was achieved by dilution of a standard solution (0.1 M) of the salts. The change in emission intensity at the emission maxima was used for determining the quenching efficiency. The alkali metal cations studied were Na^+, K^+, Rb^+ and Cs^+ and the alkaline earth metals used were Mg^{2+}, Ca^{2+}, Sr^{2+} and Ba^{2+}. The data are given in table *9*.

The fluorescence intensity was not significantly quenched by alkali or alkaline earth metal cations. Quenching by copper and mercury ions was observed as in the case of captands. As mentioned in the previous case, separation of the static and dynamic quenching constants was difficult and was not pursued to a great extent.

The association of the ligand with copper and mercury can be considered to explain the quenching. As will be discussed below, the stability constant measured from the potentiometric titration and the stability constant measured from the fluorescence studies are comparable within the error limits

of the techniques. The potentiometric titration values are based on the equilibrium of the host and the guest whereas the fluorescence data assumes a 100% complexation between the two species.

The suitability of these water soluble ditopic co-receptors (bis crown series) derived from the acid crowns, for multiple recognition still needs to be explored. Premedesa et al have shown that linear diammonium salts do bind with this type of ditopic host molecule. Since the structure of the anthracene bis crown ether is very close to the molecules designed by previous authors, an efficient selective quenching by the linear diammonium guest species also might be anticipated in this case.

4.3.4.c Absorbance studies of the chromoionophhores

Both compounds **30** and **31** were soluble in water, hence all uv studies were done in water. A typical sample solution comprised a fixed volume of the crown ether stock solution, a variable volume of metal ion solution and dilution to 2.5 ml with a pH 10 buffer solution.

The cation dependence of the uv-spectrum of the diacid derivative **30** was observable (Figure *30* and *31*). There are two changes in the uv spectra of the compounds due to addition of metal ions. The first is a bathochromic

shift in the absorption maxima ($\Delta\ \lambda_{max}$). The second observation is a change in intensity of the absorption spectrum with the nature of the metal ion. In general, as the phenolate is stabilised, the intensity of the absorption increased. The order of decrease in intensity among alkali metal ions is $K^+ > Na^+ > Rb^+ > Cs^+ > Li^+$ and among the alkaline earth metals is $Sr^{2+} > Ba^{2+} > Ca^{2+}$. The cavity available for a cation to occupy is modified by the functionalisation of the acid group. A pendant phenolic group presumably can only participate in cation binding in case of metal ions which have an optimum fit in the cavity (Figure 29).

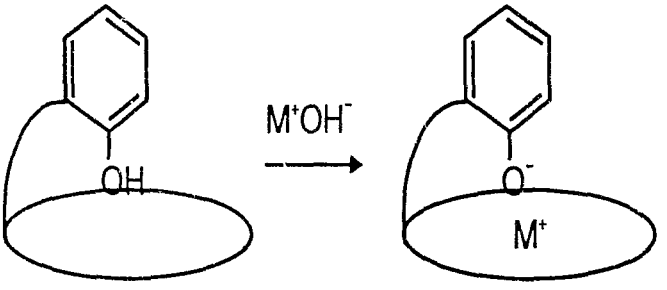

Figure 29 Cartoon of the metal complexation of compound **30**

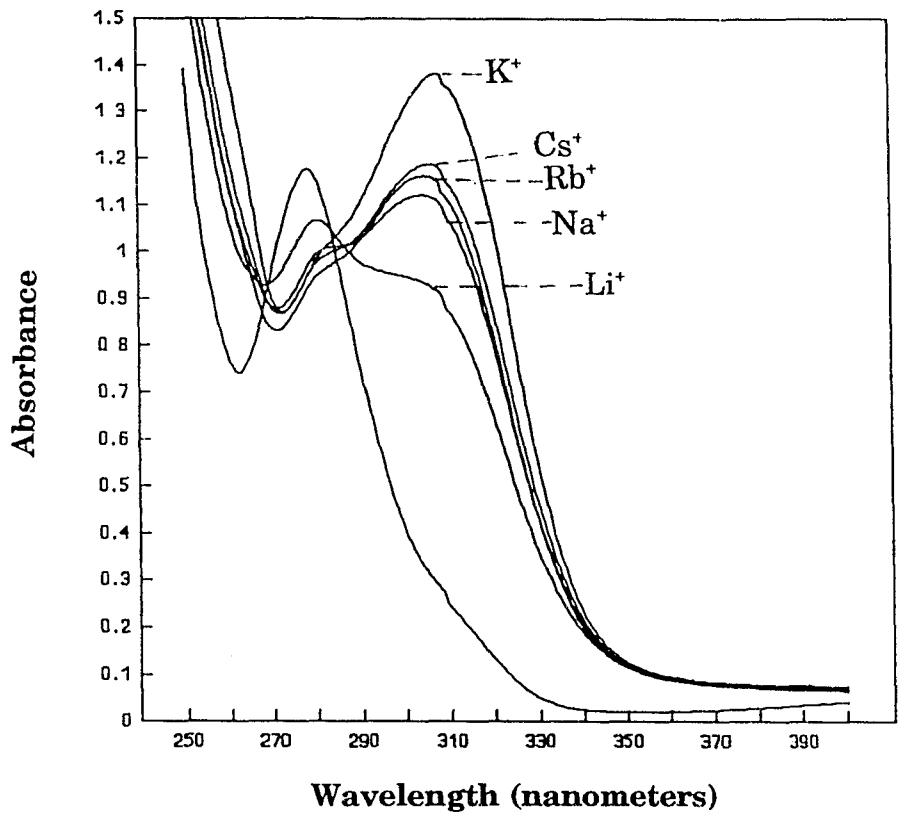

Figure *30* Effect of alkali metal ions on uv-spectrum of compound **30**[*,$,a]
* uv-spectra were taken in water, (buffered, pH=10)
$ Concentration of the ligand was 10^{-4} M
a) concentration of metal ion was 0.01 M in all cases

Since the K^+ has size compatibility with the crown ether cavity, it stabilises the phenolate ion much more than any other cations. The sequence of metal ion complex stability constants derived from this picture follows the crown ether selectivity derived from potentiometric titration (Sect. 4.3.5.c). In

both cases, as the metal ion radius increases, the size compatibility between the metal ion and the cavity is reduced and the binding constant decreases. This relationship also applies to other alkali metal ions in the same group.

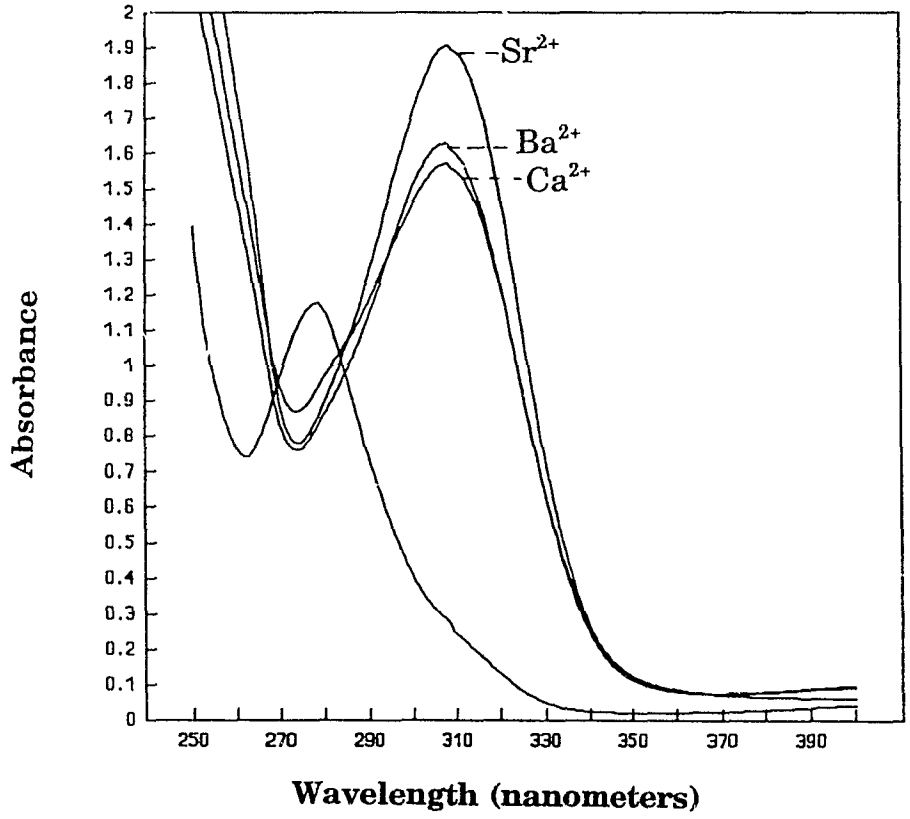

Figure *31* Effects of alkaline earth metal ion concentration on absorption spectrum of compound **30**

* uv-spectra were taken in water, (buffered, pH = 10)

$ Concentration of the ligand was 10^{-4} M

a) concentration of metal ion was 0.01 M in all cases

Rubidium and cesium interact with the phenolate in the decreasing order due to the increase in size. Lithium, being the smallest, has a stability constant that is the lowest because it interacts very poorly with phenolate ion. The same trend follows in the alkaline earth series with strontium giving the highest intensity.

The uv studies of the 2-aminophenol derivative of the crown ether tetraacid (**31**) did not show changes in the presence of metal ions. The lack of influence of the metal ion on the absorption spectrum indicates that the phenolates do not participating in cation binding. Since the compound was synthesised in the presence of triethylamine the *syn* isomer could be the most favourable product.

The question of why the phenolate does not participate in cation binding in the *syn*- isomer needs to be addressed. The reasonable approach to this problem is to look at the stability of the cation complex on either side of the crown ether. The carboxylate, being a good donor, will provide a stronger electrostatic component of the complexation with cation, and the complex will have a structure where the cation approaches the crown ether on the side opposite to the phenolic groups. This will effectively decrease the interaction of cation with the phenolic group because of the large distance.

4.3.5 Stability constant determination by potentiometric titration

Molecular recognition phenomena are defined in terms of the interaction of molecules with each other. The strength of this interaction depends on the properties of the two interacting molecules. The strength of interaction, which is an accumulation of the forces taking part in the interaction, is quantified in terms of stability constants. Understanding the chemical equilibria involved in the molecular process opens the door to the level of molecular recognition between the two interacting molecules[209].

For an equilibrium of a crown ether (Cr) and a cation M^+ to form a complex (CrM^+)

$$Cr + M^+ \underset{k_2}{\overset{k_1}{\rightleftharpoons}} CrM^+ \qquad \text{---------- 22}$$

$$K_{th} = \frac{\gamma_C[CrM^+]}{\gamma_L[Cr]\gamma_M[M^+]} \qquad \text{---------- 23}$$

where γ represents the activity coefficient and K_{th} is the thermodynamic stability constant. Since the activity coefficients are not known in most cases the equation can be rewritten as

$$K_S = \frac{[CrM^+]}{[Cr][M^+]} \qquad \text{---------- 24}$$

where the K_S is known as a concentration stability constant. The value of K_S can be measured by a variety of analytical techniques such as calorimetry,[210,211]

potentiometric titrations with ion selective electrodes,[212,213] spectroscopic studies (uv,nmr)[214-215] and conductometry.[216-219] All these methods are suitable only in the special case where the properties of the host, the guest and the complex species are the deciding factors. For example, spectrophotometry (uv-vis) can be used only when the host has a chromophoric appendage whose electronic properties are perturbed by the guest species due to complexation. Potentiometric titrations can only be used for equilibria where a component of the reaction can be detected (H^+ by pH electrode, M^+ by ion selective electrode).

In the case of a ligand with ionisable protons, a large number of equilibria exist in solution depending upon the protonation and deprotonation of the macrocycle. The stability constant is more usefully described as a cumulative association constant defined by the equilibrium between "l" ligands of charge z^-, "m" cations of charge y^+ and "h" protons

$$lL + mM^{y+} + hH^+ == L^{z-}{}_l M^{y+}{}_m H^+{}_h \qquad \text{---------- 25}$$

$$\beta_{lmh} = \frac{[L^{z-}{}_l M^{y+}{}_m H^+{}_h]}{[L^{z-}]^l[M^{y+}]^m[H^+]^h} \qquad \text{---------- 26}$$

where β_{lmh} is the cumulative association constant and the integers l, m and h represent the number of ligands, number of metal ions and the number of protons. The possible equilibria which exist in the case of a ligand with two ionisable protons can be written as

Equilibria of ionisation (acidity constants)

$$H_2L \rightleftharpoons 2H^+ + L^{2-} \quad K_{a1} = 1/\beta_{102} \qquad \text{----- 27}$$

$$HL^- \rightleftharpoons H^+ + L^{2-} \quad K_{a2} = 1/\beta_{101} \qquad \text{----- 28}$$

$$H_2L \rightleftharpoons H^+ + HL^- \quad K_{a3} = \beta_{101}/\beta_{102} \qquad \text{------ 29}$$

Equilibria of complexation

$$M^+ + L^{2-} \rightleftharpoons LM \quad K_{s1} = \beta_{110} \qquad \text{--------- 30}$$

$$H^+ + M^+ + L^{2-} \rightleftharpoons HLM \quad K_{s2} = \beta_{111} \qquad \text{--------- 31}$$

$$M^+ + HL^- \rightleftharpoons HLM \quad K_{s3} = \beta_{111}/\beta_{101} \qquad \text{--------- 32}$$

In the above mentioned equations concerning the different equilibria, the equation 28 represents the acidity constant of HL^-. By the definition of β_{lmh} the acid dissociation constants for equation 27 and 28 are denoted as $(\beta_{102})^{-1}$ and $(\beta_{101})^{-1}$. So the normal acid dissociation constant of the ligand represented by equation 29 can be derived from the first two equations as β_{101}/β_{102}. Now the pK_{a1} and pK_{a2} can be calculated as

$$pKa_1 = -\log K_{a2} = -\log (\beta_{101})^{-1} \qquad \text{---------- 33}$$

$$pK_{a2} = -\log K_{a3} = -\log (\beta_{101}/\beta_{102}) \qquad \text{--------- 34}$$

by expansion and substitution,

$$= \log (\beta_{102}) - pK_{a2} \qquad \text{---------- 35}$$

By the same logic, the log of stability constant is given by,

$$\log K_S = \log [(\beta_{111} - \beta_{101})] \qquad \text{---------- 36}$$

and by rearranging the equation

$$\log K_S = \log (\beta_{111}) - pK_{a2} \quad \text{---------- 37}$$

The titration of ligands in the absence of metal ions with a standard base leads to the values of β_{101} and β_{102} and hence pK_{a1} and pK_{a2} from the β values. The β values are calculated from the titration data together with electrode slope, intercept, pK_w of the medium and the concentration of ligand and titrant. The program SCOGS[216] uses these data to generate β values by non-linear least squares. In order to achieve true concentration stability constants the pH meter to be used as a device to determine the concentration rather than the activity (a_{H+}) of the protons in the solution. There is a linear relation between the meter reading and pC_{H+},

$$pH_m = s\,(pC_{H+}) + b \quad \text{---------- 38}$$

where pH_m is the pH meter reading, "s" is the slope typically very close to 1, pC_{H+} is the concentration of H^+ and "b" is the intercept. Values of s, b and the pK_w for the supporting electrolyte can be determined from a strong acid strong base titration. According to Jameson and Wilson's analysis[217]

$$\log K_w = (pH_{m1} + pC_{HO^-}) + pC_{H+} - pH_{m2} \quad \text{--------- 39}$$

where pH_{m1} refers to the reading in the alkaline region and pH_{m2} in the acidic region of a strong acid/strong base titration and

$$b = pH_{m2} - pC_{H+} \quad \text{---------- 40}$$

The stoichiometric concentration of H^+ and HO^- can be calculated at each point on the titration curve after applying the correction factor for dilution. In the strong base buffer region (> pH 11.5) the sum of the average value of pH_{m2}

- pC_{OH^-} and -b gives the $-pK_w$. By using all these correction values, the concentration based β can be calculated. This can be converted to the thermodynamic quantity by substituting the activity correction using a modified Debye-Huckel expression.

$$pK_a' = pK_a - 2\log \gamma_{\pm} \qquad \text{---------- 41}$$

where pK_a' is the activity based term and pK_a is the concentration based term.

In the case of ligands containing ionisable protons, the β values were determined using a pH sensitive glass electrode and calomel electrode as reference electrode. The typical solution in the cell comprises a fixed volume of the ligand solution with ionic strength set with tetramethylammonium nitrate. A standard solution of tetramethylammonium hydroxide was used as a base and was added by an automatic burette controlled by an HP85 microcomputer. The pH of the solution was recorded with each aliquot addition of titrant to the cell under constant stirring, along with the time of equilibration and the volume of the titrant added. The results were then analyzed by using the program SCOGS and the pK_as were calculated. The titration was repeated in the presence of a fixed amount of metal ion in the cell along with the ligand. The pH changes were recorded and analyzed with the determined acidity constants to give the β values and hence the stability constants.

For neutral ligands, pH metric titration is not appropriate. In such cases, the free metal ion concentration can be directly measured using ion

selective electrodes. Consider the equilibrium

$$L + M^+ \rightleftharpoons LM^+ \qquad \text{---------- 42}$$

$$\text{where} \quad K_S = \frac{[LM^+]}{[L][M^+]} \qquad \text{---------- 43}$$

From mass balance considerations

$$[L]_{tot} = [L]_{free} + [LM^+] \qquad \text{---------- 44}$$

$$\text{and} \quad [M^+]_{tot} = [M^+]_{free} + [LM^+] \qquad \text{--------- 45}$$

$$\text{thus} \quad K_S = \frac{([M^+]_{tot} - [M^+]_{free}}{([L]_{tot} - [M^+]_{tot} + [M^+]_{free})([M^+]_{free})} \qquad \text{------- 46}$$

where $[L]_{tot}$ and $[M^+]_{tot}$ are the initial concentrations of ligand and metal ions respectively whereas $[L]_{free}$ and $[M^+]_{free}$ represent the concentration of uncomplexed ligand and metal ions at equilibrium. The ion selective electrode must be calibrated under conditions closely similar to the conditions of the K_S titration. A series of calibration curves were compared and repeated until close agreement in slope and intercept was obtained. Using the well behaved and calibrated electrode, a ligand solution is titrated with the metal ion of interest to give a series of points where K_S can be evaluated from equation 46. The most reliable values of K_S are those in which the ligand is approximately half complexed; points were evaluated and retained for $0.2 < [ML^+]/[L]_{free} < 0.8$.

In the case of neutral ligands such as the captands, the titrations were done with a cell consisting of a potassium ion selective electrode and a calomel

reference electrode. The fixed volume of the standard ligand solution was taken in the cell with tetramethyl ammonium nitrate solution to control ionic strength. A water-methanol mixture (1:1, v:v) was used in case of captands to prepare the standard solution and titration. The titrant was added to the cell by using an automatic burette controlled by a microcomputer and the electrode response to the excess potassium in the solution was recorded after each addition from the burette. The electrode response was monitored and recorded along with the time taken for the equilibration. At each point in the titration, $[M^+]_{free}$ was determined from the calibration parameters of the electrode. Given the initial concentration of ligand corrected for dilution, the value of K_S at each point was calculated. The K_S values for the points having $0.2 < [LM^+]/[L]_{free} < 0.8$ were averaged to give the reported values (Table *13*)

4.3.5.a Discussion of the stability constants of Captand series

Before discussion of the data, the factors which affect complex stability need to be explored briefly. The lock and key mechanism[14] proposed in the early stages of crown ether chemistry is still applicable in all cases, but inadequate to explain the selectivity patterns shown by flexible ligands such as lariat crown ethers and tartaric acid crown ethers. In general, the stability of a complex can be attributed to factors such as electrostatic effects, ligand topology, the number and nature of the ligating atoms in the macrocycle and solvent effects. The electrostatic factor plays a major role for a charged

ligand[185]. A good example of this factor is the increased stability of the cation complexes of tartaric acid based crowns especially crown ether tetra and hexaacids in comparison to neutral crown ethers. These ligands showed the highest stability constant so far reported for alkali metal ion complexation in water at pH 7.

The stability constants for K^+ complex formation in the captand series were determined by potentiometric titration using a potassium selective electrode. The unavailability of other metal ion selective electrodes restricted further exploration of complexation properties of these ligands with other metal ions. The stability constants are larger than neutral crown ethers but considerably smaller than the cryptand series. Table *13* gives a comparison of the values.

Table *13* Logarithm of stability constants of K^+ complex of Captands and related compounds [a,c]

metal ion	**15**	**16**	**20**	18C6[b]	$B_2$2.2.2[b]
K^+	2.8	3.0	3.6	2.2	4.4

a: 1:1 water:methanol mixture, determined at 25 °C, I = 0.1M made up with $Me_4NO_3^-$
b: water solvent
c: uncertainty in the values is ± 0.2

The cryptand series synthesised by Lehn[4,10] showed high stability

constants for alkali metals. The topology of a captand is similar to cryptand (2.2.2). The decrease in the complexation towards potassium could be explained by considering the structural difference of the ligand. Even though the ligand is preorganised to a great extent to permit ion binding, the lack of flexibility and the relatively low number of ligating atoms in the three dimensional cavity must be responsible for the modest association constants. In the case of a cryptand, a three dimensional hydrophillic cavity could be envisaged to accommodate the cation, where the binding sites are distributed uniformly throughout the cavity. The other factor could be the hydrogen bonding of the amide NH-CO to a ring oxygen atom which was observed both by nmr and crystal structures of the compounds (Table *18*, *19* and *20*). The low binding constants of cyclic peptides have previously been were attributed to the collapse of the cavity by intramolecular hydrogen bonding.[220] The same analogy could be taken to a certain extent in this case also.

4.3.5.b Discussion of the stability constants of the bis crown ether series

Table *14* gives the acidity and stability constants of the bis crown ether ligands studied. The values are based on concentrations and are expressed as cumulative constants. The values in parentheses represent the stepwise formation constants.

Table *14* Logarithm of cumulative stability constants and stepwise formation constants[a] of bis crown ethers **28** and **29** in comparison to the parent compounds.

Metal ion	Stoichiometry	Compounds		
		28	**29**	**13**
H^{+b}	101 102	4.08 7.78(3.70)	4.42 8.09(3.67)	4.37 7.0(2.72)
Li^+	110 111 120	--- --- ---	2.3 * *	--- --- ---
Na^+	110 111 120	--- --- ---	2.7 * *	3.3 6.7(2.4) *
K^+	110 111 120	2.8 * 6.3	3.6 * *	4.2 7.6(3.2) *
Rb^+	110 111 120	1.9 * *	3.6 * *	--- --- ---
Cs^+	110 111 120	2.4 * *	3.3 * *	--- --- ---
Ca^{2+}	110 111 120	3.0 * *	3.7 * *	5.6 * *
Sr^{2+}	110 111 120	4.1 * 7.5	4.4 * *	5.9 8.9(4.2) *
Ba^{2+}	110 111 120	4.1 * 7.2	5.2 * *	6.5 * *
Cu^{2+}	110 111 120	* * 6.3	2.9 * *	--- --- ---
Hg^{2+}	110 111 120	* * 7.0	3.8 * *	--- --- ---
Cd^{2+}	110 111 120	--- --- ---	2.7 * *	3.0 * *

see the foot notes on next page

a: Determined at 25 °C, I = 0.1 M with Me_4NNO_3 in water, the values in parenthesis represent 1:1 association of M^+ and the ligand. The symbol * indicates the complex of the given stoichiometry was not detected. --- indicates the system was not examined. Uncertainty acidity constants in log β_{l0h} is ± 0.1; in association constants in log β_{lmh} is ± 0.2.
b: The logarithm of dissociation constants follows the conventions of pK_a

The numbers 102, 110 etc. indicate the stoichiometry of the complex as defined previously ie, 102 refers to a one ligand, 0 metal and 2 proton complex stoichiometry. The data collected were comparable to similar ligands and follow the expected trends. As expected the 110 complexes are uniformly more stable than the 111 complexes. This can be seen in the case of alkaline earth metals more clearly than the alkali metals where electrostatic effects will be more pronounced due to the higher charge.

In the case of compound **28**, the crown ether rings are more organised to give the 1:1 complex rather than 1:2 complex. The complexation stability depends on the size of the cavity as well as the bis crown alignment. The 110 complexes of Li^+ and Na^+ were not detected. The stability of the K^+ complex is in the expected range for a monocharged crown ether ligand. Bis crown ether series reported in the literature with flexible spacers gave good selectivity towards potassium in the presence of sodium. Moreover a bis crown ether with a cyclohexane ring showed a conformation dependent selectivity; the cis isomer showed an excellent potassium selectivity while the trans isomer failed to do so. This implies a conformational requirement of crown ether rings for complexation. The stability constants for potassium are higher than for

other alkali metals. The 120 complex for K^+ also showed the stability constant in the same range. The increase in stability of cesium when compared to rubidium, may be due to a sandwich complex formation which is common in the case of other bis crown ethers. The alkaline earth cations showed the same trend as expected. Because of the size difference between the Ca^{2+} and Sr^{2+}, the latter could prefer a sandwich complex and thereby achieve a higher stability constant.

The bis crown ethers synthesized from 9,10-bis(aminomethyl)anthracene (**29**) showed the stability constant order typical of a monocharged 18-crown-6 derivative. The selectivity is rather poor due to the lack of communication between the two crown ether units. The conformational orientation of the two crown ether rings could be anti to each other hence a sandwich complex is very unlikely. Even in the *syn* orientation the distance between the two crown ether rings (7.0 -8)Å) estimated from models is much higher than the diameter of any alkali or alkaline earth metal ion. This can be supported from the experimental observation by de Silva and Sandanayakake[162] on the fluorescence quenching studies of aza-crown ether based bis crown with anthracene as the spacer. The maximum stability of a diamonium salt with a spacer of 4 to 5 CH_2s (~ 5 to 6 Å), indicates the optimum average distance between the two crown ether moieties. The data are consistent with the two crown ether units which behave as separate units.

4.3.5.c Complexation of Phenolic crown ether derivatives.

Table *15* gives acidity constants and logarithms of cumulative association constants for the phenolic crown ethers. The acidity constants for the carboxyl groups and the phenol are in the expected range when compared to similar compounds. The case of *syn* (**30**) is more complex due to the presence of the small amount of the *anti* isomer (**31**) as seen by nmr. The peaks with an intensity ratio 1:3 to the intense peak due to the *syn* isomer, was accounted for the *anti* isomer.

Table *15* Logarithm of acid dissociation constants of compound **30** and **31**[a,b] in comparison to the parent crown ether **12** and **13**

Stoichiometry	**31**	**32** (anti-isomer)	**31** (syn-isomer)	**13**	**12**
101	10.24	*	11.0	4.37	4.88
102	14.0(3.76)	*	20.39(9.29)	7.09(2.72)	9.17(4.29)
103	‡	5.85	24.16(3.77)	‡	12.01(2.84)
104	‡	10.21(4.36)	27.61(3.45)	‡	14.14(2.13)

a: Determined at 25 °C, I = 0.1 M with Me_4NNO_3 in water. The symbol * indicates a proper fit was not obtained and ‡ indicates stoichiometry is inappropriate for the ligand. --- indicates the system was not examined. Uncertainty acidity constants in log β_{10h} is ± 0.1; in association constants in log $\beta_{1n,h}$ is ± 0.2.
b: The logarithm of dissociation constants follows the conventions of pK_a

Previous studies in Lehn's laboratory[187-189] have shown that by using triethylamine as base, exclusive formation of the *syn*-isomer can be achieved.

Exclusive formation of face discriminated (*syn*) isomer was reported when the dianhydride from the 18-crown-6 tetracid was reacted with aniline, 1-amino-naphthalene in presence of triethyl amine. The same observation was repeated in the reaction of dianhydride from the crown ether tetraacid and tempamine[193]. Only the *syn* isomer was obtained in presence of triethyl amine.

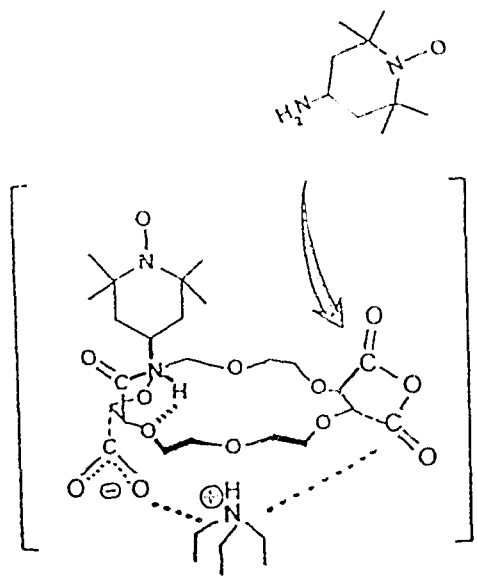

Figure *32* Schematic diagram of opening of the anhydride rings by the attack of the amine[193]

The electrostatic interaction of triethylamine with the newly formed acid group from the reaction of the first molecule of tempamine with one of the anhydride, blocks one side of the crown ether and forces the second tempamine molecule to attack from the opposite side to base (same side to the first tempamine molecule) was postulated for this interesting observation[195] (Fig *32*).

Syn

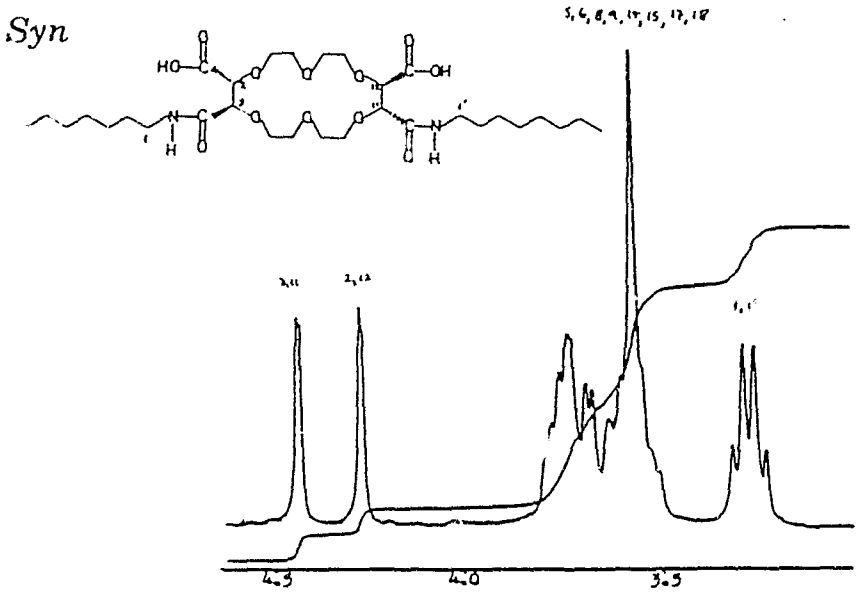

Anti

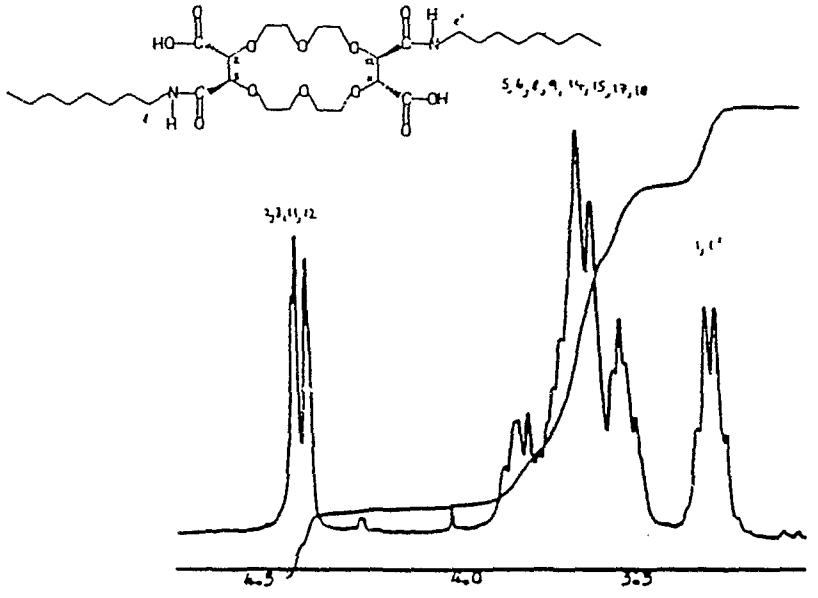

Figure *33* ^{1}H nmr of the *syn* isomers isolated and characterized by D.M Whitfield[221]

The same analogy can be used to explain the formation of *syn* isomer. The other evidence was the low coupling constant of the methine protons. So the compound was identified as *syn*- isomer. Comparison of ^{1}H nmr of *syn* isomer prepared in this laboratory by D. M. Whitfield from diacid confirms that the compound isolated was in fact a *syn* isomer[219] (Figures *33* & *34*).

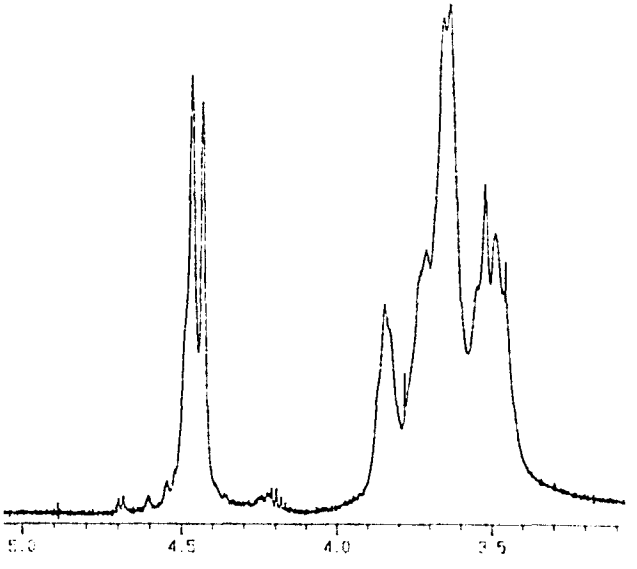

Figure *34* ^{1}H nmr of compound **31** (ring protons)

Using the ^{13}C peak intensities for comparable resonances gave a ratio of 0.28 for *anti* / *syn* isomers. The difference in the positions of the comparable signals from separate isomers were 0.3 ppm and less characteristic. The titration data were analyzed assuming two ligands at this ratio. All four pK_as

of the *syn* isomer were simple to determine, but the phenolic pK_as of the *anti* isomer were insufficiently prominent in the data to permit their determination. The carboxylic acid pK_as of *syn* and *anti* isomers are sharply differentiated and this allowed the separate determination of values for the *anti* isomer. The concentration ratio was too low to permit these values to be determined with high precision. Nonetheless, it is clear that ΔpK_a for the *syn* isomer carboxylic acids (3.77 - 3.45 = 0.32) is much smaller than the ΔpK_a for the *anti* isomer (5.85 - 4.36 = 1.49). This is contradictory to the previous observation where the difference in pK_as of the *anti* isomer is lower than the difference in pK_as of the *syn* isomer.[221] This might be explained by considering the potential for strong hydrogen bonding between the phenol and carboxyl group in the *anti* isomer as well as the acidic proton in a more shielded environment by the phenolic ring. Since the titration medium was water in this case, the hydrogen bonding between the two *syn*- carboxyl groups will be weaker than the methanol solution used in previous measurements.

Table *16* Logarithm of cumulative stability constants and derived stepwise formation constants[a] for phenolic crown ethers **30** and **31** in comparison to the parent compounds **12** and **13**

Metal ion	Stoichiometry	Compounds			
		30[c]	**31** (*syn* isomer)	**13**	**12**
Li^+	110 111	3.1 12.7(2.5)	3.6 ---	--- ---	--- ---
Na^+	110 111	3.4 12.0(1.8)	4.6 14.1(3.0)	3.3 6.7(2.4)	4.5 9.0(4.1)
K^+	110 111	4.1 12.7(2.5)	5.3 14.7(3.6)	4.2 7.6(3.2)	4.8 9.6(4.7)
Rb^+	110 111	3.1 11.8(1.6)	3.9 14.8(3.7)	--- ---	--- ---
Cs^+	110 111	3.1 12.2(2.0)	3.5 14.4(3.3)	--- ---	--- ---
Ca^{2+}	110 111	4.28 12.7(2.5)	6.1 14.7(3.6)	5.6 ---	8.6 11.9(7.0)
Sr^{2+}	110 111	5.5 13.8(3.5)	6.5 14.6(3.5)	5.9 8.9(4.2)	8.0 10.9(6.1)
Ba^{2+}	110 111	5.5 14.0(3.7)	5.7 14.3(3.2)	6.5 ---	7.2 11.0(6.2)

a: Determined at 25 °C, I = 0.1 M with Me_4NNO_3 in water, the values in parenthesis represent 1:1 association of M^+ and the ligand. The symbol --- indicates the system was not examined. Uncertainty acidity constants in log β_{10h} is ± 0.1; in association constants in log β_{1mh} is ± 0.2.
b: The logarithm of dissociation constants follows the conventions of pK_a
c: uncertainty is ± 0.4

The values for alkali and alkaline earth metal ions fall in the expected order with K^+ ion having a maximum stability constant among the alkali metals and strontium having the maximum in the alkaline earth series. The

relatively high value of the stability constants when compared to other diacid derivatives indicates the contribution of the phenol in stabilising the complex. Due to the diaxial orientation of the carboxyl groups of the tartaric acid unit, the phenolic units are aligned properly to enhance the coordination (Fig. *29*). An evaluation of the CPK model of the complex is consistent with this hypothesis.

In the case of tetraacid derived crown ether **31**, the stability constants observed were comparable to the parent crown ether tetraacid. In the case of the alkali metal ions, there is a slight increase in the stability constant possibly due to the participation of phenolic oxygen in cation binding. The stability constants for the alkaline earth cations were less than that reported for the parent tetraacid crown. This could be attributed to the removal of strong alkaline earth metal binding carboxylate groups by the linkage of phenolic groups through amide bonds to the tetracid. The order of the selectivity among the alkali metal ions is exactly same as the parent crown ether ie, $K^+ > Na^+ > Rb^+ > Li^+ > Cs^+$. The enhancement of the lithium complex stability could be attributed to the strong interaction of phenolic groups with Li^+ ions.

In general, the trends among the macrocycles are the same as observed in the case of the parent crown ethers. This factor is very important, because the known properties of the ligand need to be maintained to establish a good sensor for metal ions. A change in selectivity of the ligand after modification

or addition of a chromophoric unit would defeat the premise of incremental design of cation sensors.

4.3.6 Stability constants from Fluorescence intensities

The stability constants of the crown ether can also be determined from the quenching titrations.[222] The binding constants were calculated by using the equation where the assumption was the quenching observed was due to metal ion association only. The appropriate form of the equation is

$$(F_0 - F_S)/F_S = K_S \{S - [(F_0 - F_S)/F_0]\} C \qquad \text{---------- 47}$$

$$\log K_S = \frac{(F_0 - F_S)/F_S}{\{S - [(F_0 - F_S)/F_0]\} C} \qquad \text{---------- 48}$$

where K_S is the binding constant, F_0 and F_S are the emission intensities of the macrocycles (**15,16**) at 285 nm and for host (**20**) at 405 nm, in the absence and in the presence of different concentrations of the quencher, C is the concentration of the host and S is the molar ratio of the host to guest. The data obtained are given in table *17*; th numbers given in parenthesis are obtained from the potentiometric titrations and are the average of the values were reported. Only values for Cu^{2+} and Hg^{2+} were calculated by this method, since the quenching of the emission spectrum by other metal ions was insignificant (<20%).

Table *17* Stability constants for the host molecules from fluorescence quenching titrations[a,b]

Metal ions	Compounds				
	15	**16**	**20**	**28**[c,d]	**29**[c,d]
Cu^{2+}	3.7	4.0	3.9	2.6 (3.1)	2.6 (2.9)
Hg^{2+}	2.5	2.5	2.6	3.2 (3.5)	3.1 (3.8)

a: uncertainty in the values is ± 0.2
b: determined at 25 °C in 0.3 % methanol in water
c: determined at 25 °C, in a buffered medium (phosphate buffer pH = 10)
d: the values in parenthesis represents the values from potentiometric titrations

The major result is the relatively high stability constant for Cu^{2+} in the captand series and the somewhat lower value in bis crown ether series. The reverse is the case for mercury. This could be attributed to the size difference of the two metal ions. The smaller cation Cu^{2+} can penetrate into the cavity of captands much more easily than the larger Hg^{2+}. In the case of the bis crown series the bigger cation could form a sandwich complex more easily than the smaller one. The other significant observation is that the values obtained from the potentiometric titration and the fluorescence titration differ significantly in the case of the bis crown series. This could be due to the nature of the complex detected during the analysis. The fluorescence technique assumes a 1:1 complex and the further assumption that the amount of quenching observed is exclusively due to the static mode. The dynamic part

of the quenching would be a source of error in the stability constant determination. In potentiometric titrations with ion selective electrodes, the equilibrium concentrations of the complexed and free metal ions are monitored.

The mechanism of quenching by Cu^{2+} and Hg^{2+} could be due to either electron transfer or energy transfer. Both these metal are known electron scavengers and the reports of their quenching other fluorophores have also been studied previously.[135,156] The absolute mechanism of quenching by these metal ions can not be ascertained with the survey data obtained here.

4.3.7 Quenching of fluorescence by Cations or Anions ?

The challenge of developing an anion selective macrocycles is much greater than the counterpart of cation sensors: the size and degree of hydration of simple anions are much higher than cations,[223] and cations are generally spherical in shape whereas anions exist as linear (N_3^- SCN^-), trigonal (NO_3^-, CO_3^{2-}) spherical (halides), bent (NO_2^-), tetrahedral (PO_4^-, ClO_4^-, SO_4^{2-}) and irregular (HCO_2^-, $P_2O_7^{4-}$) shapes. One of the requirements for maximum binding is the size complementarity between the guest and the cavity of the host. The two factors above necessitate the design of bigger hosts with well defined three dimensional cavities. The overall size of the host can be modified much more simply than the cavity dimension of the host. In order to tailor a

host which fits an anion with specific shape, a complex design strategy needs to be explored. This requires an extensive synthetic chemistry and manipulation of the conformation of molecules. The concept of preorganization[16] of the host and the idea of the macrocyclic effect[13] will apply for anions as well as cations.

All efficient anion binding molecules hitherto known are based on polyamine macrocycles.[224-226] When the amines are protonated, the electrostatic interaction between the ammonium binding sites and the anions, coupled with the size of the cavity gives a reasonable binding constant and selectivity. This particular phenomenon was explored in anion binding as well as in catalysis of phosphorylation reactions of molecules of biological significance (eg. ADP to ATP).[227]

In an early experiment, quenching of captand fluorescence by anions was apparently observed. The initial observation of quenching with potassium nitrate as a quencher was somewhat unexpected. This aroused our curiosity when other salts of potassium failed to quench the fluorescence of the m-xylylene capped crown ether molecule. The effect of other anions such as chlorides, sulphates and perchlorates were tested with same metal (potassium) as cation. The quenching was observed only in case of potassium nitrate.

As finally worked out, the quenching observed can be accounted for by diffusion quenching of nitrate rather than static quenching. The preliminary confirmation came from two experiments. In both experiments the cation

concentration and ionic strength of the medium were kept constant and but the nature of the salts was varied. From the potentiometric studies it was clear that the K^+ ions do bind with the ligand with a reasonable stability constant. The first set of experiments were conducted by taking K^+ as cation and changing the ratio of chloride and nitrate in the solution. This was achieved by mixing different solutions of potassium chloride and potassium nitrate in the fluorescence cell and recording the emission of the compound. The quenching of the emission spectrum was proportional to the amount of nitrate ion present in the medium. The second set of experiments were conducted with a different cation. Tetramethyl ammonium nitrate was chosen as cation as the stability constant of this cation would be much less than the potassium complexation. The required amount of nitrate in the cell was established by mixing tetramethyl ammonium chloride and tetramethyl ammonium nitrate solutions. The emission spectra of these solutions were recorded by using the same excitation wavelength and emission wavelength.

The fluorescence quenching studies of compound **15** in the presence of nitrate ion were carried out in water. The emission spectra were given below (Figure *35* and *38*).

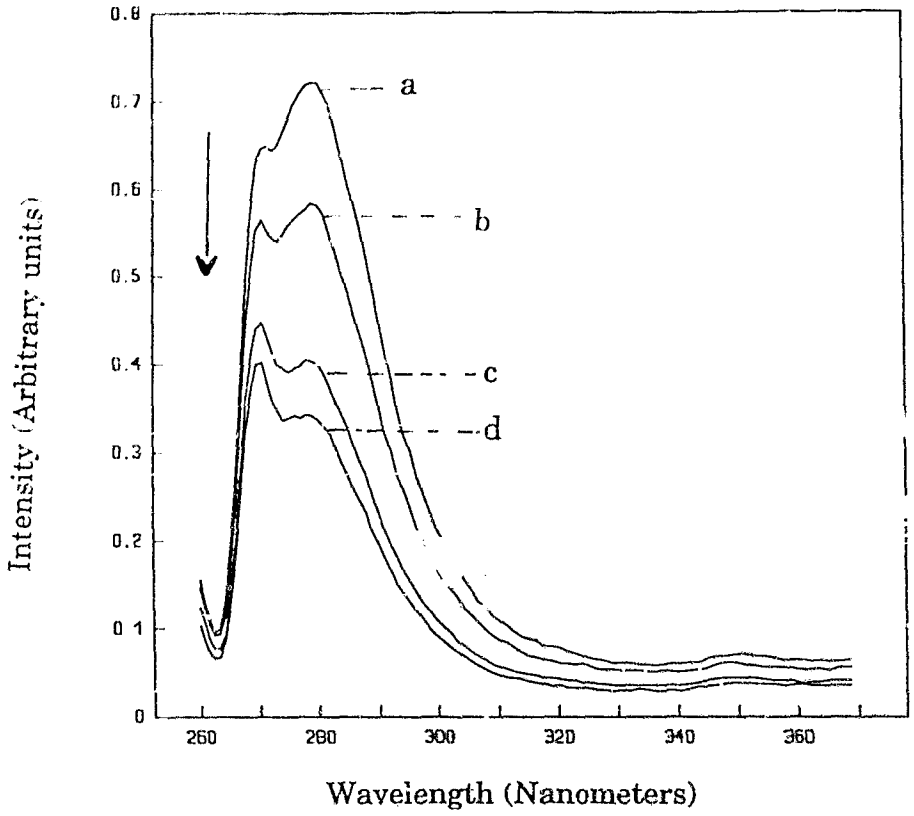

Figure *35* Emission spectra of compound **15** with varying concentrations of nitrate with K^+ as counter ion*,&

* Concentration of **15** in 3 mL cell was 1 x 10^{-5} M

&) ExWl 250 nM, EmWl 260 nM, slits 5 mm / 5 mm

a) Concentration of NO_3^- ion in the cell was 0.0 M

b) Concentration of NO_3^- ion in the cell was 3 x 10^{-3} M

c) Concentration of NO_3^- ion in the cell was 1 x 10^{-2} M

d) Concentration of NO_3^- ion in the cell was 2 x 10^{-2} M

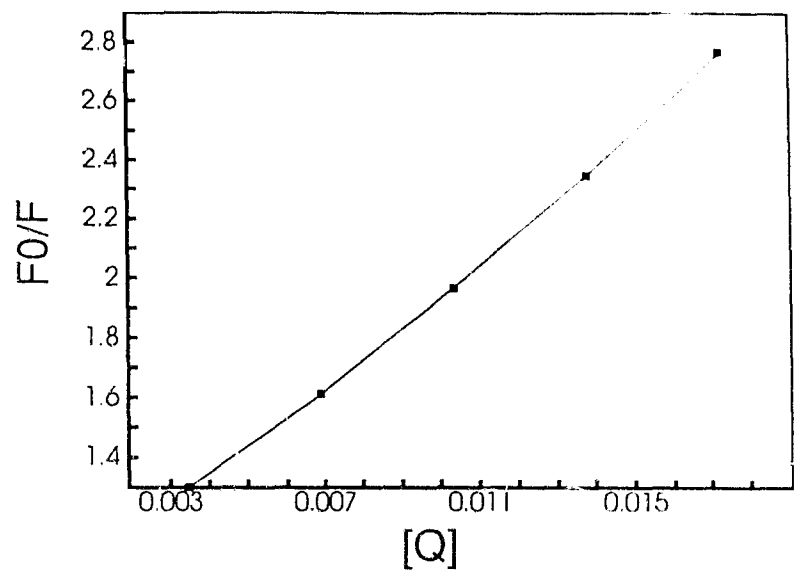

ern-Volmer plot of fluorescent quenching studies of compound **15** h nitrate and K^+ as counter ion (plot corresponds to the ssion spectrum given in figure *35*

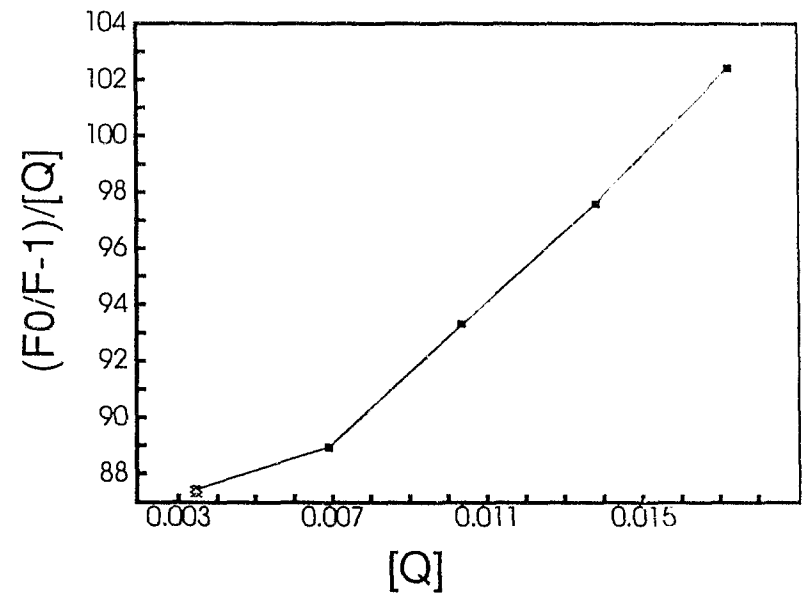

Figure *37* Plot of K_{app} versus [Q] for fluorescence studies of compound **15** with nitrate ion and K^+ as counter ion (corresponds to fig. *35*)

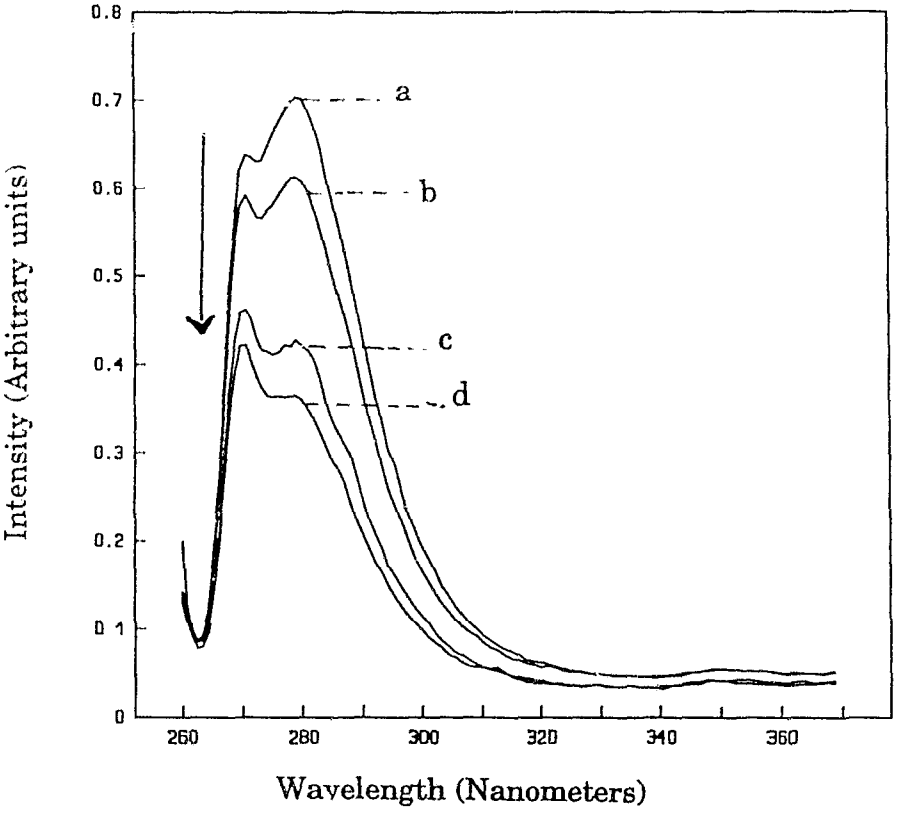

Figure *38* Emission spectra of compound **15** in presence of varying concentrations of nitrate ion with tetramethyl ammonium ion as counter ion

* Concentration of **15** in 3 mL cell was 1 x 10^{-5} M

&) ExWl 250 nM, EmWl 260 nM, slits 5 mm / 5 mm

a) Concentration of NO_3^- ion in the cell was 0.0 M

b) Concentration of NO_3^- ion in the cell was 3 x 10^{-3} M

c) Concentration of NO_3^- ion in the cell was 1 x 10^{-2} M

d) Concentration of NO_3^- ion in the cell was 2 x 10^{-2} M

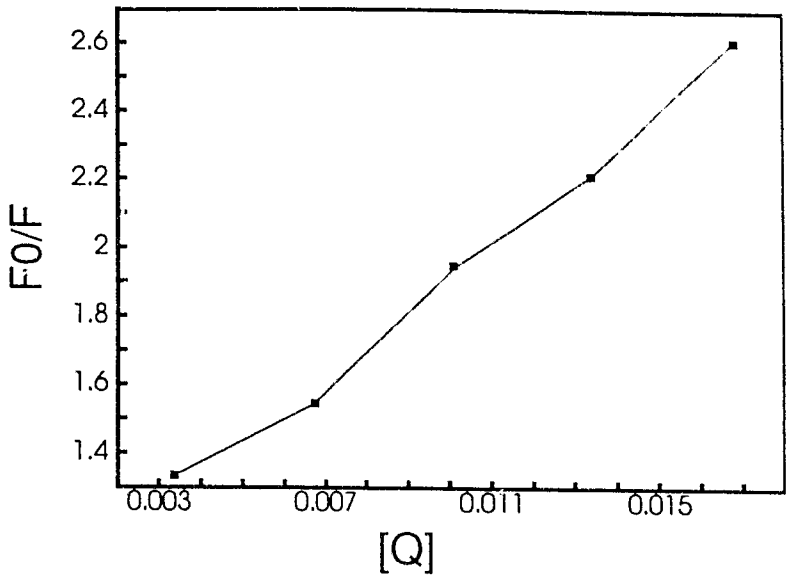

Figure *39* Stern-Volmer plot for the fluorescence emission quenching studies of compound **15** in presence of varying concentrations of nitrate ion with tetramethyl ammonium ion as counter ion (corresponds to fig.*38*)

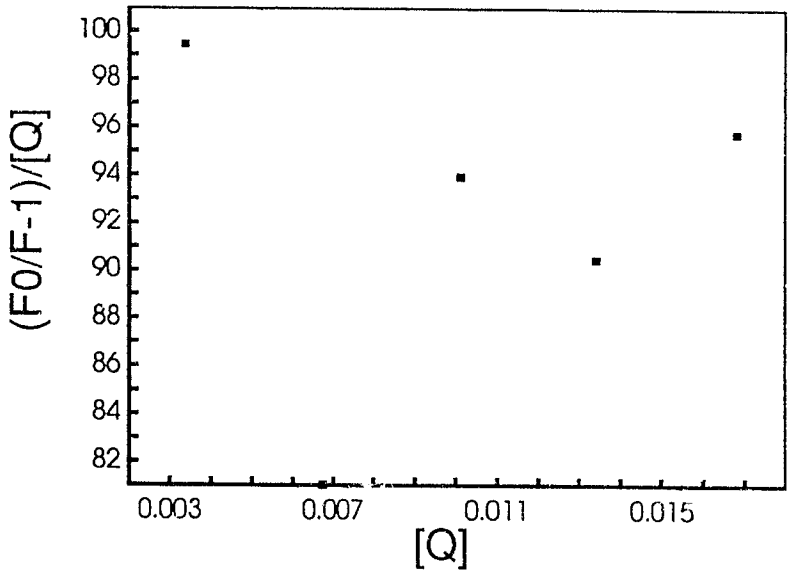

Figure *40* Plot of K_{app} versus [Q] for the fluorescence emission quenching studies of compound **15** in presence of varying concentrations of nitrate ion with tetramethyl ammonium ion as counter ion

The straight line observed in both cases indicates that the mechanism of quenching could be dynamic. If there was an association of nitrate ion and the captand, the plot would have shown a curvature towards the y axis and the rates of quenching would have been considerably different from each other.

4.3.8 Conformational studies of Captands.

The conformation of macrocycles plays an important role in the cation binding. The classic example of the change in conformation of the ligands was first established by Dunitz[17,18], based on the crystal structure of 18-crown-6 and its potassium complex. In the uncomplexed ligand, the cavity is filled by the methylene units of the macrocycle skeleton whereas in the complexed state the metal ion organises the ligand in such a way that the methylene units are expelled from the cavity and the macrocycle adopts a crown shape. The crown ether undergoes a great deal of structural rearrangement during complex formation. In more rigid macrocyles such as cavitands, the cavity is preorganised during the synthesis of the molecule and the reorganisation due to complex formation is very limited. The enhancement of stability constant due to preorganization of the host macrocycle has been under scrutiny and proven to be not valid except in the case of high rigidity. For flexible ligands the more generally used principle is "the guest organises the host".[15,16] Controlling the conformation of a macrocycle to achieve maximum

complexation is a well recognised principle in the design of macrocycles.

The conformation of tartaric acid incorporated crown ethers has been well explored and the conformation of the carboxyl groups of tartaric acid is assigned as axial-axial in all cases.[191,193,195] The incorporation of (L)-tartaric acid unit into the 18-crown-6 ring does not change the conformation of the macrocycle significantly but locks the OCH-CHO fragments into a gauche conformation. Of the two possible conformations, aa and ee of the tartaric acid units, the aa conformation is predominant in the solid state[191] and the epr studies conducted by Dugas[193] conclude that the tetraacid adopt the aa conformation in solution also. The crystal structure of the K^+ complex of 18-crown-6 tetraamide clearly demonstrates that the tartaric acid maintains an anti conformation.[17,18] A monocapped crown ether tetracid was synthesised and characterised by Lehn.[189] The crystal structure of the molecule showed an open face towards the two divergent pendent carboxyl groups and a strainless crown ether ring. The CO-NH acts as hydrogen bond donor to the crown ether ring oxygen atoms and the -CO-NH- acts as hydrogen bond acceptor to external water molecules. The free carboxyl groups also formed hydrogen bonds with two water molecules. The tartaric acid unit showed an aa coformation in all derivatives.

In an attempt to assign the conformation of captands, crystals of compound **15** and compound **16** were grown and the structures were solved by X-ray diffraction. Compound **16** crystallises as a monohydrate from

acetonitrile and belongs to a monoclinic space group of $P2_1$ (R = 0.037, for the number of observed data 3295). The positions of the CO-NH hydrogen and H_2O hydrogens were refined and others fixed. A two fold horizontal axis parallel to the two phenyl rings (top and bottom) passes through the tartaro units.

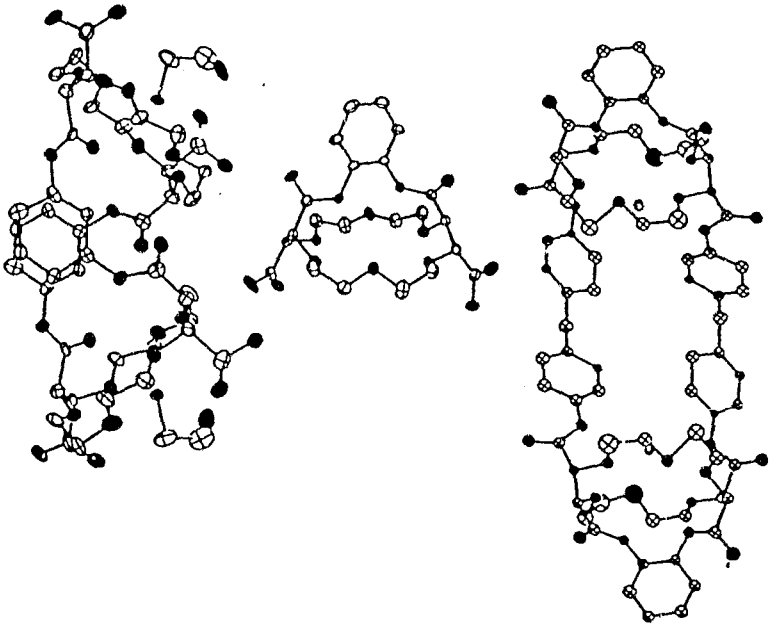

Figure *41* Crystal structures of the tartaric acid unit incorporated crown ethers[183]

The cavity of the macrocycle is open but twisted and the methylene at C18 is turned towards the cavity. The oxygen atoms in the ring skeleton

assume a boat conformation. Both tartaramide units showed the aa conformation (C19-C2-C3-C33, -175°, C31-C11-C12-C45, -167.5°). The torsion angle about the C17-C18 bond is -179.1°. In the aromatic ring, the para substituted carbons and their methylenes are bent towards the interior of the molecule. These para carbons range from 0.019 to 0.032Å out of the best plane of the four unsubstituted carbons, and methylene carbons, from 0.164 to 0.309Å. The best planes form a dihedral angle of 3° with each other. The best plane of oxygen atoms of the polyethereal ring forms dihedral angles of 2.8 and 5.9° with aromatic rings. One of the amide carbonyl oxygen (O46) acts as a hydrogen bond acceptor to the hydrogens of the external water molecule.

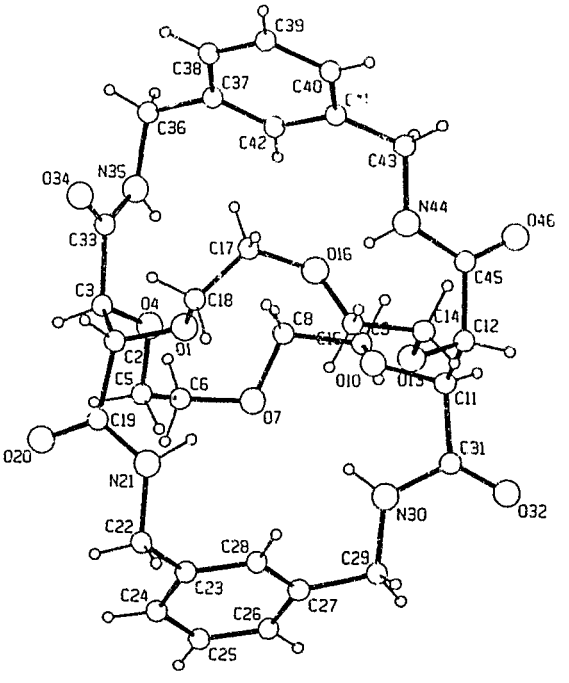

Figure *42* Crystal structure of compound **15**

Table *18* Crystallographic parameters for captands

Parameters		**15**	**16**
Formula		$C_{32}H_{40}N_4O_{10}$	$C_{32}H_{42}N_4O_{11}$
Molecular weight		640.7	658.7
Space group		$P2_12_12_1$	$P2_1$
Unit cell	a	10.594(2)Å	9.3363(7)Å
	b	17.209(3)Å	17.840(2)Å
	c	17.443(2)Å	10.3558(7)Å
	β	---	106.770(6)Å
Volume		3180(2)Å^3	1648.4(14)Å^3
Z		4	2
D_{calc}		1.338 g/cm^3	1.350 g/cm^3
Crystal dimensions		0.55x0.60x0.63 mm	0.23x0.35x0.38 mm
μ		0.94	0.96
Radiation		Mo	Mo
Θ		1-25	1-28
T		24°C	26°C
R (obs.data)		0.044	0.037
R (all data)		0.089	0.060
R_W		0.048	0.042
Unique data		5134	4030
Observed data		3440	3295
Variables		432	448
Max. residual		0.34	0.27
Extinction		3.3(30x10^{-7}	7.6(6)x10^{-7}

Compound **15** crystallised from acetonitrile in orthorhombic space group $P2_12_12_1$. All -NH hydrogens were refined and the other hydrogens were fixed.

A two fold axis runs through the tartaric acid units parallel to the benzene rings. A skeletal drawing of the molecular structure shows a chair conformation for the ether oxygens of the ring. The tartaramide units are diaxial with C33-C3-C2-C19 angle -167.9° and C31-C11-C12-C45 angle -175.0° on the polyether ring. The aromatic rings are planar to within 0.007Å and form a dihedral angle of 18.6° with each other. The best plane of the oxygen atoms of the polyethereal ring forms dihedral angles of 18.6° and 17.1° with the aromatic ring.

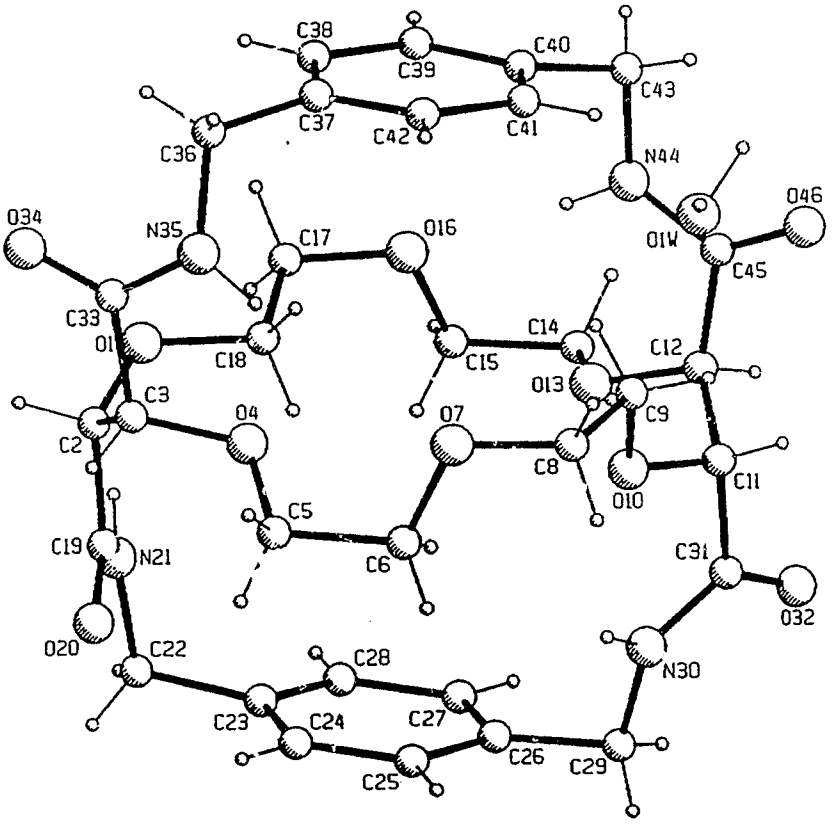

Figure *43* Crystal structure of compound **16**

The change in structure of the aromatic molecules for capping induces a change in macrocyclic ring dimensions. Transannular OO distances, O1-O10, O4-O13 and O7-O16 are 4.785 and 5.537 and 6.004 Å respectively for compound **15** and 6.199, 5.183 and 5.931 Å for compound **16**. The 1.414 Å increase in O1-O10 for p-xylylene capped crown ether results from the anti torsion around C17-C18.

The other striking feature observed in the crystal structure analysis was the hydrogen bond formation of all NH protons with the ring oxygen atoms. All hydrogen bonding resulted in stable five membered rings with NO distances in the range of 2.543 to 2.751 Å. The longest of these (N21) bifurcates to an intermolecular acceptor, amide carbonyl O46, at a NO distance of 2.942 Å. The water molecule in the crystal structure of compound **16** bridges between the captand molecules by donating linear hydrogen bonds to amide carbonyl O46 (2.849 Å) and O34 (2.916 Å). All four of the amides in compound **15** also form five membered ring hydrogen bonds to polyethereal oxygens with NO distances in the range of 2.576 to 2.717 Å The longest of these N44 bifurcates to a second acceptor O16 at an NO distance of 3.008 Å.

The other conformational evidence came from proton nmr of these molecules. The Ar-C$\underline{H}_2$ showed an AMX system with the chemical shift difference between the two methylene protons of up to 1 ppm. This indicates the different amount of shielding of methylene protons by the opposite

aromatic rings. The observed well resolved coupling of the NH protons (9Hz) with one of the methylene hydrogen indicates that one of the methylene proton forms a dihedral angle of 90° with the NH. This is one of the necessary relationships for hydrogen bonding observed in the crystal structure.

Another salient feature of ^{1}H nmr is the shielding of the ethylene glycol units from their usual position (3.7-3.8 ppm) to 3.3-3.5 ppm. This particular effect was observed in all three cases (compounds **15**, **16** and **20**). In addition to this, the glycolic protons of the ring in the compound **16** were split into a 1:3 ratio, giving two separate multiplets in a 1:3 ratio. The average structures of these molecules must therefore be same as in solution and in the solid state. This is not surprising because of their high degree of preorganization and the rigidity of the structure.

All attempts to crystallise metal complexes of the molecules were unsuccessful. This is surprising because of the open nature of the cavity in the solid state structure and the high degree of preorganization of the host. The stability constants of these macrocycles are in fact lower than the cryptand type molecules.

Attempts to crystallise compound **20** were in vain and hence the conformation of the molecule is not known in the absolute sense. The nmr was more complex to analyze. ^{13}C nmr spectrum showed 4 distinct signals for $\underline{C}$=O, Ar-$\underline{C}H_2$ and $\underline{C}$H of the ring tartaramide units. This could be explained in terms of the different shielding due to different alignments of the biphenyl

ring. One reasonable conclusion is that the rotation around the Ar-Ar bond has completely frozen due to capping. The preliminary minimisation of the structures of the "side capped (*ortho*)" and the "up and down capped (*syn*)" biphenyl crown ether was done by using MMX using standard (default parameters). The total energies obtained for either isomer were comparable and thereby the chances of forming a mixture of isomers cannot be ruled out at this time. By MMX, the tartaric acid units show a diaxial orientation in the *syn* capped structure whereas the *ortho* capped structure has a gauche form. These calculations only indicate that the formation of both isomers is feasible. The fine structure in the fluorescence emission spectrum might be due to the presence of the isomers. However there is no evidence for two separable isomers.

4.4 Conclusions and Future perspectives

The synthetic strategy developed during this study could be used for developing a water soluble photoionophore. Any rigid diamine can be used directly to couple the tartaric acid crown ethers which allows a certain degree of flexibility in choosing a chromophore as well as the properties of the molecule. The yields of the products isolated were good and the purification methods were simple to carry out. The only hurdle in this strategy is the high dilution conditions required for efficient coupling of the reactant. Even so a

reasonable amount (1g) of material can be generated in a short period of time. The high sensitivity of the technique reduces the amount of photoionophores required in the application of the sensor, and overrides the minor synthetic disadvantage.

Even though a very sensitive fluoroionophore was not developed in this exploratory study, the knowledge of this study can be used to design new molecules. The possible directions are selection of new chromophores as part of the diamine moiety and the manipulation of the preorganization of the host to introduce flexibility as well as new binding sites to enhance complexation. This would involve the extension of the distance between the amino group and the chromophore unit. Since the property of the crown ether (stability constant) did not change during the structural modifications explored, the water solubility of tartaric acid crown ethers can be further exploited.

The number of patents, papers and monographs published in this area during the last 25 years only echoes the significant contributions of supramolecular chemistry and its applications in sensor technology.[1-10,227,228] However, the promises made by the forefathers of this field towards the area of applied technology have not been fulfilled. The major problem is the transformation of information from a microscopic molecular level to a macroscopic level. This issue needs to be addressed much more carefully. Recent attempts to build supramolecular devices shows the prospects and growth in this area. The technology for the transformation of microscopic

molecular information to macroscopic visual media is one step behind the forefront of fundamental research.[22] Speaking in this line, the attempt made here, even though partly unsuccessful seeks merit for itself. So in a note to end this section it would be wiser to say that observations recorded today may provoke inspiration in a creative mind tomorrow.

It is better to debate a question
without settling it than to
settle a question without debating it....

J. Joubert

4.5 EXPERIMENTAL

General Details

Melting points were taken on a Riechardt hot-stage microscop and are uncorrected. Proton nmr spectra were recorded with a Perkin-Elmer R32 (90 MHz, CW) or Bruker AMX 360 (360.14 MHz, FT) spectrometers in $CDCl_3$, CD_2Cl_2 or CD_3OD as solvent. The 90 MHz spectra were referenced to Me_4Si as internal standard. The 360 MHz spectra were referenced with the central solvent line as standard (7.24δ for $CDCl_3$, 5.32δ for CD_2Cl_2 and 3.30 δ for CD_3OD, all relative to Me_4Si). Carbon nmr spectra were recorded with a Bruker WM250 (62.89 MHz) or Bruker AMX360 (90.57MHz) spectrometer with the central solvent line as standard (77.0 ppm for $CDCl_3$, 53.8 for CD_2Cl_2 and 49.0 for CD_3OD, all relative to Me_4Si). Mass spectra were recorded on a Finnegan 3300 GC-MS instrument with methane chemical ionization. Elemental analyses were performed by Canadian Microanalytical Services, New Westminster, B.C., and are quoted as percentages.

Synthesis of 1,4,7,10,13,16-hexaoxacyclooctadecane-2,3-dicarboxylic acid (13)

The crown ether diacid was synthesised according to the procedure reported earlier.[195] This procedure uses DMA and is the best currently available route to this compound. Sodium hydride (4.1 g, 170 mmol) was added freshly distilled DMA (500 ml) and stirred. (2R,3R)-N,N,N',N'-

Tetramethyltartaramide **7** (32.8 g, 160 mmol) was added in small portions at room temperature within 2 hours and stirred for another 2 hours. To this mixture a solution of pentaethylene glycol ditosylate **9** (75g, 160 mmol) in DMA (50 ml) was added in one portion and the mixture was stirred for another 6 hours at 80 °C. The resulting brown solution was evaporated to dryness, dissolved in water (250 ml) and extracted twice with 250 ml portions of petroleum ether, twice with 250 ml portions of diethyl ether, twice with 250 ml portions of dichloromethane and twice with 250 ml portions of Chloroform. The chlorocarbon layers were combined and evaporated to dryness to yield a solid (13.6 g, 21 %) sufficiently pure for the next step. Product **11** was characterised by comparison with the ^{1}H and ^{13}C nmr spectra of authentic samples. The diamide was then hydrolysed to give 9.9 g (90 %) of the crown ether diacid **13**, crystallised from water as previously described.[195]

Synthesis of 1,4,7,10,13,16-hexaoxacyclooctadecane-2,3,11,12-tetracarboxylic acid (12)

The reported procedure was modified by using DMA or DMSO as the solvent. This procedure is the best currently available. Sodium hydride (9.6 g, 390 mmol) was added to freshly distilled dry DMA or dry DMSO solution (300 ml) and the mixture was stirred at 0 °C. N,N,N',N'-Tetramethyltartaramide **7** (41.2 g, 200 mmol) was added in portions over 2 hours with continuous stirring. The mixture was then warmed to room

temperature and a solution of diethylene glycol ditosylate **8** (83 g, 200 mmol) in 150 ml solvent was added in one portion. The mixture was then stirred at 80 °C for another 8 hours and cooled to room temperature. The dark brown solution was then evaporated to dryness, dissolved in water (250 ml) and extracted with two 100 mL portions of petroleum ether, diethyl ether, dichloromethane and chloroform in the order specified. The chlorocarbon layers were combined and evaporated to dryness to yield 25 g (in DMA) or 29 g (in DMSO) of a pale yellow solid. The pale yellow solid was recrystallised from acetone and identified as **10**. The crown ether tetraamide was hydrolysed with 1 M HCl to give tetraacid **12**. Both of these compounds were comparable to authentic samples as determined by ^{1}H, ^{13}C nmr and Mass spectroscopy. The yield obtained by this method (DMA 22%, DMSO 26%) was higher than the previously reported method (DMF 15%).

Synthesis of 2,2'-bis(hydroxymethyl)biphenyl (17).

To a suspension of lithium aluminum hydride ($LiAlH_4$, 9 g, excess) in dry THF was added a solution of diphenic anhydride (10 g, 44.5 mmol) in 20 ml of dry THF in 2 - ml portions over 2 hours. The mixture was stirred for 5 hours at reflux, cooled and 50 ml of 4 N NaOH was added in small portions. The resulting mixture was dissolved in 250 ml of water and extracted with dichloromethane. The chlorocarbon layer was washed twice with 50 ml portions of water. The organic solution was then dried with anhydrous sodium

sulphate and the solvent was removed under reduced pressure to give 7 g (65 %) of a white solid. The compound was recrystallised from hexane to give 6.1 g of solid crystalls. ^{1}H nmr ($CDCl_3$, δ): 7.49 (d, 2H), 7.30-7.47 (m, 4H), 7.12-7.15 (m, 2H), (Ar-H), 4.3 (dd, 4H); ^{13}C nmr ($CDCl_3$, δ): 139.9, 138.6, 129.7, 129.6, 128.1 and 127.7 ppm (Ar) and 62.9 ppm (Ar-$\underline{C}H_2$-); MS: m/z 215 $(M+1)^+$.

Synthesis of 2,2'-bis(bromomethyl)biphenyl (18)

2,2'-bis(hydroxymethyl)biphenyl **17** (5 g, 23 mmol) was dissolved in carbon tetrabromide and phosphorous tribromide (2.5 g, 9.2 mmol) was added dropwise with continuous stirring over 2 hours. The mixture was stirred for another six hours and the excess phosphorous tribromide was quenched by very slow addition of water in small quantities. The solution was then diluted with 1 N sodium carbonate solution (150 ml) and extracted with dichloromethane. The halocarbon extracts were then evaporated under reduced pressure and the solid (4 g, 50 %) obtained was dissolved in 250 ml of dichloromethane and washed with water. The dichloromethane layer was then dried over anhydrous Na_2SO_4, evaporated to give 3.7 g of a pale yellow solid which was then recrystallized from hexane. ^{1}H nmr; 7.5 (d, 2 H), 7.25-7.43 (m, 4 H), 7.23 (d, 2 H, Ar-H), 4.25 (dd, 4 H, Ar-C$\underline{H}_2$-). ^{13}C nmr 4 peaks at 139.4, 135.9, 130.7, 130.1, 128.7 and 128.3 ppm (aromatic ring carbons), 31.9 ppm (Ar-$\underline{C}H_2$-)

Synthesis of 2,2'-bis(aminomethyl)biphenyl (19)

2,2'-bis(bromomethyl)biphenyl **18** (2 g, 5.8 mmol) was dissolved in 200 ml of DMA along with 3 g (16 mmol) of freshly prepared potassium phthalimide. Two drops of diethylamine was added as a catalyst. The mixture was stirred at 50 °C for 5 hours and the solvent was removed under reduced pressure. The resulting yellow paste was dissolved in 250 ml of water and extracted with dichloromethane. The halocarbon layer was washed with water, dried with anhydrous sodium sulphate and evaporated to dryness under reduced pressure to yield a white solid. The solid was dissolved in 200 ml of ethanol followed by the addition of 10 ml (excess) of hydrazine. The mixture was stirred for 5 hours at 50 °C. The resulting white solid was filtered and washed twice with 50 ml portions of ethanol. The ethanol filtrate was evaporated to dryness and 250 ml of dichloromethane was added. The resulting white precipitate was filtered and washed twice with 20 ml portions of dichloromethane. The halocarbon filtrate was dried over anhydrous sulphate and evaporated to dryness to yield 1.5 g (85 %) of a colourless oil. The oil was left under high vacuum overnight and identified as compound **19**; ^{1}H nmr (ppm): 7.54 (d, 2 H), 7.25-7.48 (m, 4 H), 7.11 (d, 2 H, Ar-H), 3.55 (dd, 4 H, Ar-CH_2), 3.0 (br.s, 4 H, -CH_2-NH_2); Its ^{13}C nmr: 141.2, 136.8, 128.8, 127.9, 127.8 and 127.6 ppm (Ar), 48.8 ppm (Ar-CH_2-NH_2); MS: m/z 213$(M+1)^+$.

Synthesis of 9,10-bis(chloromethyl)anthracene (22)

Anthracene (10 g, 56 mmol) was dissolved in 1,4-dioxane (200 ml) and conc. HCl (50 ml) was added with continuous bubbling of HCl gas for 1 hour. Trioxane (6.7 g, 74 mmol) and polyphosphoric acid (5 ml) were added along with acetic acid (10 ml). The mixture was stirred for 6 hours and filtered. The solid residue was washed twice with 100 ml portions of 1,4-dioxane and all washings were combined with the filtrate. 9,10-Bis-(chloromethyl)anthracene was precipitated from the dioxane solution by addition of water and the solid was recovered by filtration. The precipitate was then washed with water and dried to give 11 g (71 %) of a yellow powder. The yellow powder was identified as **22** from its ^{1}H and ^{13}C nmr spectra and mass spectrum. ^{1}H nmr (ppm): 8.45 (d, 4 H), 7.66 (d, 4 H, Ar-H), 5.59 (m, 4 H, Ar-CH_2-); ^{13}C nmr: 126.7, 124.3, 130.2, and 129.7 ppm (Ar) and 38.8 ppm (Ar-CH_2-Cl); MS: m/z 237 $(M+1)^+$.

Synthesis of 9,10-bis(aminomethyl)anthracene (23)

9,10-bis(chloromethyl)anthracene **22** (1.5 g, 5 mmol) was dissolved in 200 ml of dry freshly distilled DMF or DMA and freshly prepared potassium phthalimide (4.0 g, 22 mmol) was added with continuous stirring. Diethylamine (5 drops) was added and the mixture was stirred at 50 °C for 8 hours. The solvent was removed under reduced pressure and the yellow paste was dissolved in water. The solid was filtered and washed twice with 50 ml portions of water and dried under high vacuum to give 1.0g (84%) of solid. The

solubility of this compound was poor in almost all solvents and, therefore, it could not be further purified or characterised. The only structural evidence came from the mass spectrum at m/z 237 $(M+1)^+$. This crude diamine was used with out further purification for subsequent reaction.

Preparation of tetraacid chloride of 12[221]

Compound **12** (0.6 g, 1.4 mmol) was dissolved in 25 ml of phosphorous oxytrichloride and 1.14 g (5.5 mmol) of freshly sublimed phosphorous pentachloride was added with continuous stirring. The mixture was stirred at 45 °C for 12 hours and the solvent was removed under reduced pressure. The excess phosphorous pentachloride was sublimed under high vacuum. The crude white solid product was dissolved in dry toluene (10 ml) and used with out further purification or characterisation.

Synthesis of m-xylylene capped crown ether (15)

Dry toluene (500 ml, distilled over sodium) was placed in a 3 l four-neck flask equipped with two precision dropping funnels and a mechanical stirrer. A toluene solution of acid chloride **14** was placed in one of the funnels and a toluene solution of 1,3-bis(aminomethyl)benzene (0.59 g, 4 mmol) in the other funnel. Concentrations were adjusted so that equal volume addition rates gave equal mass addition rates from the two funnels. Both of the solutions were added dropwise to the reaction flask with continuous and vigorous stirring over

48 hours at room temperature. After completion of the addition, the mixture was stirred for another 12 hours and the solvent was removed under reduced pressure. The resulting pale yellow solid was dissolved in 200 ml of water and extracted twice with 100 ml portions each of petroleum ether, diethyl ether, dichloromethane and chloroform in that order. The chlorocarbon extracts were mixed and evaporated to dryness to give a 95 % yield of **15**, mp > 275 °C. The product was further purified by recrystallisation from acetonitrile. The nmr spectral data are given in Tables *19* and *20*. The mass spectrum showed a peak at 641 $(M+1)^+$. Analysis expected: C 58.34 %, H 6.42 %, N 8.50 %, found: C 58.34 %, H 6.31 %, N 8.31 %.

Synthesis of p-xylylene capped crown ether (16)

The dry toluene solution of 1,4-bis(aminomethyl)benzene (0.85 g, 6.2 mmol) and toluene solution of acid chloride **14** (0.63 g, 1.4 mmol) were placed in separate high precision dropping funnels attached to a flask equipped with a mechanical stirrer and added dropwise into the 500 ml of toluene with vigorous stirring. The addition was continued over 48 hours and the mixture was stirred for another 12 hours and the solvent removed under high vacuum. The resulting solid was dissolved in water and extracted twice with 100 ml portions each of petroleum ether, diethyl ether, dichloromethane and chloroform in that order. The chlorocarbon extracts were concentrated to give

a white solid (0.35 g, 40 %). This compound was identified as **16** from its ^{13}C and ^{1}H nmr spectra (see Tables *19* and *20*); MS: m/z 641 $(M+1)^+$, mp > 275 °C. Analysis expected ($M+H_2O$): C 58.34 %, H 6.42 %, N 8.50 %, found C 58.07 %, H 6.25 %, N 8.23 %.

Synthesis biphenyl capped crown ether (20)

A toluene solution of acid chloride **14** (0.6 g, 1.14 mmol) and 2,2'-bis(aminomethyl)biphenyl (0.65 g, 3.1 mmol) were taken in separate addition funnels and added dropwise to a high dilution flask containing 500 ml dry toluene. The solution was stirred continuously with a mechanical stirrer and the addition was continued for 48 hours. After the addition of the reagents, the mixture was stirred for another 12 hours. The solvent was removed under reduced pressure to give a solid which was dissolved in water and extracted twice with 250 ml portions each of petroleum ether, diethyl ether, dichloromethane and chloroform. The chlorocarbon extracts were evaporated to give 0.76 g (85 %) of a pale yellow solid which was identified as **20**. The nmr spectral data are given in Tables *19* and *20*. The mass spectrum showed a molecular ion peak at m/z 793 $(M+1)^+$. Analysis expected,($M+2H_2O$): C 63.50 %, H 5.83 %, N 6.55 %, found: C 63.25 %, H 5.81 %, N 6.46 %.

Attempted synthesis of monocapped crown ether (26)

The solution of crown ether bis anhydride **25** (0.92 g, 2.2 mmol) in dry

THF and a solution of 1,3-bis(aminomethyl)benzene (0.3 g, 2.2 mmol) in THF were placed in separate dropping funnels and added dropwise to 500 ml dry THF and 1 ml of triethylamine in a 3 l flask with vigorous stirring. The addition was continued for 48 hours at room temperature and the excess solvent was removed under high vacuum. The resulting white solid was dissolved in 200 ml of water and extracted twice with 100 ml portions of dichloromethane to remove unreacted organic compounds. The water layer was concentrated under reduced pressure and ammonium salt impurity was removed by passing the solution through a cation exchange resin and collecting the fractions of pH less than 3. All fractions were evaporated to dryness and the compound (0.8 g, 65 %) was identified by its proton and carbon nmr spectra. ^{1}H nmr (D_2O, δ): 7.3-7.1 (4 H), 4.3-3.9 (m, 8 H), 3.7-3.1 (br m, 16 H); ^{13}C nmr (D_2O, δ): 176.1, 172.1 ppm ($\underline{C}$=O), 143.3, 138.7, 129.3, 126.6 ppm (Ar), 81.9 and 81.0 (ring $\underline{C}H$), 72.1, 70.0, 69.6, 68.9 (ring $\underline{C}H_2$), 45.0, 43.0 (Ar-$\underline{C}H_2$); MS: m/z 541 $(M+1)^+$.

Synthesis 18-crown-6 dicarboxylic anhydride (27).

Diacid **13** (1.0 g, 2.8 mmol) was stirred at 50 °C with acetyl chloride for 8 hours. The mixture was cooled and excess acetyl chloride was removed under reduced pressure. A colourless oil (0.95 g) was obtained which was evaporated under high vacuum for another 4 hours to remove traces of acetyl chloride and acetic acid. The oil was used with out purification in the following reactions.

Synthesis of bis(18-crown-6) with a m-xylylene connecting unit (28)

A solution of anhydride **27** (0.95 g, 2.8 mmol) in THF was mixed with 1,3-bis(aminomethyl)benzene (0.2 g, 1.4 mmol) followed by the addition of 2 ml of dry triethylamine. The mixture was stirred for 7 hours at room temperature under an inert atmosphere. The excess solvent was removed under reduced pressure to give a glassy solid. The product was dissolved in water and extracted twice with 200 ml portions of dichloromethane to remove neutral impurities. The water solution was passed through a cation exchange resin to remove triethylammonium chloride. The acidic fractions (< pH 3) were collected and the water was removed under reduced pressure to give a colourless solid (1.02g, 89%) which was identified as compound **28**. The nmr spectral given in the Tables *19* and *20*; MS: m/z 805 $(M+1)^+$.

Synthesis bis(18-crown-6) with a 9,10-anthracene connecting unit (29)

A solution of anhydride **27** (0.9 g, 2.6 mmol) in 300 ml of THF was stirred with 9,10-bis(aminomethyl)anthracene **23** (0.5 g, 2 mmol) for 14 hours in presence of 2 ml of triethylamine at room temperature. The solvent was removed under reduced pressure. The resulting yellow pasty solid was dissolved in water and extracted with dichloromethane. The chlorocarbon layer was washed with water and evaporated to dryness to yield 0.9 g (76 %) of **29** as yellow powder. The nmr spectral data are given in Tables 19 and 20.

Synthesis of 18-crown-6 tetracarboxylic bisanhydride (25)

The procedure to prepare **25** was exactly the same as discussed above for **27**. The tetraacid **12** (1.0 g, 2.3 mmol) and 20 ml of acetyl chloride were mixed and stirred at 50 °C for 14 hours. The excess acetyl chloride and traces of acetic acid were removed under high vacuum to give 0.94 g of **25** as colourless oil. The crude oil was dissolved in dry THF and used without further purification.

Synthesis of Phenol derivative of crown ether diacid (30)

2-Aminophenol (0.3 g, 3.7 mmol) crown ether bisanhydride **25** (0.93 g, 2.7 mmol) were dissolved in 150 ml of dry THF followed by the addition of 1 ml (xs) of triethylamine. The mixture was stirred for 6 hours at room temperature. The solvent was then removed under reduced pressure and the resulting brown solid was dissolved in water and extracted twice with 50 ml portions of dichloromethane. The chlorocarbon extract was washed twice with 100 ml portions of water and evaporated under vacuum. The brown solid residue was dissolved in water and passed through a cation exchange column to remove traces of ammonium salt. The fractions of pH < 3 were collected and evaporated to dryness to give 1.0 g (84 %) of **30**. The product was identified by nmr spectral data (see Tables *19* and *20*). Analysis expected: C 51.54 %, H 6.27 %, N 3.01 %, found C 52.50 %, H 6.45 %, N 3.19 %.

Synthesis of phenol derivative of crown ether tetracid (31)

Bis anhydride **25** (0.92 g, 2.2 mmol) and 1 ml of dry triethylamine were dissolved in THF and a solution of 0.5 g (4.5 mmol) of 2-aminophenol in THF was added to it *dropwise within 4 hours* with constant stirring at room temperature. The excess solvent was removed under high vacuum. The brown solid residue was dissolved in water and extracted twice with 100 ml portions of dichloromethane. The chlorocarbon layer was washed twice with 50 ml portions of water and evaporated under reduced pressure to give 1.41 g (99 %) of **31** as a solid which was dissolved in water. The traces of ammonium salt impurity were removed by passing the solution through a cation exchange resin and collecting fractions of pH less than 3. All fractions were evaporated to dryness to give 1.3 g of **31** as a viscous oil. The product was identified by its proton and carbon nmr spectral data (see Tables *19* and *20*). Analysis expected ($M+2H_2O$): C 51.07 %, H 5.2 %, N 4.25 %, found: C 51.14 %, H 5.35 %, N 4.17 %.

Stability constant determination

Solutions of 0.05 M nitric acid and 0.05M tetramethylammonium hydroxide (TMAOH) were prepared and standardised against primary standards. The primary standards were potassium hydrogen phthalate for TMAOH or TRIS (tris-hydroxymethylaminomethane) for HNO_3. A constant ionic (0.1 M) strength was maintained by the addition of

tetramethylammonium nitrate (TMAN) to both standard acid and base as well as using a 0.1 M TMAN medium for titrations. Standard metal ion solutions (0.1 M) were made from the corresponding metal ion chlorides. All metal chlorides were reagent grades. The equivalent weight of the ligands were determined from the concordant values of the titrations and the purity of the ligand was assessed before the stability constant titrations.

Aliquots of 2-10 µl of titrant solution (TMAOH in case of charged ligands and KCl in case of neutral ligands) were added to a temperature controlled cell using an automatic burette (Metrohm 655 Dosimat). All electrodes were conditioned before use. The pH electrode was conditioned in a 0.1 M TMAN solution while the potassium selective electrode was conditioned in a 0.01 M KCl solution. The pH electrode was calibrated and the linearity was tested between pH 7.4 and 4.1 using commercially available buffers. A calomel electrode was used as a reference electrode with an external solution of 0.1 M TMAN connected to the sample solution through a porous plug. All potentials and pH readings were taken using a Metrohm 632 pH meter. The pH meter and the burette were connected to a HP85 microcomputer which allowed control of the aliquot volume, dosing speed, volume cut off, recording the responses of electrodes, time taken to equilibration etc. Since the computer monitors the equilibrium before each addition, the cases where equilibrium was not found were discarded. The data points were plotted to see the endpoints and then transferred to the UVIC main frame computer. The

program SCOGS was used to analyze the data and to calculate acidity constants and stability constants. All titrations were done under a positive argon pressure.

In a typical pK_a determination titration, a 4 ml solution of the ligand (~ $4x10^{-4}$ M) in 0.1 M TMAN was titrated with standardized base containing 0.1 M TMAN to beyond the strong acid - strong base end point (60 µl per ligand equivalent with 0.05 M base) in 2-4 µl aliquots (~ 18 points per ligand equivalent). The data file was stored and processed using SCOGS to get β_{10h} for the ligand. The carbonate content of the solutions were determined before titrations by titrating strong base TMAOH against strong acid HNO_3 and any necessary corrections were applied. The slope and intercept corrections for the pH meter was also included. The value of the slope was set to unity (ie. s = 1) whereas the intercept correction was taken as -0.23. The pK_{medium} was also calculated from the strong acid-strong base titrations and included in the calculations (13.78 for TMAN at 0.1 M). The stability constants were determined by repeat pK_a titrations in the presence of the metal cations. The SCOGS calculation included previously determined β_{10h} values.

Stability constants for the neutral ligands (captands) were determined using an ion selective electrode. The cell assembly comprised of a reference electrode (calomel electrode) and a potassium selective electrode. The potassium selective ISE was preconditioned in 1:1 v/v methanol-water mixture and titrated with a 0.1 M KCl solution. The titrations were repeated to get a

concordant values of slope and intercept. The titrant was taken in an automatic burette (Metrohm 655 Dosimat) and added to the cell in aliquots scaled to give concentration corresponding to increase of 0.2 pK^+. 10 ml of 1:1 v/v methanol-water solution was placed in a temperature controlled cell and the ionic strength was maintained constant using 0.1 M TMAN. In a typical titration, 20 uL of the ligand solution was introduced into the cell and titrated against the standard KCl solution. Since the burette was driven by a microcomputer, the added volume of the titrant was stored along with the response of the electrode. The collected data was then analyzed by using the slope and intercept from the electrode calibration titrations to derive $[M^+]_{free}$ values at each point in the titration. Values were calculated at each point and averaged over the range of $0.2 < [M^+]_{free}/[ML] < 0.8$.

Fluorescence studies.

In case of neutral ligands such as the captands, the ligands were dissolved in 50 % methanol:water and 0.02 ml of the stock solution was diluted to 3 ml with water and the required amount of metal ion solution. All metal ion solutions (0.1 M) were prepared by dissolving the chloride salts in deionised water. The appropriate concentration of the metal ions for individual fluorescence spectrum was obtained by diluting the stock solution with water. The excitation wavelength was determined from the absorption spectrum, taking the absorption maximum as the excitation wavelength. The emission

wavelength was scanned from 10 nm higher than the excitation wavelength. The purity and absorption of all metal ion solutions and the solvent were recorded separately and subtracted from the emission spectrum of the compound whereever necessary. Since the medium of the fluorescence study was water, the Raman scattering was observed. Emission and Raman scattering were differentiated by changing the excitation wavelength. Only the position of the Raman scattering band changed with change in excitation wavelength. All fluorescence spectra were recorded with excitation slits and emission slits set to 5 nm and uncorrected spectra were recorded.

In the case of charged ligands such as the bis crown ethers, a lithium / phosphate buffer of pH 10 was used. A few mL of the stock solution of the ligand was added to the cell containing buffer solution. The emission of the buffer was recorded and subtracted from the emission of the ligands. The metal ion effect was monitored using different volumes of 0.1 M metal chloride stock solution added to the cell.

The absorption spectra of phenol derivatives of the crown ether diacid and crown ether tetraacid were done according to the same procedures given above. The solutions were prepared individually with the ligand solution, metal chloride solution and made up to 3 ml with a pH 10 buffer solution.

Crystal structure determination

All crystals were grown by using a slow evaporation method from

solutions of the ligand in acetonitrile. All structure determinations were done by F. R. Fronczek and R.D. Gandour, Louisiana State University. The standard experimental procedure was followed closely from ref. 232. Intensity data were collected by ω-2Θ scans of variable rate designed to yield measurement with $I = 50\sigma(I)$ for all significant reflections, using an Enraf-Nonius diffractometer equipped with Mo Kα radiation (λ = 0.71073Å) and a graphite monochromator. Unit cell dimensions and crystal orientations were by a least squares fit to the setting angles of 25 reflections having $20° < 2\Theta < 24°$. A maximum of 120 sec. was placed on the scan time spent on any reflections. The scan rates varied from 0.61 to 4.0 deg. min^{-1}. One hemisphere of data ($h \pm k \pm l$) having $2° < 2\Theta < 55°$, $0 \leq h \leq 9$, $-11 \leq k \leq 11$, $-13 \leq l \leq 13$, was collected. Data reduction included corrections for back ground, Lorentz, polarisation and a 4.5 % linear intensity decay correction. A total of 4030 unique data was collected, of which 3295 had $I > 3\sigma(I)$ and were used in the refinements. The structures were solved by direct methods and refined by full-matrix least squares minimizing $\Sigma w (|F_o| - |F_c|)^2$ with weights $w = \sigma^{-2}(F_o)$ using the scattering factors of Cromer and Waber and the Enraf-Nonius SPD programs[233]. Non-hydrogen atoms were refined anisotropically, and hydrogen atoms were located on difference maps and refined isotropically.

Table *19* ^{1}C nmr spectral data of compounds

Compound	$\underline{C}H_2$-NH	Ring $\underline{C}H_2$-O	$\underline{C}H$ (ring)	$\underline{C}$ (Ar ring)	$\underline{C}$=O
15	42.4	69.4, 70.4	80.9	125.0, 127.1, 128.5, 138.8	169.3
16	43.4	70.3, 70.4	78.1	128.9, 139.2	169.2
17	41.6(2 peaks), 42.2,42.5	67.4,67.9,68.2, 68.5,70.7,71.2, 71.3,71.6,77.3	81.3,81.9, 82.4,83.0	126.7,127.2, 127.6,127.9, 128.0,128.4, 128.5,128.6, 129.0,129.4, 129.5,129.6, 130.0,130.5, 134.7,135.0, 135.5,135.9, 138.4,138.7, 139.2,139.5	169.4, 169.5, 170.1, 170.3
28	42.8	69.6,69.7,69.8, 69.9,70.2,70.5, 71.2	80.5,81.3	126.2,127.0, 128.5,138.7	169.4, 171.7
29	35.6	69.3,69.5,69.8, 69.9,70.0,70.5, 71.2,71.4,	80.7,81.3	124.6,124.9, 126.2,126.3, 130.1,130.2, 130.3	168.8, 171.5
31 (*syn*)		68.8,69.2,70.5, 71.0,	79.9,81.2	118.7,120.4, 123.6,124.8, 127.4,148.8	169.2, 171.7
30		69.4,69.6,69.9, 70.1,70.4,70.5, 71.0,71.2,	80.7,80.9	119.3,120.3, 123.4,125.2, 127.3,149.2	169.1, 171.2

Table *20* ^{1}H nmr spectral data of compounds

Compounds	-C<u>H</u>$_2$-O (ring)	C<u>H</u>- (ring)	C<u>H</u>$_2$-Ar	-N<u>H</u>-	Ar-<u>H</u>
15	3.3-3.6(m,16H)	4.3(s,4H)	3.6(d,2H), 5.0(dd,2H)	7.6(d,4H)	7.2(s,6H)
16	3.2-3.3(m,10H), 3.5-3.6(m,6H)	4.4(s,4H)	3.7(d,2H), 4.9(t,2H)	6.7(d,4H)	7.1(s,6H)
20	3.1-3.5(m,16H)	4.6-4.7(m,4H)	3.6-4.2(m,2H), 4.8(m,2H)	---	6.9-7.6(m,12H)
28	3.4-3.6(m,40H)	4.5(dd,4H)	3.8-3.9(m,2H), 4.9(m,2H)	---	7.2-7.4(m, 3H), 7.5(t,1H)
29	2.9-3.6(m,40H)	4.3(dd,4H)	5.4(dd,2H), 5.6(dd,2H)	---	7.5(AA'XX',2H), 8.4(AA'XX',2H)
30	3.4-3.8(m,20H)	4.4(d,2H)	---	9.4(b,1H)	6.8(t,1H)7.0(d,1H), 7.1(t,1H),7.3(d,1H)
31 (*syn*)	3.5-3.9(m,16H)	4.3(d,4H)	---	8.7(b,2H)	6.8(t,2H),6.9(t,2H), 7.0(t,2H), 7.3(d,2H)

CHAPTER 5

Epilogue

In the last two decades, research in the area of molecular recognition has provided an enormous amount of knowledge of how individual small molecules interact with one another to form complicated structures based on so called "weak" interactions such as electrostatic interaction or hydrogen bonding. During this period two schools have evolved. One school focuses on structure oriented functions wherein the structure of the molecule dictates the function of the molecule. The other school is function oriented, where the required function such as catalysis or metal cation sensing dictates the architecture of the molecule. Contributions from the Stoddart[234] and Lehn[6,22] laboratories on self assembling systems are based on the first premise whereas Breslow's[235] or Tabushi's[236] work on artificial enzymes are good examples of the second school of thought. Prior work from the Fyles group on metal ion sensors[95] and artificial ion channels[237] is also function driven.

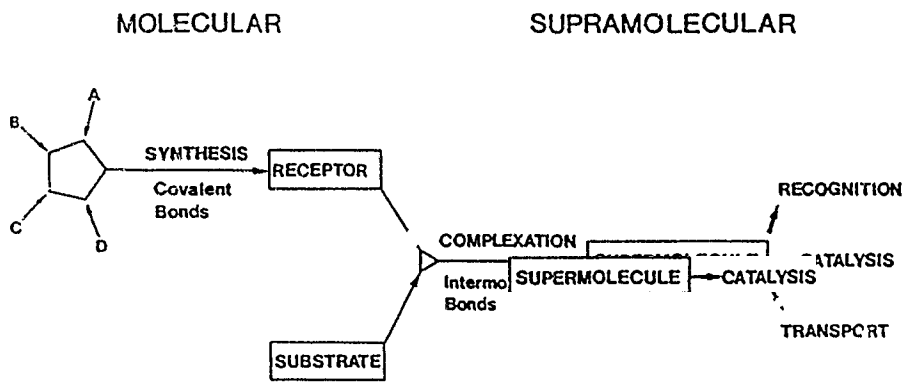

Figure *44* Supramolecular chemistry, past and future

These distinctions can be illustrated by the analogy of hardware and software in a computer system. From the first school, the designed molecule acts as software which can execute only the information implanted in the structure. The function oriented strategy is related to hardware where same structures can in principle execute more than one function.

Figure *44* shows an analysis of supramolecular chemistry according to Lehn's formalism. Both schools of thought subscribe to this analysis, but differ in where they place the emphasis. From my perspective, the interesting features are the functions of the supermolecule, that is the hardware or function driven approach.

The first part of this thesis was focused on analyzing metal ion concentration in solutions by exploiting the existing knowledge of macrocyles and their complexation properties. The binding of crown ethers with metal cations changes the potential of the membrane in which the crown ether is incorporated. This change reflects the amount of metal complex which is in a linear relationship with the metal ion concentration in the given solution. The third chapter was focused on monitoring the concentrations of alkali and alkaline earth metal ions in water by using photometry. The ground state and excited state properties of the photoionomeric hosts can be perturbed by guests (metal ions in this case). Both efforts were directed towards converting or transforming the individual molecular interactions into a readable macroscopic form, and thereby providing a means to analyze microscopic molecular

recognition processes. The second chapter deals with the related functional process of metal ion movement on a macroscopic scale. If successful it would have been an ideal example of how to convert a microscopic molecular interaction into a macroscopic process. All these areas are then fundamentally the same, and primarily driven by function oriented considerations.

The successful results observed in the immobilisation studies can be extended to immobilise any macrocycle to a polymer for developing sensors for any species of interest in any medium. The fluoroionophores unfortunately failed to perform the required function sufficiently well, so further work will be required. However the results are not insignificant in terms of the water solubility, as well as the fluorescence quenching observed in some instances. For example, the metal dependent emission observed in the case of the biphenyl capped crown ether (**26**) with Na^+ and Cs^+ could be extended to develop fluoroionophores for these metal ions. As stated earlier the research in this area of water soluble fluoroionophores is relatively new and the problems of finding a well behaved fluoroionophore for use in water requires better molecular models to perform this challenging function.

For the last 20 years the complexation step (Figure *44*) has dominated developments. The complexity of the next step of tailoring a supermolecule into molecular and supramolecular devices, demands more expertise and merging of different disciplines of science and engineering. This thesis is directed to the next 20 years of translating supramolecular structures to

molecular devices to carry out specific functions.

REFERENCES

1. C. J. Pedersen, *J. Am. Chem. Soc.*, 89, (**1967**), 2495.

2. A. D. Hamilton, *Comprehensive Heterocyclic Chemistry*, 7, (**1984**), 731.

3. I. O. Sutherland, *Chem. Soc. Rev.*, 51, (**1986**), 63.

4. J. M. Lehn, *Structure and Bonding*, 16, (**1973**), 1.

5. Host Guest Complex Chemistry I, *Top. Curr. Chem.*, 98, (**1981**), 101, (**1983**), 121, (**1984**), Springer Verlag, NY.

6. J. M. Lehn, *Angew. Chem. Int. Ed. Engl.*, 27, (**1988**), 89.

7. J. S. Bradshaw and P. E. Stott, *Tetrahedron*, 36, (**1980**),461.

8. E. Webber and F. Vogtle, *Top. Curr. Chem.*, 98, (**1981**), 1.

9. D. J. Cram, *Science*, 219, (**1983**), 1173.

10. J. M. Lehn, *Acc. Chem. Res.*, 11, (**1978**), 49.

11. J. M. Lehn, *Pure and Appl. Chem.*, 50, (**1978**), 871.

12. R. G. Pearseon, Ed. Hard and Soft acids and Bases, Dowden, Hutchinson and Rossi, Stroudsberg, Pa., (**1973**).

13. D. K. Cabbiness and D. W. Margerum, *J. Am. Chem. Soc.*, 91, (**1969**), 6540.

14. P. R. Mallinson, *J. Chem. Soc. Perkin Trans. 2*, (**1975**), 261.

15. J. M. Lehn and J. P. Sauvage, *J. Am. Chem. Soc.*, 97, (**1975**), 6700.

16. D. J. Cram, *Angew. Chem. Int. Ed. Engl.*, 25, (**1986**), 1039.

17. J. D. Dunitz and P. Seiler, *Acta. Crystallogr.*, Sect. B.30, (**1974**), 1330.

18. E. Maverick, P. Seiler, W. B. Schweizer and J. D. Dunitz, *Acta. Crystallogr.*, Sect. B.36, (**1980**), 615.

19. K. E. Koenig, G. M. Lein, P. Stuckler, T. Kaneda and D. J. Cram, *J. Am. Chem. Soc.*, 101, (**1979**), 3553.

20. S. P. Artz and D. J. Cram, *J. Am. Chem. Soc.*, 106, (**1984**), 2160.

21. R. M. Izatt, J. S. Bradshaw, S. A. Nielsen, J. D. Lamb and J. J. Christensen, *Chem. Rev.*, 85, (**1985**), 271.

22. J. M. Lehn, *Angew. Chem. Int. Ed. Engl.*, 29, (**1990**), 1304.

23. a) B. Alpha, J. M. Lehn, G. Mathis, *Angew. Chem. Int. Ed. Engl.*, 26, (**1987**), 266, 1266. b, J. M. Lehn, Supramolecular Photochemistry, V. Balzani (Ed),Reidel, Dordrecht, Netherlands, (**1987**).

24. J. J. Grimaldi, S. Boileau, J. M. Lehn, *Nature* (London), 265, (**1977**), 229.

25. a) D. F. Eaton, *Tetrahedron*, 43, (**1987**), 2390. b) J. F. Nicoud, R. J. Tweig, Non Linear Optical Properties of Organic molecules and Crystals, Academic Press, NY, (**1987**).

26. S. Shinkai, *Pure and Appl. Chem.*, 59, (**1987**), 425.

27. V. E. Carmichael, P. J. Dutton, T. M. Fyles, T. D. James, J. A. Swan and M. Zojaji, *J. Am. Chem. Soc.*, 111, (**1989**), 767.

28, T Kunitake, *Ann. NY. Acad. Sci.*, 471, (**1986**), 70.

29. T. M. Fyles, Frontiers in Bioorganic Chemistry, 1, (**1990**), 71.

30. P. Oggenfuss, W. E. Morf, U. Oesch, D. Ammann, E. Pretsch and W. Simon, *Analytica. Chimica Acta.*, 180, (**1986**), 299.

31. R. L. Solsky, *Anal. Chem.*, 62, (**1990**), 21R.

32. J. Koryta, *Anal. Chim. Acta*, 206, (**1988**), 1.

33. J. D. R. Thomas, *A.C.S. Symp. Ser.*, 390, (**1989**), 303.

34. R. G. Bates, *A.C.S. Symp. Ser.*, 390, (**1989**), 142.

35. A. Evans, Potentiometry and Ion-Selective Electrodes, Wiely, New York, (**1987**), 304.

36. G. S. Calabress, *Top. Curr.Chem.*, 143, (**1988**), 49.

37. T. P. Byrne, *Sel. Electrode Rev.*, 10, (**1988**), 107.

38. K. Reichenbach, K. Thiele and U. Funke, *Bioelectro. Anal.*. 1, Symp. Ist, E. Pungor Ed., Akad, Kido: Budapest, Hung., (**1987**), 341.

39. R. W. Cattrall and I. C. Hamilton, *Ion Sel. Electrode. Rev.*, 6, (**1984**),125.

40. Toshiba Corp. Jpn. Patent JP 58/86449, A2 (83/86449), 24 may **1983**, *Chem. Abstr.*, 99, (**1983**), 115221j.

41. Toshiba Corp. Jpn. Patent JP 59/214752, A2 (84/214752), 4 Dec. **1984**, *Chem. Abstr.*, 102, (**1985**), 142508v.

42. S. Yanagisawa, N. Shirai, K. K. Showa Denko, Jpn. Patent JP 58/39940, A2 (83/39940), 24 mar **1983**, *Chem. Abstr.*, 99, (**1983**), 205248c.

43. S. Yanagisawa, N. Shirai, K. K. Showa Denko, Jpn. Patent JP 58/58458, A2 (83/58458), 7 Apr. **1983**, *Chem. Abstr.*, 99, (**1983**), 205253a.

44. G. J. Moody, B. B. Saad, J. D. R. Thomas, *Sel. Electrode. Rev.*, 10, (**1988**), 71.

45. R. W. Carttrall and D. W. Drew, *Anal. Chim. Acta*, 77, (**1975**), 9.

46. K. Suzuki, H. Wada, T. Shirai, S. Yanagisawa, *Jpn. Anal.*, 29, (**1980**), 816.

47. U. Oesch and W. Simon, *Anal. Chem.*, 52, (**1980**), 692.

48. a) V. J. Wotring, D. M. Johnson and L. G. Bachas, *Anal. Chem.*, 62, (**1990**), 1506. b) J. E. W. Davies, G. J. Moody, W. M. Price and J. D. R. Thomas, *Lab Practice*, 22, (**1973**), 20.

49. I. A. Mostert, *Microchim. Acta*, 1, (**1985**), 33.

50, a) J. G. Schnider and M. M. Schindler, *Fres. Z. Anal. Chem.*, 320, (**1985**), 258., *Chem. Abstr.* 102, (**1985**), 159595u. b) R. S. Lawton, A. M. Yacynych, *Anal. Chim. Acta.*, 160, (**1984**), 149.

51. a) K. Kimura, T. Miura, M. Matsuo and T. Shono, *Anal. Chem.*, 62, (**1990**), 1510., b) G. J. Moody, R. B. Oke and J. D. R. Thomas, *Analyst*, 95,(**1970**), 910.

52. R. W. Murray, *Proc. Robert. A. Welch Found. Conf. Chem. Res.*, 30, (**1986**),168.

53. L. Ebdon, E. T. Ellis and G. C. Corfield, *Analyst* (London), 107, (**1982**), 288.

54. L. Ebdon, B. A. King, G. C. Corfield, *Anal. Proc.*, 22, (**1985**), 354.

55. S. Oka, Y. Sibazaki, S. Tahara, *Anal. Chem.*, 53, (**1981**), 588.

56. S. G. Cutler, P. Meares and D. G. Hall, *J. Electroanal. Chem.*, 85, (**1977**),145.

57. S. Daunert and L. G. Bachas, *Anal. Chem.*, 62, (**1990**), 1428.

58. K. Kimura, M. Yoshinaga, S. Kitazawa and T. Shono, *J. Polymer. Sci., Polymer. Chem. Ed.*, 21, (**1983**), 2777.

59. Y. Nakatsuji, S. Furuyoshi and M. Okahara, *Makromol. Chem.*, 187, (**1986**), 105.

60. D. J. Harrison, A. Teclemarium and L. L. Cunningham, *Anal. Chem.*, 61, (**1989**), 246.

61. T. M. Fyles, Inclusion Aspects of Membrane Chemistry, T. Osa and J. L. Atwood (Ed), Klawer Academic Publishers, Netherlands, (**1991**), 59.

62. C. R. Martin and H. Freiser, *Anal. Chem.*, 53, (**1981**), 904.

63. E. Lindner, E. Graf, Z. Niegreisz, K. Toth, E. Pungor and R. P. Buck, *Anal. Chem.*, 60, (**1988**), 295.

64. A. Berg, P. D. Wal, M. S. Patasinska, E. T. R. Sudholter and D. N. Reinhoudt, *Anal. Chem.*, 59, (**1987**),2827.

65. S. C. Ma, N. A. Chaniotakis and M. E. Meyerhoff, *Anal. Chem.*, 60, (**1988**), 2293.

66. T. Okada, K. Hiratani and H. Sugihara, *Analyst*, 112, (**1987**), 587.

67. K. Toth, E. Graf, G. Horvai, E. Pungor and R. P. Buck, *Anal. Chem.*, 58, (**1986**), 35.

68. A. S. Attiyat, G. D. Christian, J. L. Hallman and R. A. Bartsch, *Talanta*, 35, (**1988**), 789.

69. G. J. Moody, B. Saad and J. D. R. Thomas, *Analyst*, 112, (**1987**), 1143.

70. G. D. Carmack, PhD Dessertatior, University of Arizona, (**1977**).

71. H. James, G. D. Carmack and H. Freiser, *Anal. Chem.*, 44, (**1972**), 853, 856.

72. G. D. Carmack and H. Freiser, *Anal. Chem.*, 45, (**1973**), 1976.

73. G. D. Carmack and H. Freiser, *Anal. Chem.*, 47, (**1975**), 2249.

74. G. D. Carmack and H. Freiser, *Anal. Chem.*, 49, (**1977**), 767.

75. T. Satchwill and D. J. Harrison, *J. Electroanal. Chem.*, 202, (**1986**), 75.

76. H. J. Neilsen and E. H. Jansen, *Anal. Chim. Acta*, 86, (**1976**), 1.

77. N. Ogata, K. Sanui and H. Fujimura, *J. Appli. Poly. Sci.*, 26, (**1981**), 4149.

78. H. Sakamoto, K. Kimura and T. Shono, *Eur. Poly. J.*, 22, (**1986**), 97.

79. K. Kimura, H. Sakamoto, M. Yoshinaga and T. Shono, *J. Chem. Soc. Chem. Commun.*, (**1983**), 978.

80. a) W. E. Morf and W. Simon, Ion Selective Electrodes in Analytical Chemistry, H. Freiser (Ed), Plenum Press., New York, (**1978**), 211. b) W. E. Morf, The Principles of Ion Selective Electrodes and of Membrane Transport, Elseveir, Amsterdam, (**1981**), 274. c) D. Amman, W. E. Morf, P. Ankew, P. C. Meier, E. Pretsch and W. Simon, *Ion Selective Electrode Rev.*, 5, (**1983**), 3.

81. a) G. Eisenman, Ed, Glass Electrodes for Hydrogen and other Cations, M. Dekker, New York, (**1967**)., b) IUPAC Recommendations for Nomenclature of Ion Selective Electrodes, *Pure and Appl. Chem.*, 48, (**1976**), 127.

82. R. G. Bates, *Pure and Appl. Chem.*, 36, (**1973**), 407.

83. Recommendations for Nomenclature of Ion Selective Electrodes, *Pure and Appl. Chem.*, 48, (**1988**), 129.

84. L. M. Dulyea, T. M. Fyles and G. D. Robertson, *J. Membr. Sci.*, 34, (**1987**), 87.

85. P. L. Anelli, F. Montanari, V. Pollak and S. Quici, *Gazz. Chimi. Ital.*, 116, (**1986**), 127.

86. Vedejs, *Org. React.*, 22, (**1975**), 401.

87. House, Modern Synthetic Reactions, 2nd Ed., W.A. Benjamin, New York, (**1972**), 49.

88. Heck, Organotransition Metal Chemistry, Academic Press, New York, (**1974**), 65.

89. H. Freiser (ed), Ion Selective Electrodes in Analytical Chemistry, Plenum Press, New York, 2, (**1980**), 86.

90. L. Cunningham and H. Freiser, *Anal. Chim. Acta.*, 180, (**1986**),271.

91. U. Fiedler and J. Ruzicka, *Anal. Chimi. Acta.*, 67, (**1973**), 179.

92. R. M. Izatt, G. A. Clark, J. D. Lamb, J. E. King and J. J. Christiansen, *Thermochim. Acta*, 97, (**1986**), 115.

93. K. Kimura, H. Tamura and T. Shono, *J. Electroanal. Chem. Interfac. Sci.*, 105, (**1979**), 335.

94. C. J. Pedersen, *J. Am. Chem. Soc.*, 89, (**1967**), 2495; *ibid*, p. 7017.

95. T. M. Fyles and C. A. McGavin, *Anal. Chem.*, 54, (**1982**), 2103.

96. R. D. Noble and J. D. Way (Eds.), Liquid Membranes Theory and Applications, American Chemical Society, Washington, D.C., (**1987**), 1.

97. D. Paul and S. Newman, Ed., Polymer Blends, Vol. 1 and 2, Academic Press, New York, (1978).

98. S. Rowland, Ed., Water in Polymers, *ACS Symposium Series* No. 127, American Chemical Society Washington, D.C., (**1980**)

99. P. R. Keller, Membrane Technology and Industrial Separation Technique, Noyes Data Corp., Park Ridge, NJ, (**1976**).

100. S. T. Hwang, K. Kammermeyar, Membrane Separations, Techniques of Chemistry, Vol. 7, Wiely, New York, (**1975**).

101. J. F. Hoffmann, Membrane Transport Processes, Vol. 1, Raven Press, New York, (**1978**); D.C. Tosteson, Yu.A. Ovchinnikor and R. Later, ibid, Vol. 2, (**1978**).

102. A. S. Michaels, *Desalination*, 35, (**1980**), 329.

103. a) F. Bovey and F. Winslow, Ed, Macromolecules, An Introduction to Polymer Science, Academic Press, New York, (**1979**); b) C. Schonbein, British Patent, 11, 402, 1846.

104. A. Fick, *Ann. Phys. Chemie.*, 94, (**1855**), 59.

105. J. Baranetzky, *Pogg. Ann.*, 147, (**1872**), 195.

106. H. Bechhold, *Z. Phys. Chem.*, 48, (**1910**), 257.

107. K. Maier and E. Schenermann, *Kolloid. Z.*, 171, (**1960**), 122.

108. K. Meyer and J. Seivers, *Helv. Chim. Acta.*, 19, (**1936**), 649, 665, 987.

109. W. Juda and W. McRae, US Patent, 27636,851, (**1953**).

110. S. Loeb and S. Sourirajan, UCLA Report, 60-60, (**1960**).

111. R. E. Kesting (Ed), Synthetic Polymeric Membranes, A. Wiely, Interscience Publication, (**1985**), 7.

112. N. Lakshminarayanaiah, *Chem. Rev.*, 65, (**1965**), 548.

113. T. R. E. Kressman, *Rept. Progr. Appl. Chem.*, 47, (**1962**), 293.

114. W. Pusch and A. Walch, *Angew. Chem. Int. Ed. Engl.*, 21,(**1982**), 660.

115. M. Hofer (Ed.), Transport Across Biological Membranes, Potman, London, (**1981**).

116. J. D. Goddard, *J. Phys. Chem.*, 89, (**1985**), 1825., T. M. Fyles and S. P. Hansen, *Can. J. Chem.*, 66, (**1990**), 1445.

117 R. N. Robertson (Ed), The Lively Membranes, Cambridge University Press, New York, (**1983**).

118. R. N. O'brian, B. Zaho and T. M. Fyles, *J. Membr. Sci.*, 20, (**1984**), 305.

119. M. Yoshikawa, H. Ogata, K. Sanui and N. Ogata, *Polym. J.*, 15, (**1983**), 609.

120. T. M. Fyles, V. A. Malik-Diemer, C. A. McGavin and D. M. Whitfield, *Can. J. Chem.*, 60, (**1982**), 2259.

121. T. M. Fyles, C. A. McGavin and D. E. Thompson, *J. Chem. Soc. Chem. Commun.*, (**1982**), 924.

122. T. Uragani, S. Watanabe, R. Nakamura, F. Yoshida and M. Sugihara, *J. Appl. Poly. Sci.*, 28, (**1983**), 1613.

123. M. Tasaka, *Pure and Appl. Chem.*, 58, (**1986**), 1637.

124. C. Gostoli and G. C. Sarti, *J. Membr. Sci.*, 41, (**1989**),211.

125. S. I. Andeersson, N. Kjellander and B. Rodesjo, *Desalination*, 56, (**1985**), 345.

126. R. Marr and A. Kopp, *Int. Chem. Eng.*, 22, (**1984**), 44.

127. D. W. Mcbride, R. M. Izatt, J. D. Lamb and J. J. Christensen, Inclusion Compounds III, J. A. Davies and J. L. Atwood (Ed), Accademic Press, London, (**1984**).

128. B. M. Kim, *J. Membr. Sci.*, 21, (**1984**), 5.

129. N. Kahana, A. Deshe and A. Warshawsky, *J. Poly. Sci., Poly. Chem. Ed,* 23, (**1985**), 231.

130. P. Blais, Reverse Osmosis and Synthetic Membranes, S. Sourirajan, (Ed), NRCC Publications, Ottawa, (**1977**), 167.

131. H. Strathmann, K. Kock, P. Amar and R.W. Baker, *Desalination*, 16, (**1975**), 179.

132. M. A. Frommer and R. M. Messalem, *Ind. Eng. Chem. Prod. Res. Dev.*, 12, (**1973**), 328.

133. E. B. Sandell, Colorimetric Determination of Traces of Metals, New York, London, Interscience, (**1959**).

134. K. L. Cheng, K. Ueno and T. Imamura, Hand Book of Organic Analytical Reagents, Boca Raton, CRC Press, (**1982**).

135. F. Vögtle and C. Ohm, *Chem. Ber.*, 117, (**1984**), 948.

136. B. Lange and C. J. Vejdelek, Photometrische Analyse, Verlag Chemie, Weinheim/Bergstr. Germany, (1980), B. Budesinsky and B. Menclova, *Chem. Anal.*, 56, (**1967**), 30.

137. M. Takagi and K. Ueno, *Topics in Curr. Chem.*, Springer Verlag, Berlin -Heidelberg, 121, (**1984**), 39.

138. M. Takagi and H. Nakamura, *J. Coord. Chem.*, 15, (**1986**), 53.

139. S. Shinkai, Y. Ishikawa, H. Shinkai, T. Tsuno, H. Makishima, K. Ueda and O. Manabe, *J. Am. Chem. Soc.*, 106, (**1984**), 1801.

140. D. J. Cram, R. A. Carmack and R. C. Helgeson, *J.Am. Chem. Soc.*, 110, (**1988**), 571.

141. S. Ogawa, R. Narashima and Y. Arai, *J. Am. Chem. Soc.*, 106, (**1984**), 5760.

142. W. R. Seitz, *Anal. Chem.*, 56, (**1984**), 16A.

143. O. S. Wolfbeis, *Trends in Anal. Chem.*, 4, (**1985**), 184.

144. M. Takagi, H. Nakamura and K. Ueno, *Anal. Lett.*, 10, (**1977**), 1115.

145. H. Nakamura, M. Takagi and K. Ueno, *Talanta*, 26, (**1979**), 921.

146. H. G. Lohr and F. Vögtle, *Acc. Chem. Res.*, 121, (**1984**), 65.

147. H. Nishida, M. Tazaki, M. Takagi and K. Ueno, *Mikrochim Acta*, 1, (**1981**), 281.

148. K. W. Street, Jr. and S. A. Krause, *Anal. Lett.*, 19, (**1986**), 735.

149. H. Nishida, Y. Katayama, H. Katsuki, H. Nakamura, M. Takagi and K. Ueno, *Chem. Lett.*, (**1982**), 1853.

150. A. P. Silva and K. R. A. S. Sandanayake, *J. Chem. Soc. Chem. Commun.*, (**1989**), 1183.

151. T. Kaneda, K. Sugihara, H. Kamiya and S. Misumi, *Tetrahedron Lett.*, 22, (**1981**), 440.

152. S. Kitazawa, K. Kimura and T. Shono, *Bull. Chem. Soc. Jpn.*, 56, (**1983**), 3253.

153. H. Nakmura, H. Saka, M. Takagi and K. Ueno, *Chem. Lett.*, (**1981**), 1305.

154. H. Nakumura, H. Nishida. M. Takagi and K. Ueno, *Anal. Chim. Acta.*, 139, (**1982**), 219.

155. H. G. Lohr, F. Vögtle, W. Schul and H. Puff, *Chem. Ber.*, 117, (**1984**), 2839.

156. J. M. Larson and L. R. Sousa, *J. Am. Chem. Soc.*, 99, (**1977**), 307.

157. J. M. Larson and L. R. Sousa, *J. Am. Chem. Soc.*, 100, (**1978**), 1944.

158. H. S. Brown, C. P. Muenchausen and L. R. Sousa, *J. org. Chem.*, 45, (**1980**), 1682.

159. H. Forrest and G. E. Pacey, Talanta, 36, (1989), 335.

160. U. Herrmann, B. Tummler, G. Maass, P. KooTze Mew and F. Vögtle, *Biochemistry*, 23, (**1984**), 4059.

161. B. Tummler, U. Herrmann, G. Maass, H. Eibl, *Biochemistry*, 23, (**1984**), 4068.

162. A. P. Silva and K. R. A. S. Sandanayake, *Angew Chem. Int. Ed. Engl.*, 29, (**1990**), 1173.

163. J. Janata, *Anal. Chem.*, 59, (**1987**), 1351.

164. S. Borman, *Anal. Chem.*, 59, (**1987**), 1161A.

165. T. J. Kulp, I. Camins, St. M. Angel, C. MunKholm and D. R. Walt, *Anal. Chem.*, 59, (**1987**), 2849.

166. O. S. Wolfbeis and B. P. H. Schaffar, *Anal. Chim. Acta.*, 198, (**1978**), 1.

167. M. R. S. Fuh, L. W. Burgess, T. Airschfeld, G. D. Christan and F. Wang, *Analyst*, 112, (**1987**), 1159.

168. J. Janata and A. Bezegh, *Anal. Chem.*, 60, (**1988**), 62r.

169. G. F. Kirkbright, R. Narayanaswamy and N.A. Welti, *Analyst*, 109, (**1984**), 1025.

170. J. I. Peterson, S. R. Goldstein and R. V. Fitzgerald, *Anal. Chem.*, 52, (**1980**), 864.

171. C. Munkholm, D. R. Walt, F. P. Milanowich and S. Klainer, *Anal. Chem.*, 58, (**1986**), 1430.

172. A. M. Scheggi, F. Baldini, *Opty. Acta.*, 33, (**1986**), 1587.; L. A. Saari and W. R. Seitz, *Anal. Chem.*, 55, (**1983**), 667.

173. P. Caglar, R. Narayanaswamy, *Analyst* (London), 112, (**1987**), 1285.

174. M. A. Butler and D. S. Ginley, *Proc. Symp. Chem. Sens.*, 87-9, (**1987**), 502.

175. H. VanRyswyk and A. B. Ellis, *J. Am. Chem. Soc.*, 108, (**1986**), 2454.

176. J. F. Place, R. M. Sutherland and C. Dachne, *Biosensors*, 1, (**1985**), 321.

177. F. Farahi, P. A. Leilabady, J. D. C. Jones and D. A. Jackson, *J. Phys. E. Sci. Instrum.*, 20, (**1987**), 435.

178. A.S. Waggoner and A. Grinvald, *Ann. NY. Acad. Sci.*, 309, (**1977**), 217.

179. H. Windisch, W. Muller and H. A. Tritthart, *Biophys. J.*, 48, (**1985**), 877.

180. Biomimetic and Bioorganic Chemistry III, *Topics in curr. Chem.*, 136, (**1986**), Springer-Verlag, New York.; G. W. Gokel, Crown Ethers and Cryptands, Monographs in Supramolecular Chemistry, J. F. Stoddart (Ed), Royal Society of Chemistry, Cambridge, England, (**1991**)

181. A. P. Silva and S. A. Silva, *J. Chem. Soc. Chem. Commun.*, (**1980**), 1709.

182. J. P. Konopelski, F. K. Hibert, J. M. Lehn, J. P. Desvergne, F. Fages, A. Castellan and H. B. Laurent, *J. Chem. Soc. Chem. Commun.*, (**1985**), 433.

183. P. J. Dutton, T. M. Fyles and S. J. McDermid, *Can. J. Chem.*, 66, (**1988**), 1097.

184. A. Ashok and T. M. Fyles, *Can. J. Chem.*, 68, (**1990**), 1338.

185. T. M. Fyles, Cation Binding by Macrocycles, I. Inoue and G. W. Gokel (Ed.), Marcel Dekker Inc., New York, (**1990**), 203.

186. T. M. Fyles, V. V. Suresh, F. R. Fronczek and R. D. Gandour, *Tetrahedron Lett.*, 31, (**1990**), 1101.

187. J. P. Behr, M. Bergdoll, B. Chevrier, P. Dumas, J. M. Lehn and D. Moras, *Tetrahedron Lett.*, 28, (**1987**), 1989.

188. J. P. Behr, C. J. Burrows, R. Heng and J. M. Lehn, *Tetrahedron Lett.*, 26, (**1985**), 215.

189. J. M. Lehn and P. G. Potvin, *Can. J. Chem.*, 66, (**1988**), 195.

190. R. Hosseini, These Doctorat es Sciences, University of Louie Pasteur, Strasbourg, France (**1985**).

191. P. J. Dutton, F. R. Fronczek, T. M. Fyles, R. D. Gandour and V.V. Suresh, *Can. J. Chem.*, in Press.

192. T. M. Fyles and D. M. Whitfield, *Can. J. Chem.*, 62, (**1984**), 507.

193. H. Dugas, P. Keroack and M. Ptak, *Can. J. Chem.*, 62, (**1984**), 489.

194. A. Anantanarayan, V. A. Carmichael, P. J. Dutton, T. M. Fyles and M. J. Pitre, *Synth. commun.*, 16, (**1986**), 1771.

195. T. M. Fyles, C. A. McGavin and D. M. Whitfield, *J. Org. Chem.*, 49, (**1984**), 753.

196. Values were obtained by minimising the molecular structure using PCMODEL (Version. 3), Serena Software, (**1989**).

197. R. H. Mitchel and V. S. Iyer, *Synlet*, (**1989**), 55.

198. L. A. Frederick, T. M. Fyles, N. P. Guruprasad and D. M. Whitfield, *Can. J. Chem.*, 59, (**1981**), 1724.

199. J. R. Lakowicz, Principles of Fluorescence Spectroscopy, Plenum Press, New York, (**1983**).

200. N. J. Turro, Modern Molecular Photochemistry, University Science Books, CA, (**1978**).

201. B. R. Martin and F. Richardson, *Quart. Rev. Biophys.*, 12, (**1979**), 181.

202. A. Jablonski, *Z. Phys.*, 94, (**1935**), 38.

203. J. A. Barltrop and J. D. Coyle, Excited States in Organic Chemistry, Wiely London, (**1975**), 148.

203. H. Knibbe, D. Rehm and A. Weller, *Ber. Bunsenges*, 72, (**1968**), 257.

204. D. V. O'Connor and W. R. Ware, *J. Am. Chem. Soc.*, 98, (**1976**), 4706.

205. M. Kasha, *Discuss. Faraday Soc.*, 9, (**1950**), 14.

206. M. R. Wright, R. P. Frosch and G. W. Robinson, *J. Chem. Phys.*, 33, (**1960**), 934.

207. R. F. Steiner and E. P. Kirby, *J. Phys. Chem.*, 73, (**1969**), 4130.

208. I. B. Berlman, Handbook of Fluorescence Spectra of Aromatic Molecules, 2nd Edn, Academic Press, new York, (**1971**).

209. R. L. Bruening, R. M. Izatt and J. S. Bradshaw, Cation Binding by Macrocycles, Y. Inoue and G. W. Gokel (Ed.), Marcel Dekker Inc., New York, (**1990**), 111.

210. J. J. Christensen, J. Ruckman, D. J. Eatough and R. M. Izzat, *Thermochem. Acta*, (**1972**), 303.

211. R. M. Izatt, R. E. Terry, D. P. Nelson, Y. Chan, D. J. Eatough, J. S. Bradshaw, L. D. Hansen and J. J. Christensen, *J. Am. Chem. Soc.*, 98, (**1976**), 7626.

212. C. Micheaux and J. Reisse, *J. Am. Chem. Soc.*, 104, (**1982**), 6985.

213. J.M. Lehn and J.P. Sauvage, *J. Am. Chem. Soc.*, 37, (**1975**), 6700.

214. D. J. Cram and P.Ho, *J. Am. Chem. Soc.*, 108, (**1986**), 2998.

215. J. J. Dechter and J. I. Zink, *J. Am. Chem. Soc.*, 98, (**1976**), 845.

216. K. H. Wong, G. Knizer and J. Smid, *J. Am. Chem. Soc.*, 92, (**1970**), 666.

217. B. G. Cox, J. Garcia-Rosas and H. Schneider, *J. Am. Chem. Soc.*, 103, (**1981**), 1054.

218. I. G. Sayce, *Talanta*, 15, (**1968**), 1397, *ibid*, 18, (**1971**), 653.

219. R. F. Jameson and M. F. Wilson, *J. Chem. Soc.*, (**1972**), 2607.

220. E. R. Blout, *Biopolymers*, 20C, (**1981**), 1901.

221. D. M. whitfeild, PhD Thesis, University of Victoria, (**1983**), pp 97.

222. P. Tundo and J. H. Fendler, *J. Am. Chem. Soc.*, 102, (**1980**), 1760.

223. Y. Marcus, Ion Solvation, Wiely Chichester, (**1985**), 105.

224. F. P. Schmidtchen, *Topics in Curr. Chem.*, 132, (**1986**), 101.

225. F. P. Schmidtchen, A. Gleich and A. Schummer, *Pure and Appl. Chem.*, 61, (**1989**), 1535.

226. B. Dietrich, J. Guilhem, J. M. Lehn, C. Pascard and E. Sonveaux, *Helv. Chim. Acta*, 67, (**1984**), 91.

227. M. W. Hosseini and J. M. Lehn, *J. Am. Chem. Soc.*, 109, (**1987**), 7047.

228. J. P. Behr, J. M. Lehn, A. C. Dock and D. Moras, *Nature*, 295, (**1982**), 526.

229, E. Kimura (Ed), Current Topics in Macrocyclic Chemistry in Japan, Hiroshima School of Medicine, (**1987**).

230. S. Tanaka (Ed), Chemomeasuring by High Performance Chemical Sensor Systems, Special Project Research, (**1986-1988**).

231. J. P. Behr, J. M. Lehn and P. Vierling, *J. Chem. Soc. Chem. Commun.*, (**1976**), 621.

232. F. R. Fronczek, R. D. Gandour, T. M. Fyles, P. J. Hocking, S. J. McDermid and P. D. Wotton, *Can. J. Chem.*, 69, (**1991**), 12.

233. D. T. Cromer and J. T. Waber, International Table for X-ray Crystallography, Kynoch Press, Brimmingaham, (**1974**), Table 2.2B.

234. D. Philp and J. F. Stoddart, *Synlet*, (**1991**), 445, 459, 462 and the reference cited therein.

235. R. Breslow, *Pure and Appl. Chem.*, 62, (**1990**), 1859 and the references cited therein.

236. I. Tabushi, *Tetrahedron*, 40, (**1984**), 269 and the references cited therein.

237. V. E. Carmichael, P. J. Dutton, T. M. Fyles, T. D. James, C. McKim, J. A. Swan and M. Zojaji, Inclusion Phenomena and Molecular Recognition, J.L. Atwood (Ed.), Plenum Press, New York and London, (**1990**), pp. 145.